GA-A--19536

DE89 013999

FINAL REPORT

DIII-D RESEARCH OPERATIONS

NOVEMBER 1, 1983 THROUGH OCTOBER 31, 1988

by

PROJECT STAFF

Work prepared under
Department of Energy
Contract DE-AC03-84ER51044

GENERAL ATOMICS PROJECTS 3410/3415/3436/3455
DATE PUBLISHED: MAY 1989

GENERAL ATOMICS

TABLE OF CONTENTS

SECTION 1

INTRODUCTION AND SUMMARY

1. INTRODUCTION AND OVERVIEW

This report summarizes Research Operations on the Doublet III and DIII–D tokamaks for the contract period November 1, 1983 to October 31, 1988. The General Atomics tokamak research program has strived to advance the understanding and bounds of tokamak physics. Research at General Atomics has emphasized plasma shaping and high beta operations. The expanded boundary divertor that was invented in Doublet III was capitalized on in the design of the DIII–D device [1,2]. The DIII–D tokamak quickly demonstrated these high beta and enhanced confinement features of non-circular divertor geometry that have been adapted in next generation tokamak designs such as CIT and ITER.

Results of the research of this five year period are contained in over 150 journal articles as well as in additional archived technical reports and conference proceedings. A list of these publications is given in Section 6. The DIII–D research program in the ongoing 5-year contract period builds on these past results. The goal of the ongoing research program is to advance understanding and predictive capability resulting in a demonstration of a high-β plasma with noninductively driven toroidal current and good confinement.

The past 5-year contract period can be characterized by four phases:

1. 1984 Doublet III operation and the design phase of the DIII–D vessel vessel modification project.
2. 1985 Conversion of Doublet III to DIII–D.
3. 1986 Commissioning of DIII–D and initial experiments.
4. 1987-88 DIII–D research operations.

The characteristics of the Doublet III and DIII–D tokamaks as given in Table 1-1 indicate that the DIII–D vacuum vessel is larger and capable of higher plasma current. The emphasis in this report is on 1988 since annual reports are available for the earlier years [3-6].

TABLE 1-1.
CHARACTERISTICS OF DOUBLET III AND DIII–D

	Doublet III*	DIII–D**
Major radius, m	1.43	1.67
Minor radius, m	0.44	0.67
Magnetic field (on axis), T	2.6	2.2
Maximum plasma current, MA		
Limiter	1.05	3.0
Divertor	0.95	2.2
Maximum beta achieved, %	4.5	6.8
Energy confinement times (ms)		

* In operation with a single magnetic axis.

** Achieved values at end of FY88.

The DIII–D tokamak and high power neutral beam system have operated very reliably with 78% availability for physics experiments in FY88. Wall conditioning techniques were developed which provide unusual experimental flexibility that allows high quality experimental operations to be resumed rapidly after venting the device to atmospheric conditions. Radial profile diagnostics are available, and being further improved, for transport experiments. Two radio frequency plasma heating systems each with 2 MW system power are operational, ten 0.2 MW 60 GHz gyrotrons are available for electron cyclotron heating and a 2 MW 30 to 60 MHz transmitter is available for ion cyclotron heating. A radiation roof shield has been completed and wall shields are being constructed to allow experiments to be carried out with deuterium, as well as with hydrogen, plasmas.

At the close of this contract period the DIII–D research program had demonstrated a number of significant results that included:

- High plasma betas (6.8%) were achieved in single null divertor configuration (5% in double null). The maximum beta was found to scale as $\beta(\%) = 3.5\ I/aB$ (MA m^{-1} T^{-1}). A theoretical understanding of the beta limit has emerged.
- Plasma confinement was shown to be improved by H–mode, a high quality confinement regime in contrast to L–mode. DIII–D has demonstrated that this improved confinement regime is a universal tokamak feature since it has been achieved with neutral beams, electron cyclotron heating, ohmic heating, as well as with both divertor and limiter discharges.
- The divertor configuration has been shown to be capable of long-pulse operation. Discharges up to 5 seconds have been sustained in DIII–D without increasing impurity accumulation. Divertor sweeping was demonstrated to distribute divertor heat loads.
- Electron cyclotron heating (ECH) has been demonstrated to heat electrons up to 5 keV, generate H–mode, stabilize sawteeth, and suppress edge localized modes (ELMs).
- Neutral beam current drive has sustained plasma current up to 0.34 MA in DIII–D and produced plasmas with high poloidal betas at the entrance to the second stability regime.

A listing of DOE milestones completed during FY84 through FY88 are given in Table 1-2. Milestones 35 and 41 were deleted. Milestones 47, 48, 49, 52, 54 and 55 are scheduled for 1989.

This final report is organized on a technical rather than chronological basis. Section 2 describes scientific progress and Section 3 describes operations and hardware development. Section 4 describes the national and international collaborative efforts that play such an important role in the DIII–D research program. Contributions of support services such as quality assurance, planning and control, computer operations, safety and visitor programs are described in Section 5.

TABLE 1-2
MILESTONES COMPLETED DURING FY84 THROUGH FY88

	Task Description	Date Completed
21.	Begin three beamline operation	11-83
22.	Initial very high power neutral injection experiments (beam power > 7.5 MW)	11-83
23.	Evaluate parameter dependence of the plasma beta/confinement with very high power heating (> 6.0 MW) in non-circular discharges	2-84
24.	Complete component testing of 1.5 MA poloidal system	4-84
25.	Complete operation with present vacuum vessel and vent for installation of new vessel	9-84
26.	Document beta and confinement results for wide wide range of plasma configuration and heating power	1-85
27.	Evaluate effects of high power electron cyclotron heating on plasma performance	12-84
28.	Achieve 1.l5 MA plasma current in the new vessel	5-86
29.	Inject 6 MW into a plasma in the new vessel	10-86
30.	Inject 10 MW into a plasma in the new vessel	5-87
31.	Report on comparison of experimentally observed beta limits with theoretical limits	9-84
32.	Initial comparison of outside launch ECH heating	1-87
33.	Evaluate confinement in beam-heated high beta discharges	9-87
34.	$T_e(r)$, $n_e(r)$ from Thomson scattering	1-87
36.	Achieve plasma current of 3.0	1-87

TABLE 1-2 (Continued)

	Task Description	Date Completed
37.	Correlate beta results with previous Doublet III results	3-88
38.	Compare observed beta limits with first stability regime theories	3-88
39.	Assessment of energy confinement in DIII–D	11-88
40.	Report final assessment of outside launch ECH heating	8-87
42.	Evaluate β limit of a discharge with $I/aB > 3$	3-88
43.	Evaluate β limit of a divertor discharge with $I/aB > 2.3$	3-88
44.	Report comparison of modeling of divertor neutral pressure with experimental results (with PPPL or LLNL)	12-87
45.	Initiate inside launch ECH experiment	3-88
46.	Evaluate confinement in double null divertors	7-88
50.	Initiate ICH IBW experiments	10-88
51.	Complete radiation shielding roof	10-88
53.	Report on the physical mechanism of the β limit	10-88
56.	Begin experiments using 1.4 MW generated ECH power	8-88

REFERENCES FOR SECTION 1

[1] Davis, L., J. Luxon, P. Anderson, R. Callis, A. Colleraine, P. Rock and R. Stambaugh, "DIII–D Vessel Modification Project, Final Report for the Period FY83 through FY86," General Atomics Report GA-A19327, June 1988.

[2] Program Staff, "System Design Description of DIII–D," General Atomics Report GA-A19264, 1989.

[3] Project Staff, "Doublet III Annual Report for the Period October 1, 1983 to September 30, 1984," General Atomics Report GA-A18024, UC-20, 1985.

[4] Project Staff, "Doublet III Annual Report for the Period October 1, 1984 to September 30, 1985," General Atomics Report GA-A19468, UC-20, 1986.

[5] Project Staff, "Doublet III Annual Report for the Period October 1, 1985 through September 30, 1986, General Atomics Report GA-A19133, UC-420, 1988.

[6] Project Staff, A.P. Colleraine, Editor, "DIII–D Annual Report for the Period FY87," General Atomics Report GA-A19222, UC-420, 1988.

SECTION 2

SCIENTIFIC PROGRESS

2. SCIENTIFIC PROGRESS

2.1. INTRODUCTION

The General Atomics tokamak research program has always sought to advance the state of the art by testing and stretching the bounds of tokamak operation. This emphasis on advanced tokamak features began with the early Doublet series of devices, Doublet I, Doublet II and IIA. The program reached the forefront of fusion research in some areas on Doublet III. This report describes the transition in the advanced line of research from the Doublet III device whose performance has caused important future machine designs (CIT, ITER) to be patterned after it.

The central theme of the Doublet III and DIII–D research programs has been enhanced tokamak performance through non-circular plasma shaping. The Expanded Boundary Divertor was invented on Doublet III and has produced remarkable confinement and high beta results on DIII–D. DIII–D routinely operates with the highest plasma elongation and lowest safety factors of any tokamak in the world.

Plasma elongation has proven essential to operating at high beta values. With our present understanding of beta limit physics, to which Doublet III and DIII–D were major contributors, we know that circular tokamaks are limited to $\beta_T \sim 3\%$. In 1982 Doublet III achieved $\beta_T = 4.5\%$, then a record, which began steady progress in surmounting the circular plasma limit. DIII–D has reached $\beta_T = 6.8\%$ and expects to go higher.

Achieving high beta requires a high quality of energy confinement. Doublet III showed that confinement in the expanded boundary divertor configuration was twice that of limiter plasmas. When DIII–D was brought into operation, the H–mode regime of improved confinement (discovered on the ASDEX tokamak in Germany) was quickly found. The H–mode regime has been very important in reaching higher beta. DIII–D has made important contributions to understanding the physics of the H–mode regime.

Because the H–mode improvement originates in the plasma boundary, the DIII–D research program has always had an explicit element focused on the plasma boundary. Complete and detailed studies have been made of neutral refueling of diverted plasmas. Operational techniques were developed to control impurity levels in the plasma, leading to long pulse (5 sec) quasi-stationary H–mode discharges. These results have helped establish H–mode as a viable operating scheme for steady state tokamak reactors.

In keeping with the GA thrust toward advanced tokamak features, the long range goal of DIII–D is to provide the research basis for steady state operation. To that end, the program contains rf heating and non-inductive current drive elements. A 60 GHz Electron Cyclotron Heating program was begun on Doublet III and continues on DIII–D. This program seeks to provide the basis for ECH as a primary heating system in future devices as well as developing applications of ECH such as MHD mode stabilization. To provide ion heating complementary to the electron heating with ECH, an Ion Bernstein Wave heating program was begun on DIII–D.

Non-inductive current drive is being pursued with a variety of techniques. Neutral beam current drive work has already yielded exciting results, including an unexpected close approach to the theoretically predicted "second regime" of high beta stability. Experiments are being planned and hardware made ready for tests of current drive by electron cyclotron waves and ICRH fast waves.

The scientific progress described herein details a dynamic program of advanced tokamak research. In plasma shape, achieved beta values, enhanced confinement operation, ECH and current drive work, the Doublet III and DIII–D programs are providing the physics basis for effective tokamak reactors. This program has carried the tokamak far beyond its low beta beginnings.

2.2. CONFINEMENT

2.2.1. FY88 HIGHLIGHTS

With the development of the single-null divertor H–mode firmly established in FY87, confinement experiments in FY88 focused on searching for other methods of improving confinement over the L–mode values, and to further studying the details of the L– to H–mode transition. H–mode like confinement is typically obtained in divertor discharges with neutral beam injection (NBI) heating. Several other methods of achieving H–mode

confinement were obtained in FY88. These included limiter discharges limited on the inside wall of the vessel heated by NBI and divertor discharges with no auxiliary heating at all. Confinement values significantly above ohmic levels were obtained for the first time on DIII–D with ohmic H–mode discharges and high current, NBI heated H–mode discharges. Studies of the transition from L–mode to H–mode yielded the parametric scaling of the threshold conditions.

In support of our high β program, GA focused on confinement at low safety factor q in FY88. Previous studies in H–mode discharges had indicated that energy confinement scaled linearly with plasma current and was independent of toroidal field [1,2]. These studies were performed with hydrogen neutral beams injected into deuterium plasmas with a safety factor above three. We found that for plasmas with $q \leq 3$, the confinement becomes independent of plasma current and, instead, becomes linearly dependent on the toroidal field [3,4]. This has the consequence that the beta value in low q discharges will increase inversely with the toroidal field up to the beta limit.

Confinement scaling with plasma current for both low and higher q discharges is shown in Fig. 2.2-1. Data from the current scan at 2.1 T shows a linear increase in confinement up to the highest current. The value of q at the highest current is still above three. The data at 1.5 and 0.9 T show a rollover of confinement when the current rises to values where $q \leq 3$. This rollover is not due to coherent MHD activity associated with operation at high β values. The data in Fig. 2.2-1 also indicate that at fixed plasma current and q below three, the confinement is a function of the toroidal field. Other experiments at low q show that the confinement scales linearly with toroidal field down to 0.7 T. This toroidal field dependence was reminiscent of Simomura [5] scaling where a maximum achievable confinement value is suggested based on confinement values achieved in a saturated ohmic confinement regime. To test whether confinement in DIII–D followed this idea, we searched for confinement regimes with τ_E greater than the saturated ohmic value.

Saturated ohmic confinement values were exceeded in DIII–D with two different types of discharges. The first example was obtained with ohmic heating only in divertor discharges that exhibit transient periods of H–mode behavior at low toroidal field, low q, and low density [6]. Confinement times during these periods are up to twice the normal ohmic heating values as shown in Fig. 2.2-2. The power threshold condition for these ohmic H–mode discharges appears to be similar to the condition for NBI heated H–mode discharges. The broad density profiles differ from improved confinement examples from other devices (i.e., ASDEX IOC mode and pellet injection) where the improvement is

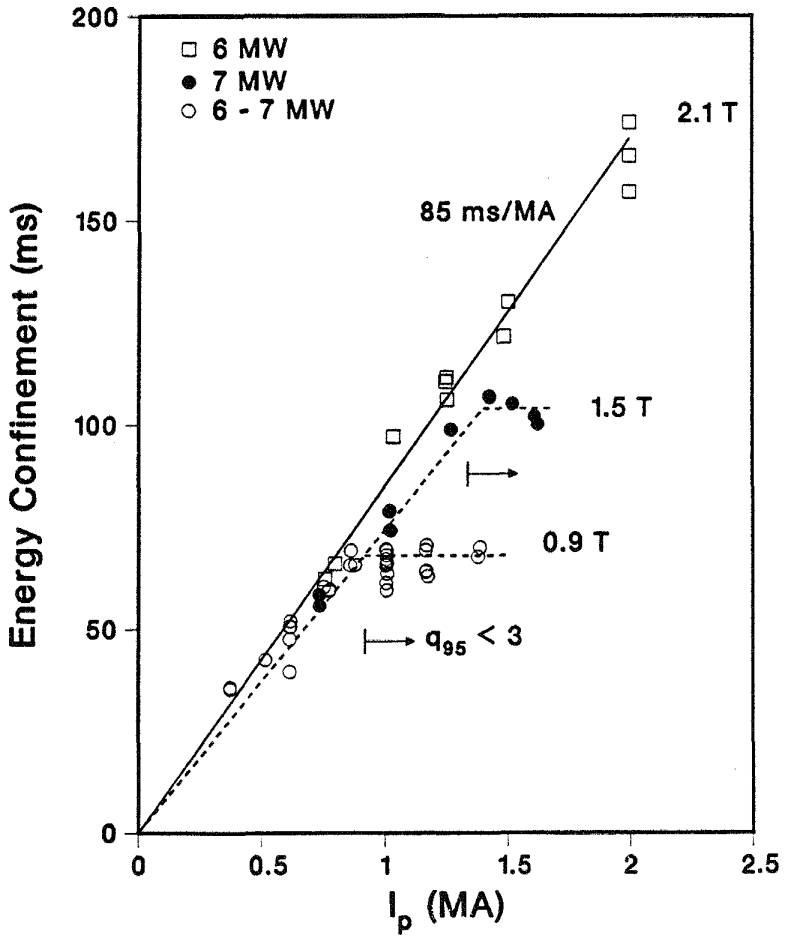

Fig. 2.2-1. Energy confinement time as a function of plasma current for three toroidal field values. At 2.1 T the safety factor q_{95} remains above three at all currents. Data with $q_{95} < 3$ are indicated by arrows for the other two toroidal field values.

attributed to peaked density profiles. The second example with confinement above the saturated ohmic value occurred in discharges heated with two source NBI at 2 MA and 2.1 T. Taking advantage of the favorable scaling of confinement with current at high q, confinement in these H–mode discharges was up to 220 msec at a total heating power of 4 MW as compared to 150 msec for the saturated ohmic confinement time. Even at 10 MW, the confinement is still comparable to the saturated ohmic level. These examples demonstrated that saturated ohmic confinement is not the maximum possible in auxiliary heated plasmas and that the rollover in confinement scaling with current near $q = 3$ is not due to hitting a saturated confinement limit. At the lower current values, the rollover may be due to an unfavorable interplay between sawteeth and ELMs. At higher currents,

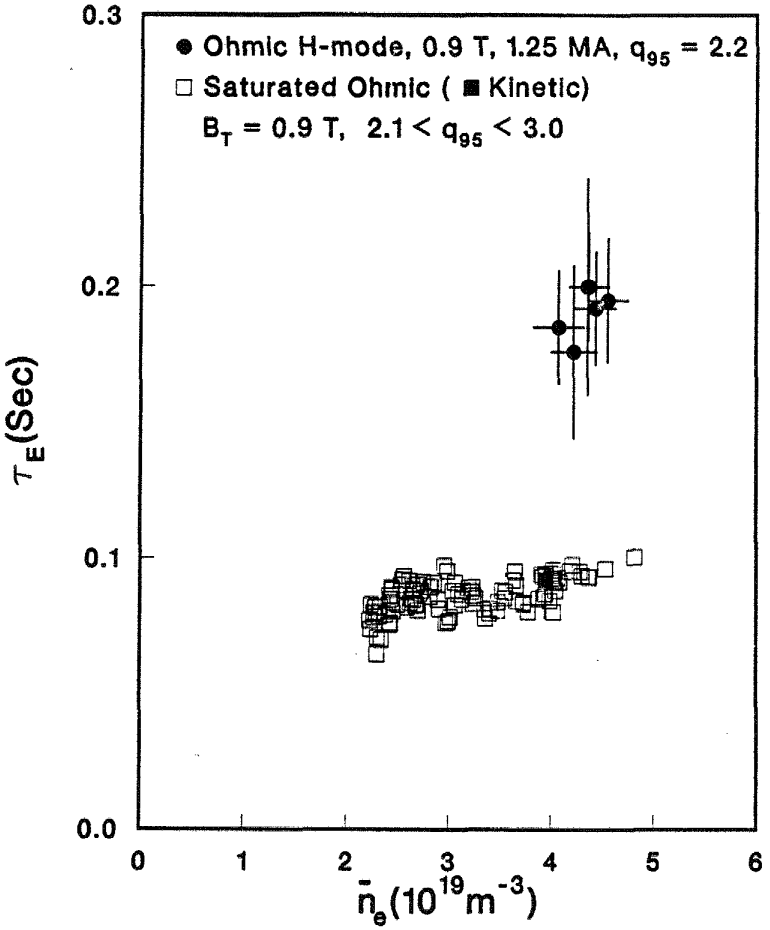

Fig. 2.2-2. Energy confinement time versus line average density for ohmic H–mode discharges and steady-state saturated ohmic discharges. Since H–mode discharges were not in steady state, a correction for the time rate of change of plasma stored energy was included.

the ELM frequency becomes too low for the ELMs to play a significant role in coupling to the energy loss from sawteeth. This remains an area for future investigation.

H–mode confinement quality was also obtained in limiter discharges limited on the inside wall of the vessel. The best confinement values obtained in these discharges were comparable to the ohmic confinement values as well as to divertor H–mode plasmas with corresponding parameters [7]. The rather large variation in τ_E shown in Fig. 2.2-3 for these discharges was predominantly due to various helium wall conditioning scenarios. The best confinement times were obtained from the first few shots in the morning following a night of baking and discharge cleaning in helium. Because these discharges are limited on the inside wall, they can be made with high elongations and triangularities. We expect to exploit these characteristics for our advanced shape high β program.

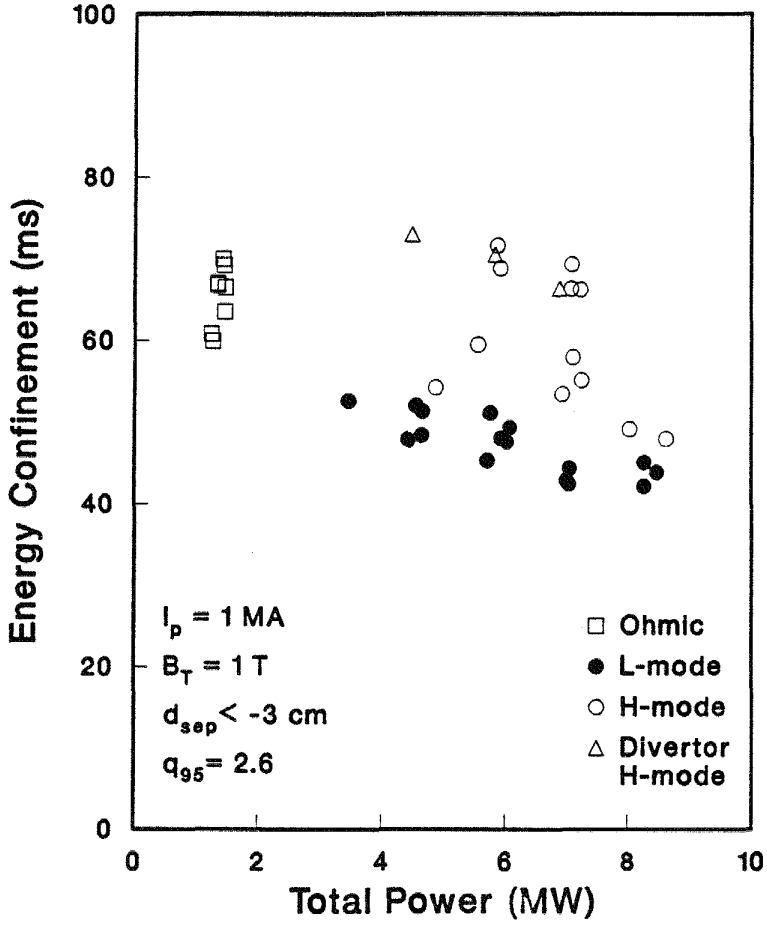

Fig. 2.2-3. Confinement time comparison of limiter H–mode discharges with similar divertor H–mode discharges and limiter ohmic and L–mode values before transition to H–mode.

In FY88, GA conducted detailed experiments aimed at identifying the necessary conditions for achieving H–mode and performed a critical comparison of the scaling of these conditions with various theories [2,8]. We investigated conditions leading to the L to H transition in single-null, NBI heated ($H^\circ \rightarrow D^+$) discharges in DIII–D through systematic scans of plasma parameters over the ranges:

$$1 < I_p\,(\mathrm{MA}) < 2,\ 1 < B_T\,(\mathrm{T}) < 2,\ 3 < \bar{n}_e\,(10^{19}\ \mathrm{m}^{-}3) < 8 \quad ,$$

and the bottom X–point to divertor plate distance,

$$1 < \delta\,(\mathrm{cm}) < 23 \quad .$$

To achieve an H–mode discharge, a minimum or threshold level of heating power must be applied. The threshold power was found to scale with $n_e B_T$, independent of I_p and q. As NBI power was increased during the L–phase of the discharge, T_e $(r/a = 0.97)/B_T$ approached a critical value of ~115 eV/T before each L to H transition. This critical value was constant over the entire range of conditions studied, suggesting that this parameter is important for the threshold condition. Just prior to the L to H transition, we observed that near the edge region of the plasma $(r/a = 0.97)$ the electron and ion temperatures were similar and the ion collisionality was above one. These observations conflict with transport bifurcation theories that require $T_i \neq T_e$ at the plasma edge and indicate that ion orbit loss may not be important in establishing a radial electric field E_r as required by some bifurcation theories. After the transition, the plasma remains in the first stability regime for ideal ballooning modes indicating the L to H transition is not a switch into the second stability regime. We observed edge ion rotation consistent with a negative E_r. This is in direct conflict with predictions of the L to H transition theory by S. I. and K. Itoh [9].

Motivated by experiments on other devices, we examined confinement in discharges with counter-injected neutral beams (beam injection in a direction counter to the direction of the plasma current). We found that the H–mode threshold was reduced by about 2 MW with counter-injection into single-null divertor discharges, but there was no confinement improvement over co-injection for H–mode, L–mode, or limiter discharges [10]. Suppression of sawtooth oscillations was achieved in many H–mode discharges. In these plasmas without sawteeth, metallic impurity build-up in the central region of the plasma caused cooling, and ultimately, a reduction of confinement after about 1 sec of beam heating.

We evaluated confinement in double-null divertor, H–mode discharges for both co- and counter-injection neutral beam heating [11]. No significant confinement differences were found between single-null and double-null discharges.

Based on a comparison of Doublet III and DIII–D limiter discharges, we observed no apparent effect on confinement quality $\tau/I\sqrt{k}$ which could be attributed to the differences in size, plasma minor radius a or vessel major radius R, of the two devices. The plasma radius was increased by about 60% in DIII–D and the major radius was increased 17%. This resulted in a 26% decrease in the inverse aspect ratio. We concluded that either there is no confinement dependence on a and R individually or that the dependence is such that the a and R scaling offset each other for this comparison. The latter finding is consistent with Kaye-Goldston [12] confinement scaling predictions for this comparison. Also, we ruled out a strong dependence (quadratic or stronger) of confinement on aspect

ratio, since a 26% variation in aspect ratio had no effect on confinement and this level of variation was similar to the fluctuation level in the confinement values.

2.2.2. FY84 TO FY87 SUMMARY

FY84 was the final year of operation of Doublet III. During FY85 and part of FY86, the vacuum vessel was replaced with a larger vessel that essentially utilized all of the available space within the toroidal field coils. During FY84, confinement experiments focused on identifying improved confinement regimes relative to confinement in hydrogen beam heated limiter discharges. FY85 was a productive year of detailed analysis and publication. We made a final assessment of confinement scaling laws and their exceptions [13], and described a detailed test of neoclassical transport theory for the ions [14].

The results of detailed ion transport analyses of high power neutral beam heated discharges in Doublet III challenged the fusion community to rethink the relative roles of electron and ion transport in a tokamak. Based on measured profiles of electron density, electron temperature, and ion temperature, the plasma transport equations were inverted to give the electron and ion thermal diffusivities [14]. We found the ion thermal diffusivity over most of the plasma radius to be larger than the neoclassical value and to have a spatial variation different than that predicted by neoclassical theory. This result indicated that the usual treatment of ion transport in tokamaks, assuming some multiple of neoclassical diffusivity, was no longer valid.

To find ways to maximize energy confinement time, GA performed confinement scaling experiments on Doublet III. Linear scaling with plasma current and a weak, square root dependence on elongation was established before FY84. During FY84, we found power scaling to be described equally well by two different functional forms for both limiter and divertor discharge data: an offset linear form for the plasma energy content and a power law form [13]. These two descriptions of confinement degradation with power still hold for many tokamaks throughout the world. Several different regimes of operation on Doublet III were explored and confinement was compared to the confinement obtained in standard hydrogen beam heated limiter discharges. Deuterium beam heating was found to be better than hydrogen beam heating; discharges limited radially inward on the inside of the vacuum vessel had somewhat better confinement than those limited on the outside, and divertor discharges exhibited the best confinement values.

Although divertor operation in Doublet III was good in terms of impurity control, we did not observe sharp transitions from L–mode to H–mode like behavior. Confinement from limited to diverted discharges continued to improve, but the confinement in divertor discharges was a factor of 2 less than that observed in ASDEX H–mode discharges with comparable parameters. Experimental evidence from Doublet III, PDX, and ASDEX suggested that this was due to poor neutral particle confinement in the divertor region [15]. ASDEX with its tightly closed divertor chamber provided a roughly 40 msec confinement or delay before neutrals in the divertor recycled back to the main plasma. This allowed the edge temperature time to rise to a critical value necessary to achieve a transition to H–mode when enough neutral beam heating was applied. The effective neutral particle confinement time in the divertor region of Doublet III was estimated to be 5 ms, too short to allow a large enough temperature increase at the plasma edge. We observed a clear L to H transition in DIII–D with its more tightly closed divertor region, provided by divertor plasma plugging, which further supports the notion that achieving a good H–mode requires sufficient neutral particle confinement in the divertor.

In FY86 we observed a clear correlation between edge incoherent magnetic fluctuations and edge transport based on further analysis of Doublet III divertor data with improved confinement [16]. The fluctuations and associated transport were consistent with a model based on an assembly of saturated microtearing modes. This model offered an explanation to the observation that an apparent improvement in edge transport could result in an increased temperature across the entire profile, not just at the edge. The low-frequency fluctuations exhibited the incoherence, frequency range, and radial-amplitude decrease expected of an assembly of microtearing modes with mode number $m \geq 8$. It was suggested that stabilization of these modes changed the current density profile responsible for the increase observed in the temperature profile everywhere.

The new device, DIII–D, began operation in mid-FY86. In an attempt to modify the boundary physics of limiter discharges and obtain confinement improvement similar to H–mode, GA investigated electrically biasing the primary limiter [17]. The results showed that while particle (and impurity) confinement improved, there was no improvement in energy confinement.

In early FY87, we achieved clear transitions from L–mode to H–mode confinement during deuterium neutral beam heating of divertor discharges [18]. At plasma currents of 1 MA, confinement values of 120 msec were achieved with 3 to 6 MW of NBI [19]. Early scaling studies showed that the confinement was independent of heating

power, plasma density, and toroidal field over the range $3 < P_T(MW) < 6$, $3.0 < \bar{n}_e$ $(10^{19}m^{-3}) < 5.5$, and $1.2 < B_T(T) < 2.1$.

With the improved confinement in H–mode, the neutral beam pulse length proved to be too short to allow a new equilibrium to be reached. Consequently, longer pulse sources (LPSs) were installed to replace the short pulse sources (SPSs). The LPSs caused a much higher gas flow into the DIII–D vessel than the SPSs did. As a result, the H/(H + D) ratio obtained with H° injection into D^+ plasmas with the LPSs (τ_E = 70 ms at I_p = 1.0 MA and P_T = 7.0 MW) compared unfavorably with those for the SPSs (τ_E = 115 ms at I_p = 1.0 MA). The results for the virtually pure D^+ plasmas obtained with the SPSs were reproduced with the LPSs by injecting D°into a D^+ plasma (τ_E = 115 ms at I_p = 1.0 MA).

For the remainder of FY87, confinement studies focused on H–mode divertor discharges with H° neutral beam injection with the LPSs into D^+ plasmas. We observed the following scaling relationships for these discharges [1]:

1. τ_E decreased weakly with beam power from 4 to 7 MW (see Fig. 2.2-4). (The ELM frequency increased as P_B was increased, and the ELM behavior accounted for some and perhaps all of the τ_E degradation with power.)
2. τ_E was independent of toroidal field for B_T = 0.9 to 2.1 T (for $q > 3$).
3. τ_E increased linearly with I_p in the range 0.75 to 2.0 MA (for $q > 3$).
4. τ_E systematically decreased as the H/(H + D) ratio increased.

For H° injection into H^+ discharges, we made the following observations:

1. τ_E was 50 to 80% of that obtained for the pure deuterium case for $P_T = 4 - 7$.
2. The density and power thresholds for obtaining the H–mode were higher than for D^+ targets.
3. τ_E decreased with increasing beam power (Fig. 2.2-4). Part of this decrease may have been related to the ELM frequency dependence on P_B.

The H–mode was obtained with He° injection into He^{++} plasmas above 5.0 MW with I_p=1.0 MA. The confinement time was comparable to that obtained for H° injection into H^+ plasmas (Fig. 2.2-4). Confinement times observed for L–mode discharges were independent of ion species and were consistent with Kaye-Goldston scaling [12]. For pure D^+ plasmas, H–mode discharges had a τ_E which was 2 to 2.5 times that of L–mode discharges (Fig. 2.2-4). Pure H^+ discharges exhibited no more than a 50% increase in τ_E in H–mode versus L–mode (Fig. 2.2-4).

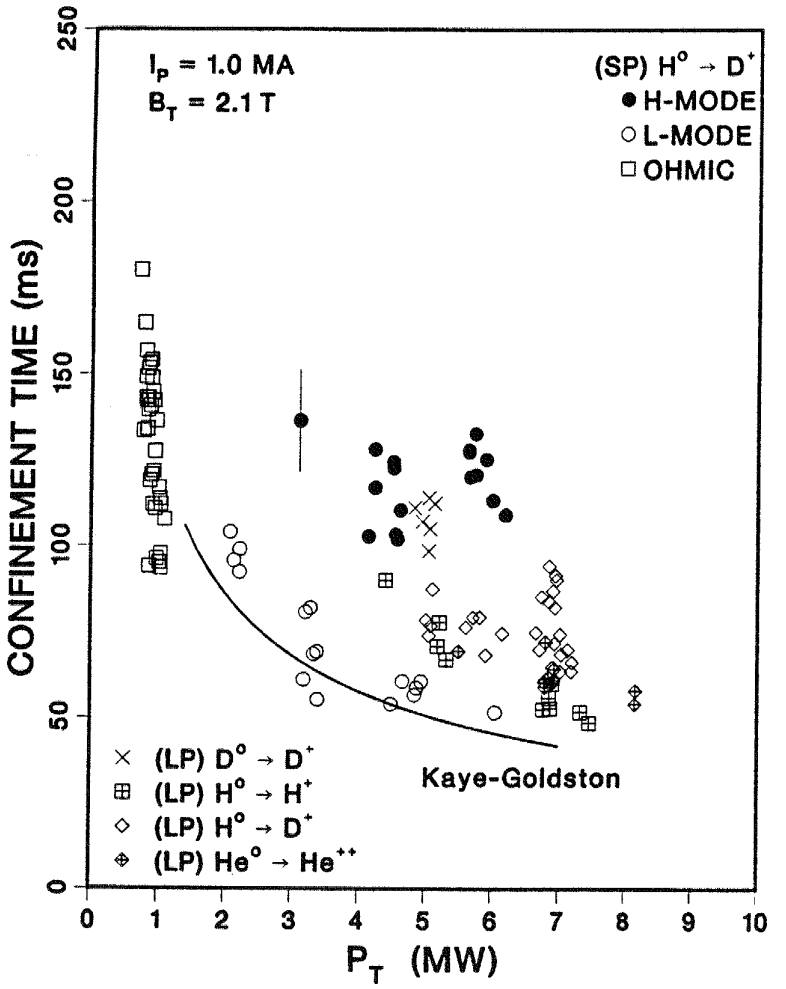

Fig. 2.2-4. Energy confinement time versus total power; (•) and (○) refer to data obtained with SPSs for injection of H° into D^+ plasmas. Solid line is Kaye-Goldston prediction for DIII–D. Remaining symbols are for confinement for various ion species combinations with LPS injection.

Edge localized modes (ELMs), present in most H–mode discharges, can have a substantial effect on confinement. Two general classes of ELMs were distinguished in DIII–D: low frequency, large amplitude ELMs (giant ELMs) which could expel up to 15% of the total stored energy within a few milliseconds, and high frequency, small amplitude events (grassy ELMs) which did not alter confinement from that obtained during ELM-free periods. The giant ELM frequency was higher in H^+ discharges than in D^+ discharges, increased with beam power, and was reduced by degassing the graphite in the vessel. Reducing the gaps between the plasma and the top and bottom vessel walls was found to be a reliable technique for suppressing giant ELMs in favor of grassy ELMs in many D^+ discharges.

The edge electron pressure gradient increased by a factor of about two from the ohmic to the L–phase and by an order of magnitude within 100 ms after the L to H transition. The increase in pressure was primarily a result of an increase in n_e with a small increase in T_e. This pressure gradient was maintained for a few hundred milliseconds until the occurrence of a giant ELM which decreased the edge pressure gradient markedly by expelling particles from the plasma. There was little change in the T_e profile.

Several observations suggested that the ELM was initiated by a ballooning instability and that the ELM itself represents a brief return to L–mode confinement [20]. Under the reasonable assumption that T_i equals T_e at the plasma edge, we found that prior to the ELM, the total pressure gradient at the plasma edge reached the stability limit for ideal ballooning modes (Fig. 2.2-5). The maximum gradient in electron pressure attained prior to an ELM was proportional to the square of the poloidal field, as expected from ballooning mode theory. Furthermore, the incoherent magnetic fluctuations measured in the divertor decreased markedly after the L to H transition, rose to L–mode levels during the period of the ELM, and returned to H–mode levels as the pressure gradient rebuilt.

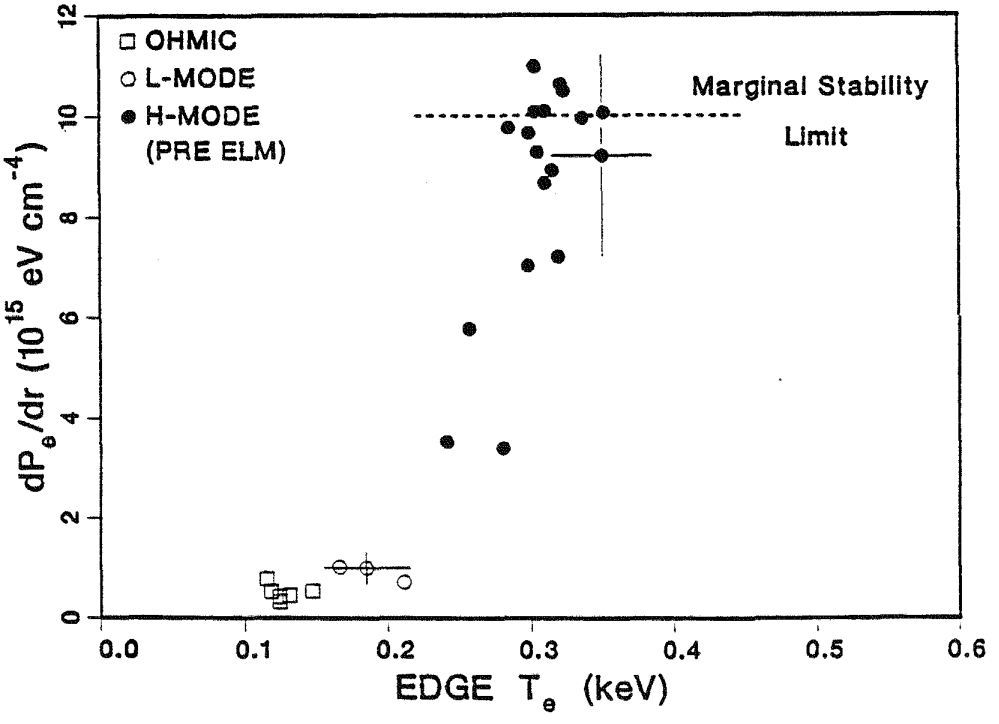

Fig. 2.2-5. Electron pressure gradient at plasma boundary versus edge electron temperature for 1.25 MA discharge with $P_T = 7$ MW. The dashed line corresponding to marginal stability was determined with the assumption that the ion and electron pressure gradients are equal.

We compared transport properties of H–mode and L–mode discharges with identical control parameters ($I_p = 1.25$ MA, $B_T = 2.1$ T, $\bar{n}_e = 7 \times 10^{13}$ cm^{-3}, $P_B = 6.8$ MW, H° injection into D^+ targets and H/(H + D) = 40%) [2,21]. The high densities and moderate temperatures of these discharges strongly coupled T_e and T_i. Due to this strong coupling, thermal diffusivities were calculated for a one-fluid plasma where $\chi = 0.5\ (\chi_e + \chi_i)$ (Fig. 2.2-6). The primary loss for $r < 2a/3$ was conduction in both H and L discharges. τ_E for the L–mode discharge was exactly one-half of τ_E for the H–mode discharge; correspondingly, the one-fluid thermal diffusivity for the L–mode discharge had about twice the value for the H–mode discharge for $r > 0.5a$. The thermal diffusivity for the ohmic and H discharges were essentially equal (Fig. 2.2-6). The comparison showed that the confinement improvement in H–mode occurred over a significant portion of the plasma, not just the plasma edge.

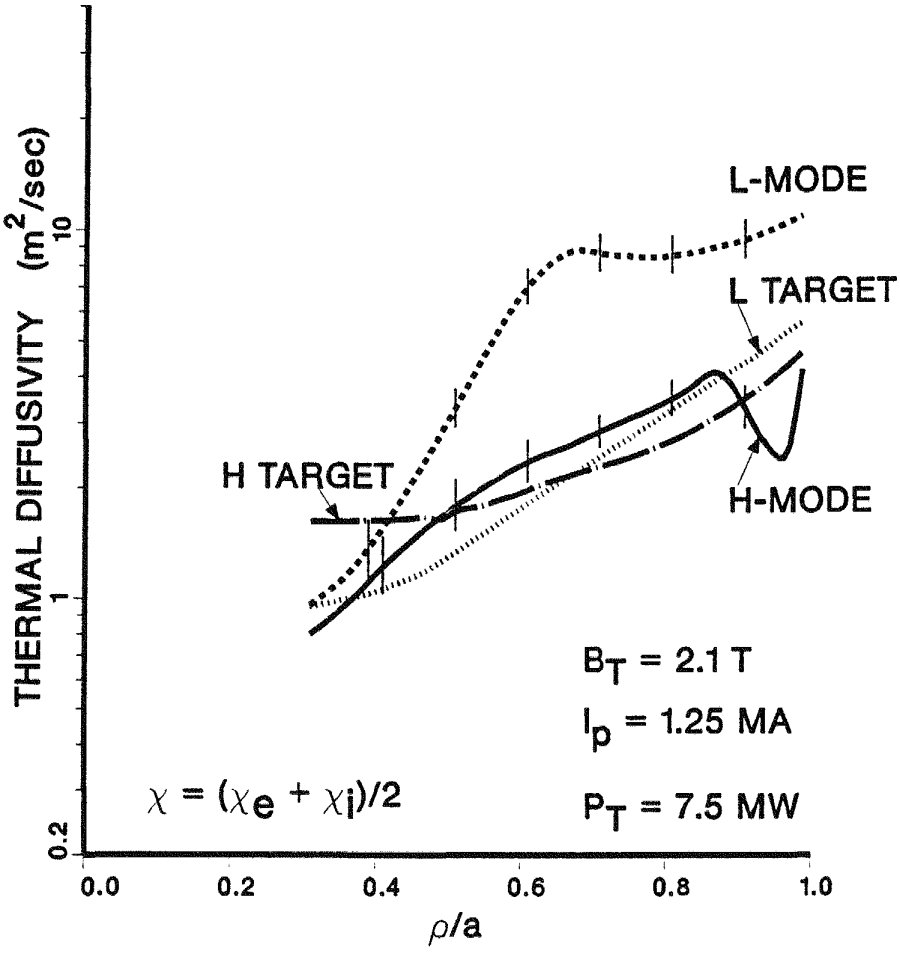

Fig. 2.2-6. One fluid thermal diffusivity (average of χ_e and χ_i) versus flux coordinate for ohmic plasmas (L target and H target) and for L and H discharges with the same parameters.

2.2.3. REFERENCES FOR SUBSECTION 2.2

[1] Schissel, D.P., *et al.*, "Energy Confinement Properties of H–mode discharges in the DIII–D Tokamak," General Atomics Report No. GA-A19243, February 1988, to be published in *Nuclear Fusion* in February 1989.

[2] Burrell, K.K., *et al.*, "Energy Confinement in Auxiliary-Heated Divertor and Limiter Discharges in the DIII–D Tokamak," General Atomic Report No. GA-A19443, October 1988, to be published in *Proc. of Twelfth International Conference on Plasma Physics and Controlled Nuclear Fusion Research*, Nice, France, 1988.

[3] Kellman, A., *et al.*, "Confinement Studies in Low q, H–mode Discharges," *Bull. Am. Phys. Soc.* **33**, 1964 (1988).

[4] DeBoo, J.C., *et al.*, "Energy Confinement Studies in the DIII–D Tokamak," *Bull. Am. Phys. Soc.* **33**, 1915 (1988).

[5] Shimomura, Y., *et al.*, "Empirical Scaling of Energy Confinement Time of L–mode and Optimized Mode and Some Consideration of Reactor Core Plasma in Tokamak," *JAERI-M* **87-080**, May 1987.

[6] Osborne, T., *et al.*, "H–mode With Ohmic Heating Alone in DIII–D," *Bull. Am. Phys. Soc.* **33**, 1915 (1988).

[7] Jackson, G.L., *et al.*, "Enhanced Confinement in DIII–D Beam-Heated Limited Discharges," *Bull. Am. Phys. Soc.* **33**, 1963 (1988).

[8] Carlstrom, T.N., *et al.*, "H–mode Transition Studies in DIII–D," *Bull. Am. Phys. Soc.* **33**, 1964 (1988).

[9] Itoh, S.I., and Itoh, K., "Model of L–mode to H–mode Transition in Tokamak," *Phys. Rev. Lett.* **60**, 2276 (1988).

[10] Schissel, D.P., *et al.*, "Results of Counter-Neutral Beam Injection on the DIII–D Tokamak," General Atomics Report No. GA-A19503, December 1988, submitted to *Phys. Fluids B.*

[11] Ferron, J.R., *et al.*, "High β Discharges in DIII–D Double Null Divertor Equilibria," *Bull. Am. Phys. Soc.* **33**, 1960 (1988).

[12] Kaye, S.M., and Goldston, R.J., "Global Energy Confinement Scaling for Neutral-Beam-Heated Tokamaks," *Nuclear Fusion* **25**, 65 (1985).

[13] DeBoo J.C., *et al.*, "Doublet III Operating Regimes With Improved Energy Confinement," *Nuclear Fusion* **26**, 211 (1986).

[14] Groebner, R.J., *et al.*, "Experimentally Measured Ion-Thermal Conductivity Profiles in the Doublet III Tokamak: Comparison With Neoclassical Theory," *Nuclear Fusion* **26**, 543 (1986).

[15] Ohyabu, N., *et al.*, "Model for Divertor Function in H–mode Onset and Proposal For H–mode Operation With the Island Divertor," *Journal of Nuclear Materials* **145** to **147**, 844 (1987).

[16] Ohyabu, N., *et al.*, "Correlation of Magnetic Fluctuations and Edge Transport in the Doublet III Tokamak," *Phys. Rev. Lett.* **58**, 120 (1987).

[17] Shimada, M., *et al.*, "Limiter Biasing Experiments in DIII–D," *Bull. Am. Phys. Soc.* **31**, 1503 (1986).

[18] Luxon, J., *et al.*, "Initial Results from the DIII–D Tokamak," in Plasma Physics and Controlled Nuclear Fusion Research 1986 (*Proc. 11th Int. Conf., Kyoto, 1986*), Vol. 1, IAEA, Vienna, 159 (1987).

[19] Burrell, K.H.,*et al.*, "Observation of an Improved Energy Confinement Regime in Neutral-Beam-Heated Divertor Discharges in the DIII–D Tokamak," *Phys. Rev. Lett.* **59**, 1432 (1987).

[20] Gohil, P., *et al.*, "Study of Giant Edge-Localized Models in DIII–D and Comparison With Ballooning Theory," *Phys. Rev. Lett.* **61**, 1603 (1988).

[21] Jahns, G.L., *et al.*, "Comparison of Transport in H– and L–Phase Discharges," General Atomics Report No. GA-A19376, December 1988, submitted to *Nuclear Fusion.*

2.3. BETA AND STABILITY

2.3.1. INTRODUCTION

The feasibility (from the viewpoint of physics, engineering, and economics) of reaching ignition in a tokamak reactor depends on the ability to operate reproducibly and reliably at high volume averaged toroidal beta, β_T, with good confinement. A good figure of merit for the effective utilization of the toroidal field is $\beta_T \times \tau_E$, since ignition is obtained when $\gamma \times \frac{B_T^2}{2\mu_0} \times \beta_T \tau_E = 1$. B_T is the vacuum toroidal field, τ_E is the global energy replacement time, and the coefficient γ contains the reactivity of D–T and profile

effects, $\gamma^{-1} \approx 8$ atm-sec. Our experimental efforts this year have been concentrated in obtaining quiescent high beta discharges, more reproducibly and reliably and with good confinement. We have emphasized evaluating the limiting beta and in understanding the mechanisms responsible for the beta limit.

2.3.2. BETA LIMIT SCALING

The maximum achievable beta in DIII–D scales linearly with normalized current, $I_N = I/aB$ (MA/mT), consistent with many theoretical scaling studies based on ideal MHD instabilities, and is well described by:

$$\beta_T(\%) \leq 3.5\ I/aB\ (\mathrm{MA/mT}) \quad . \tag{2-1}$$

This scaling has been confirmed in neutral beam heated single null divertor H–mode discharges over the range of normalized current from $0.6 < I_N < 1.8$, or equivalently $9 > q_{95} > 3$, as is shown in Fig. 2.3-1. This same linear dependence of the beta limit on normalized current, with the same coefficient of 3.5 $\frac{\%}{\mathrm{MA/m/T}}$, was found in Doublet III for both limiter and divertor discharges. As normalized beta, $\beta_N = \beta_T/I_N$ %/(MA/m/T), increases toward the limit of 3.5 shown in Fig. 2.3-1, a discharge may evolve in one of three ways: 1) stable operation at high beta, 2) sudden disruption, or 3) saturation (sometimes followed by a slow but complete collapse of beta).

2.3.3. STABLE HIGH BETA OPERATION

Stable high beta discharges have been obtained both in single null divertor and double null divertor discharges. Beta $\geq 6\%$ has been obtained in single null discharges with I_N from 1.7 to 2.5 MA/m/T. $\beta_T = 5\%$ has been obtained in double null discharges. The highest values of β_T, obtained at high normalized current, $I_N > 2$, are below the anticipated beta limit of $\beta_T = 3.5\ I_N$ as seen in Fig. 2.3-1, and they show no signs of beta-related loss of confinement.

The maximum beta achieved to date is 6.8%, in a single null divertor discharge, where $\beta > 6\%$ was sustained for 0.8 sec, or almost 20 energy replacement times, as shown in Fig. 2.3-2. This was an H–mode discharge, the equilibrium and flux contours and important discharge parameters are shown in Fig. 2.3-3(a). Also shown, in Fig. 2.3-3(b), is the equilibrium flux contours and important discharge parameters of the highest beta discharge in the double null configuration. These were initial high beta experiments in the double null configuration, and with more careful cleaning and conditioning of the area of

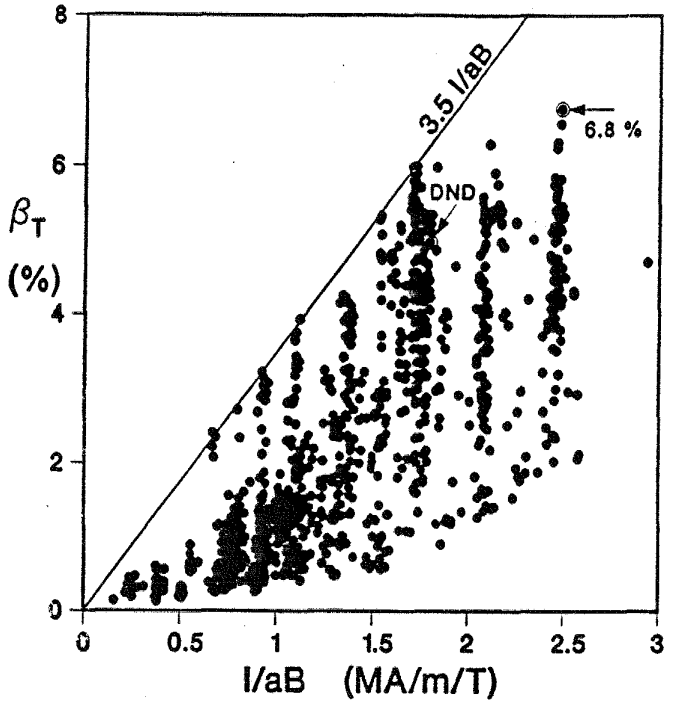

Fig. 2.3-1. Operating regime of DIII–D divertor discharges. The highest beta achieved to date in single null divertor (6.8%) and double null divertors (DND) are noted.

the vessel with high plasma interaction, we anticipate obtaining double null discharges up to $\beta_T \approx 3.5\ I/aB$.

Under the proper conditions, it is possible for a discharge to run stably very close to the operation limit. In one such discharge, $\beta_T \geq 3\ I/aB$ was sustained for more than 1 sec, as shown in Fig. 2.3-4. Under nearly identical conditions, discharges may experience saturation or sudden disruption.

2.3.4. MHD BEHAVIOR NEAR THE BETA LIMIT

Discharges that approach the beta limit in DIII–D exhibit one of three distinct types of behavior: 1) quiescent operation, 2) sudden disruption, and 3) beta saturation and collapse. These distinctively different types of behavior are often observed in otherwise very similar discharges as is shown in Fig. 2.3-4. The three discharges shown were from a series of repeated discharges, having identical shape, plasma current, and q_{95}, and with the wall conditions as identical as possible. One of these discharges was stable near the beta limit with $\beta_T > 3\ I/aB$ for 1 sec and reached a maximum normalized beta of 3.5 during that time. A second discharge, with no changes in discharge programming from the first, also reached a maximum normalized beta of 3.5 but ended with a sudden disruption

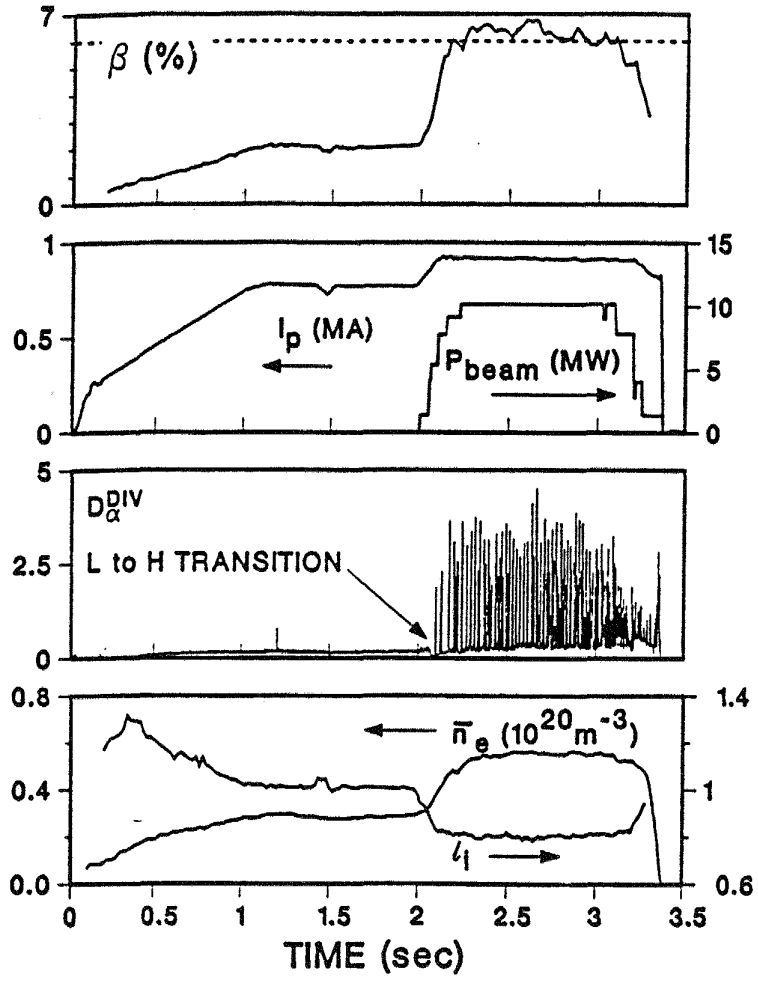

Fig. 2.3-2. Time traces for maximum beta discharge (58922).

at 3.37 sec. A third discharge, similar to the previous two with the exception of a small increase in the electron density prior to the neutral power injection, shows a decrease in beta beginning at 2.75 sec, and the discharge continues at a lower saturated level of beta.

Sudden disruptions, associated with the rapid growth of an $n = 1$ perturbation, are the ultimate limit to beta in DIII–D. Disruption at high β_N is accompanied by the rapid growth (typically 20 to 200 μsec or 10 to 100 poloidal Alfvèn times) of a non rotating mode with toroidal mode number $n = 1$ [Fig. 2.3-4(b)]. The growth of this mode follows a sawtooth crash and an edge localized mode, ELM, suggesting that the changes in pressure and current density profiles resulting from the sawtooth crash trigger the $n = 1$ external kink.

β = 6.8%
I_P = 0.92 MA
B = 0.59 T
a = 0.63 m
κ = 2.0
q_{95} = 2.3
I_N = 2.5 MA/m/T
β_N = 2.7%-T-m/MA
P_{BEAM} = 9 MW ($H^0 \rightarrow D^+$)
1 MW ($D^0 \rightarrow D^+$)
$\bar{n}_e$ = 0.56 × 10^{20}/m^3
$T_e(0)$ = 1.0 keV
$T_i(0)$ = 0.8 keV

(a)

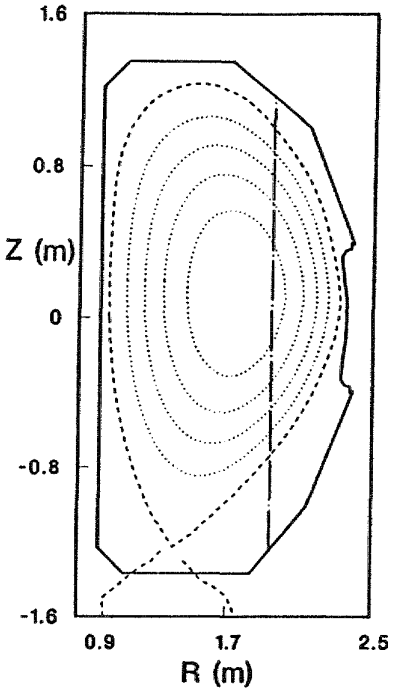

β = 5.0%
I_P = 0.88 MA
B = 0.8 T
a = 0.62 m
κ = 2.1
q_{95} = 3.6
I_N = 1.8 MA/m/T
β_N = 2.8%-T-m/MA
P_{BEAM} = 9.6 MW ($H^0 \rightarrow D^+$)
$\bar{n}_e$ = 0.63 × 10^{20}/m^3
$T_e(0)$ = 1.4 keV
$T_i(0)$ = 1.4 keV

(b)

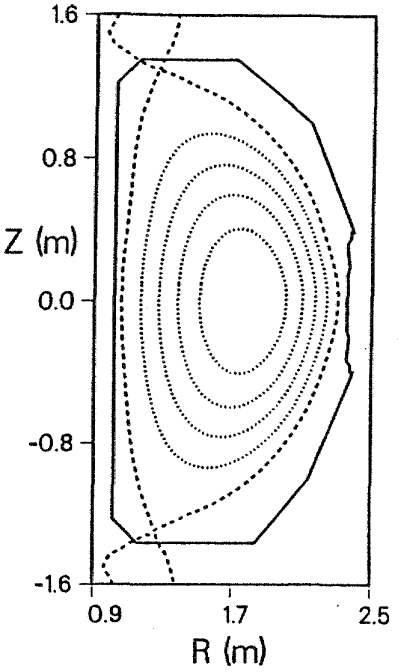

Fig. 2.3-3. Equilibrium flux plots for high beta discharges. (a) 6.8% single null divertor, (b) 5.0% double null divertor.

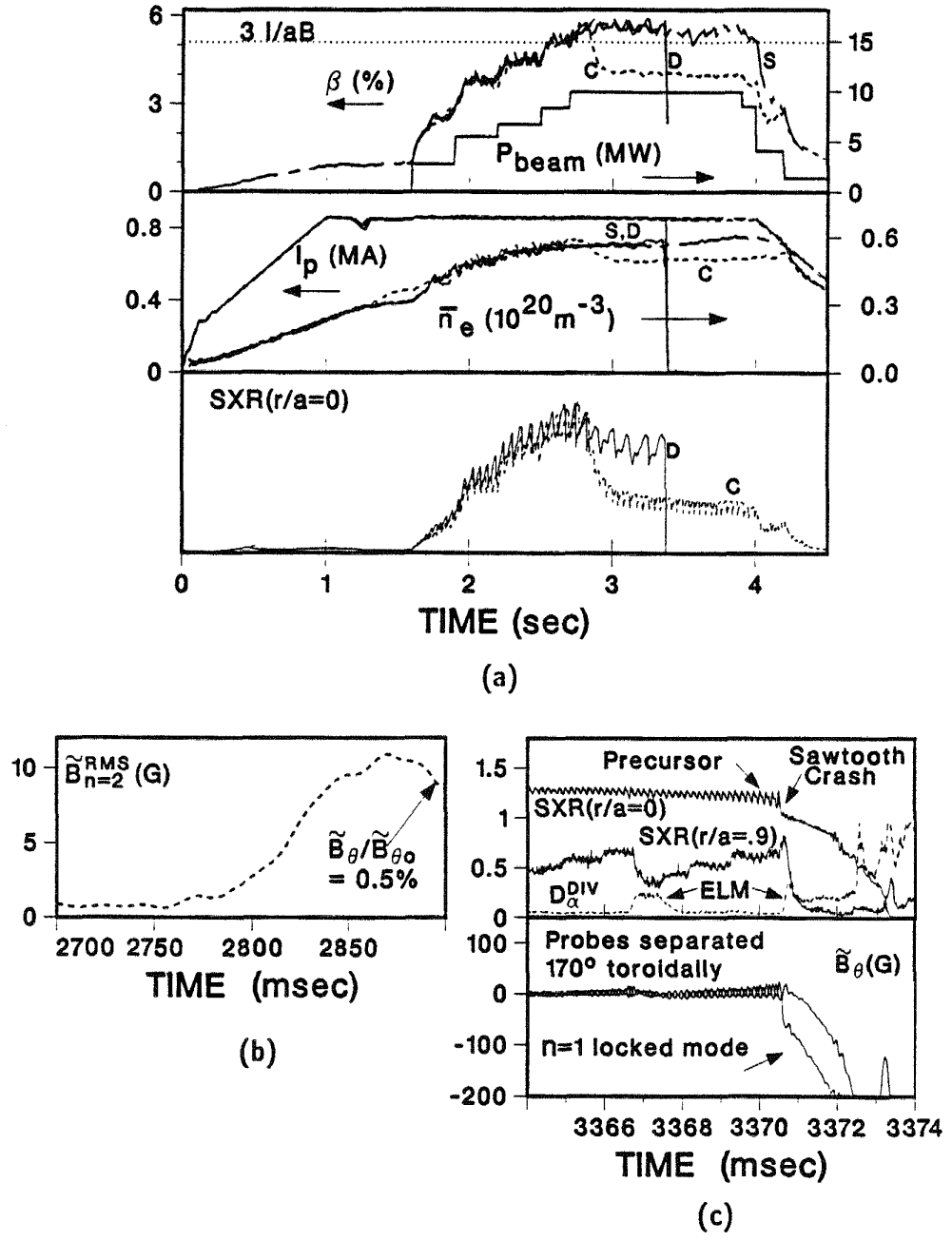

Fig. 2.3-4. (a) Traces of a series of nearly identical discharges; chain-dashed traces (S), discharge runs stably at high beta; solid traces (D) discharge disrupts; dashed traces (C), discharge saturates at lower β value; (b) expanded trace of rms level of $n = 2$ magnetic fluctuations for the discharge that exhibits saturation; (c) expanded traces of discharge that disrupts.

Beta saturation and/or collapse associated with MHD modes of low toroidal mode number, $n = 1, 2, 3, 4$, is the most frequently observed behavior near the beta limit in DIII–D, and prevents these discharges from reaching the ideal kink mode limit. The growth time of these modes is typically 10 to 100 msec, or $\approx 10^4$ to 10^5 poloidal Alfvèn times [Fig. 2.3-4(c)]. These modes often saturate at some moderate level ($\tilde{B}_\theta / B_{\theta 0} \leq 0.5\%$) and the discharge continues with degraded energy confinement time as shown in Fig. 2.3-4. At moderate q, $2.5 \leq q \leq 5$, the modes do not saturate but lead to a complete collapse, the collapse being a direct consequence of a large $n = 1$ mode ($\tilde{B}_\theta / B_{\theta 0} \geq 1\%$).

These low n continuous modes are believed to be resistive pressure driven modes. Equilibria using experimentally measured pressure profiles have all been calculated to be stable against ideal modes $n = 4$, 3, and 2, with no wall stabilization. Resistive stability calculations have been completed with the code CART-II. As beta is increased, the modes $n = 1$, 2, 3, and 4 are calculated to be unstable, and the prevalent mode is of the resistive ballooning type with a linear growth rate dependence on resistivity and toroidal mode number of $\gamma \propto \eta^{1/3} n^{2/3}$.

2.3.5. IDEAL STABILITY

Stability against ideal infinite n ballooning modes and low n ideal kink modes for high β H–mode DIII–D equilibria has been evaluated in detail. The plasma is stable to the ideal ballooning modes over the major portion of the plasma volume. The profiles of the pressure gradient for a sequence of discharges at increasingly larger values of beta are shown in Fig. 2.3-5 for a single null divertor discharge with $q_{95} = 3.1$. The pressure profile is from the measured electron and ion temperatures, the measured electron density, the measured Bremstrahlung (for ion defect), and the calculated beam pressure, and the equilibria pressure and current profiles are reconstructed self-consistently from the measured magnetic data and kinetic profile data. The pressure gradient marginally stable to ballooning modes, calculated following the procedure outlined by Greene and Chance (1981) in the code MBC, is also shown in Fig. 2.3-5. Even at the highest beta values, the pressure gradient is below that marginally stable to ballooning modes over the region $0.4 \leq \sqrt{V_N} \leq 0.95$.

As beta is increased, the pressure gradient approaches that marginally stable to ballooning modes in the central region of the the plasma. Near the plasma boundary, the pressure gradient approaches the first marginal ballooning stability limit, particularly just preceding the occurrence of an edge localized mode (ELM). Even in low β H–mode discharges, the pressure gradient just before an ELM approaches the marginal ballooning

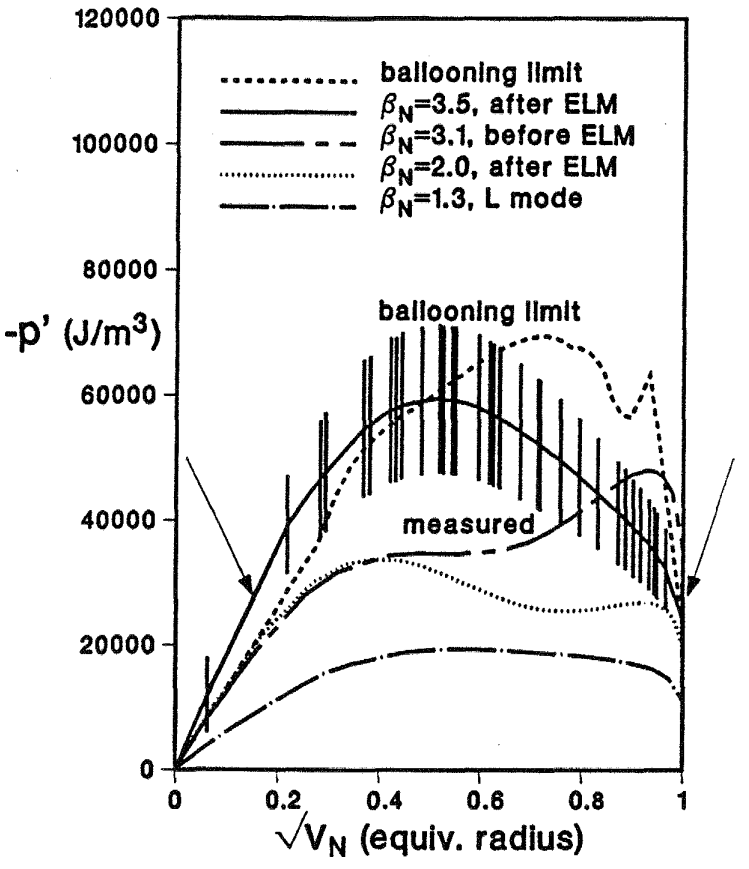

Fig. 2.3-5. Ballooning mode stability: The marginal limit is calculated for the equilibria at $\beta_N = 3.5$. The arrows indicate the regions where ballooning mode stability likely limits the pressure gradient.

limit, as shown in Fig 2.3-6. This observation suggests that the ballooning modes limit locally the pressure gradient in the edge region and may be responsible for the appearance of giant ELMs. Although we believe that ballooning modes do not limit the overall volume average beta achievable, they likely limit the pressure gradient in the center of the discharge and near the edge, constraining the allowed pressure profiles as beta is increased.

Stability against ideal modes was calculated with the code GATO using equilibria reconstructed using external magnetic measurements and the pressure profile. The reconstructed pressure profile near the peak in a sawtooth cycle is shown as the solid curve in Fig. 2.3-7(a). For this case stability to the $n = 1$ kink is found with only weak wall stabilization, $r_{\text{wall}}/a = 2.2$. The actual location of the resistive vessel for DIII–D single null divertor plasmas is $r_{\text{wall}}/a = 1.3$–1.5. This suggests that the discharge should be stable against the $n = 1$ kink, but the DIII–D vessel has many large ports, and the "effective" wall location for stability might be somewhat larger.

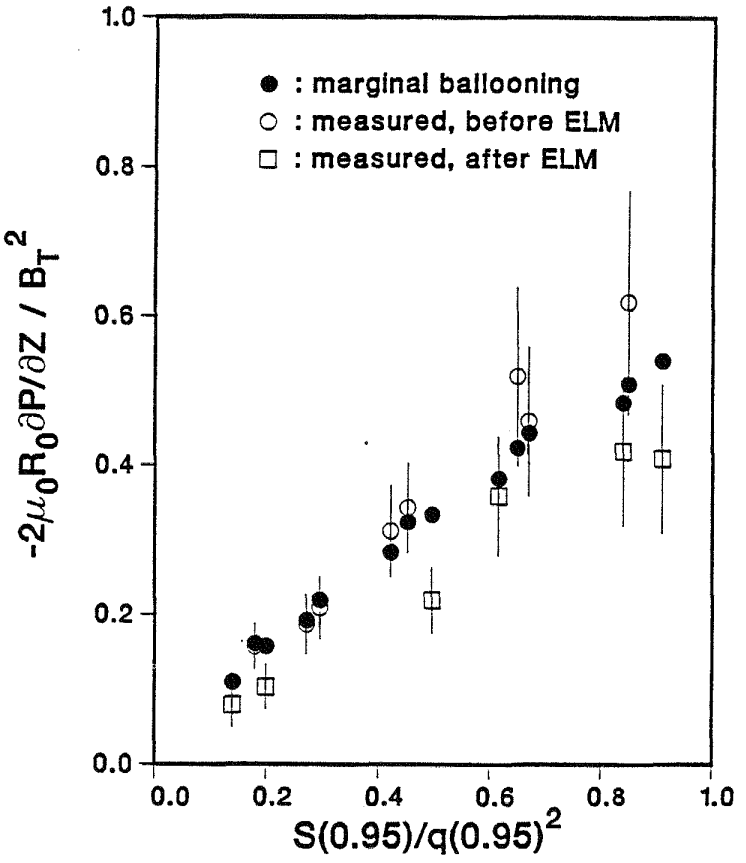

Fig. 2.3-6. Comparison of normalized edge pressure gradients before and after a giant ELM to the computed first marginal ballooning stability limits.

The influence of the sawtooth on the kink mode stability was modeled by generating equilibria with the same discharge cross section, the same plasma current and q, and total pressure (β_T) as the measured case, but with pressure and current profiles consistent with those following a sawtooth crash and the occurrence of an ELM. The pressure on axis was decreased by approximately 20% based on SXR emission data. The pressure gradient at the plasma boundary was decreased by a factor of four, consistent with previous observation on the effect of an ELM. The resultant pressure profile is shown as the dashed curve in Fig. 2.3-7(a). The current profile was slightly broadened consistent with a sawtooth crash resulting in a 30% decrease in the shear near the $q = 2$ surface. This new equilibrium is more unstable to the $n = 1$ ideal kink, as is shown in Fig. 2.3-7(b). For moderate wall stabilization ($r_{wall}/a \approx 1.7$) the profile changes caused by the sawtooth plus ELM can reduce the calculated kink mode beta limit to the observed value of $\beta_N = 3.5$.

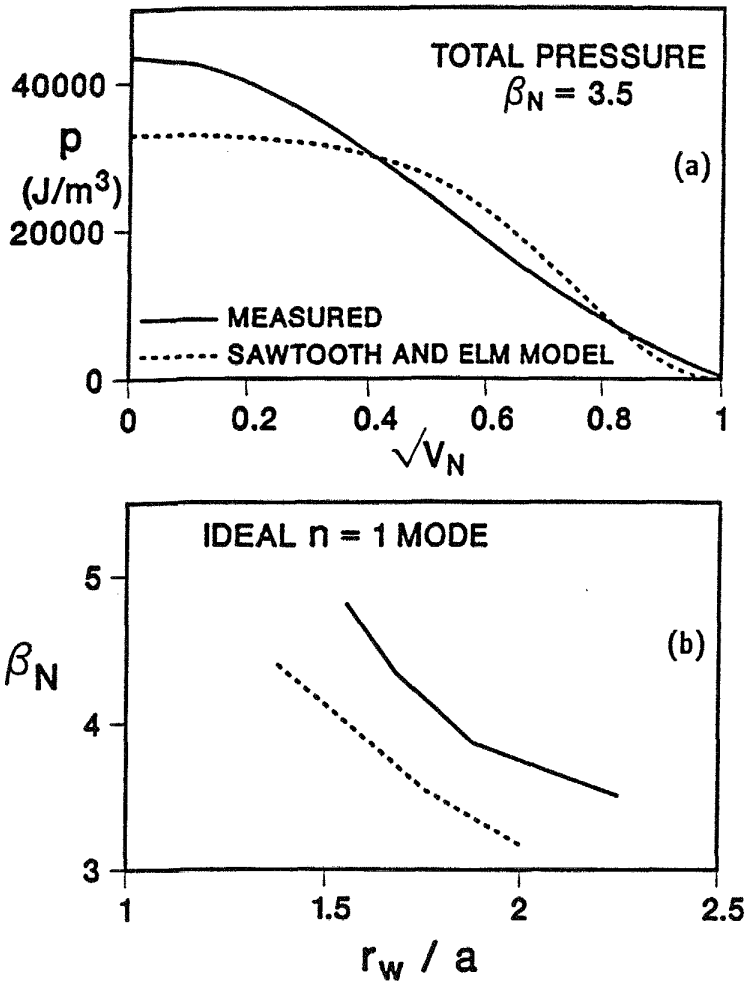

Fig. 2.3-7. (a) Pressure profiles for stability analysis; and (b) stability boundary for the $n = 1$ ideal kink, instability is above and to the right of the curves.

2.3.6. VERTICAL STABILITY AND HIGH ELONGATION DISCHARGES

The maximum achievable beta scales with normalized current, I_N, and the normalized current is given in terms of the safety factor, q, the elongation, κ, and the aspect ratio, A, $A = R/a$, by

$$I_N \approx \frac{1}{Aq} \times \frac{1+\kappa^2}{2} \tag{2-2}$$

It is clear that at a given safety factor, normalized current increases strongly with elongation, and we expect that the limiting beta value would similarly increase. Theoretically, from considerations of both ballooning stability and ideal kink stability, favorable effects of elongation on the beta limit begin to fail at elongations between 2 and 3. In preparation for high beta experiments at high elongation planned for 1989 and 1990, we began

evaluating the control and stability of discharges with $\kappa > 2$ This work was carried out in collaboration with scientists from Oak Ridge National Laboratories, and the Center for Plasma Physics Research, Lausanne Switzerland.

Vertical stability was modeled representing the plasma as a single massless filament. The induced vessel currents were decomposed into orthogonal modes of which it is easily shown that the first antisymmetric mode dominates. The addition of one pair of active poloidal field coils leads to a low order dynamical system model, 2^{nd} order. Several salient features of a vertical control system are readily obtained with this model:

1. The largest vertical field index with which a plasma can be safely operated depends critically on the choice of coil pairs. This coil pair is a set on the inboard side of the plasma.

2. There is a critical index in the problem, associated with the active coil. For n more negative than this value there are no stable solutions without derivative gain.

3. The voltage requirement for the active coil set scales approximately as $V = V_o \delta z I_p e^{-n/n_c}$

4. The voltage requirement for the active coil, V_o, depends strongly on the location of the coil, more than an order of magnitude for the different coil sets on DIII–D.

Initial experiments were carried out on DIII–D that verify that the plasma response is consistent with this simple model. Plasma elongation up to $\kappa = 2.5$ have been obtained, see Fig. 2.3-8.

2.3.7. HELIUM GLOW WALL CONDITIONING

Helium Glow Wall Conditioning (HeGWC) has become the primary technique for cleaning and conditioning the DIII–D plasma facing surfaces. In January 1988, we increased the graphite coverage of the machine from approximately 9% of the vessel surface area to 40%. Following the addition of this graphite, previously successful discharge cleaning and wall conditioning techniques failed to give reproducible high quality discharges. Only after beginning HeGWC, were H–mode discharges again reproducibly obtained. HeGWC successfully removes low z impurities, primarily as CO, and reduces fueling from the wall by desorbing hydrogenic species from the graphite surfaces. Since HeGWC has become routine, baking of the vacuum vessel and low temperature pulsed discharge cleaning (Taylor discharge cleaning) are necessary only after venting the vessel

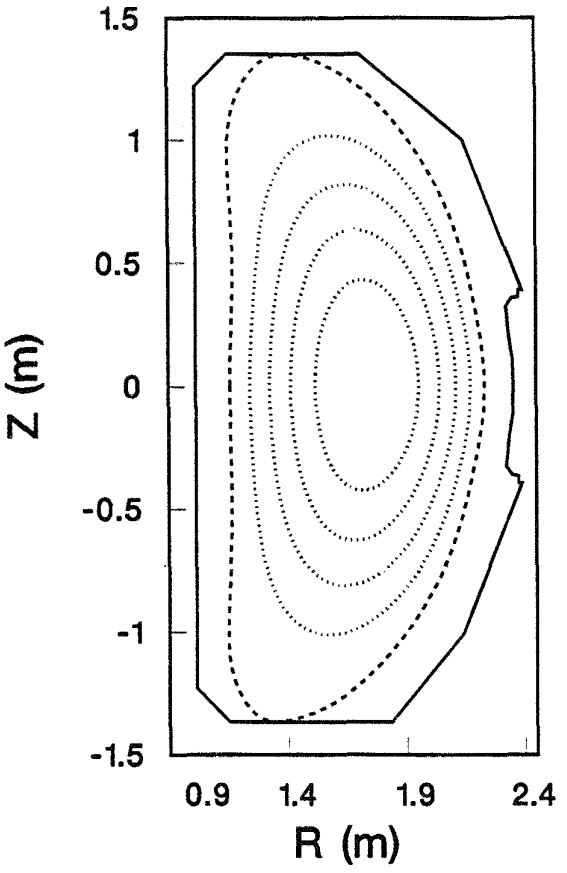

Fig. 2.3-8. Equilibrium cross section for high elongation discharge, $\kappa = 2.5$, triangularity, $\delta = 0.6$, internal inductance, $\ell_i = 0.94$.

or when a complete changeover from hydrogen to deuterium (or deuterium to hydrogen)is required. In addition, by applying HeGWC before every tokamak discharge, high quality plasma discharges are obtained much more reproducibly and reliably. Specifically, HeGWC has allowed faster and reliable recovery from disruptions, and has been indispensible in low q, high beta, and high current operation. We also believe that HeGWC has played a major role in the achievement of Ohmic H–mode and Limiter H–mode.

2.3.8. SUMMARY FY84 TO FY87

During FY84, the last year of operation of Doublet III, high beta was a major emphasis of the experimental program. The beta value of 4.5% which had been established in 1982, a world tokamak record at the time, was again reached on several occasions. However, despite numerous attempts it was never exceeded in Doublet III. Very near the end of Doublet III's experimental life, this came to be understood in terms of the simple

"Troyon" scaling law for the beta limit in a tokamak: $\beta(\%) = C\ I/aB$ (MA, m, T). This scaling was derived in several theoretical studies of stability against ideal $n = 1$ kink mode or ideal high-n ballooning modes, where the value of the coefficient C varied somewhat depending on the instability and on the parameterization used for profiles. Doublet III data with I/aB varying from 0.5 to 1.4 were found to fit this scaling law well with a value of $C = 3.5$, in the middle of the range of theoretical predictions [1]. The maximum beta of 4.5% is now understood to be consistent with this scaling at the maximum value of I/aB achievable in Doublet III. As noted above in Eq. 2-2, the maximum value of I/aB is limited by the discharge shape (determined primarily by the geometry of the vacuum vessel and coils) and by the minimum achievable value of q (in general a hard limit of $q \gtrsim 2$ due to kink instabilities). DIII–D, with its larger ϵ (0.4 versus 0.3 for Doublet III) and larger κ (2.0 or greater versus 1.6 for Doublet III) was expected to be capable of much higher beta values. An important feature of the Doublet III results was to establish the universality of this scaling, independent of discharge shape or topology (Fig. 2.3-9). The beta limit of 3.5 I/aB was found to be valid for all Doublet III discharges, including limiter, single null divertor, and double null divertor configurations, and with elongations varying from 1.0 to 1.6.

An effort to understand the physics of the beta limit continued during the construction of DIII–D in FY85. Extensive data analysis and stability calculations were carried out for the Doublet III high beta discharges. In contrast to the DIII–D results described above, it was found that virtually all discharges with sufficient heating power to reach or exceed the limiting beta value (3.5 I/aB) ended in a disruption [2]. Although discharges may disrupt at any value of β, the probability of disruption increased rapidly as $\beta_N = \beta/(I/aB)$ approached 3.5, and became 100% at $\beta_N \approx 3.6$. Fishbone oscillations and MHD modes with $n = 3$ and 4, similar to those observed in DIII–D, were seen in some high beta discharges, but they did not appear to play a role in the beta limit. The large amplitude $n = 2$ mode which causes beta saturation in some DIII–D discharges was not seen in Doublet III. Stability calculations showed that Doublet III discharges with $q < 3$ had reached marginal stability for high-n ballooning modes at most in the central 30 to 40% of the profile, while discharges with $q > 3$ may have reached marginal ballooning stability over a somewhat larger part of the profile [3]. However, as in DIII–D no gradual deterioration of confinement was observed (Fig. 2.3-10). Instead, the disruptions were sudden, usually occurring a few milliseconds after a sawtooth fall and perhaps showing some degradation of confinement during those last few milliseconds. The immediate precursor to the disruption was always a non-rotating mode with toroidal mode number n=1 and

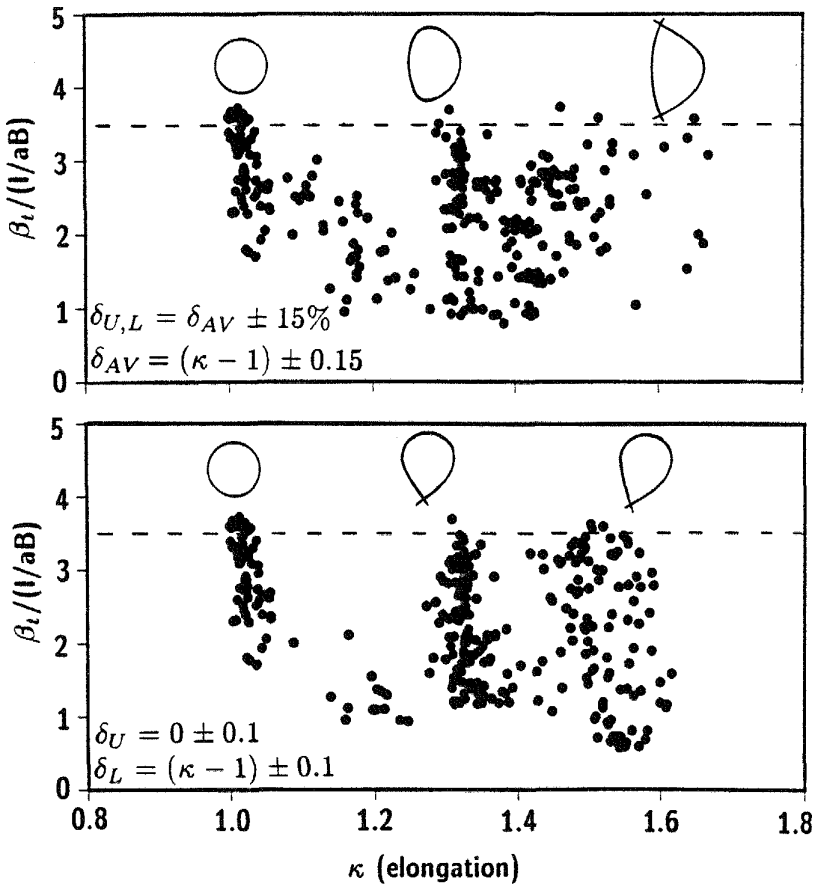

Fig. 2.3-9. Beta normalized by I/aB vs discharge shape for Doublet III. The maximum normalized beta is constant as elongation and triangularity are varied together; (a) up-down symmetric discharges varying from circular to dee-shaped limiter discharges to double-null divertor discharges; (b) asymmetric discharges varying from circular limiter discharges to highly elongated and triangular single-null divertor discharges.

poloidal mode number $m = 2$. However, with a realistic amount of wall stabilization the ideal $n = 1$ kink mode was calculated to be stable for all of these discharges.

These and other observations led to a picture for the beta limit [4] which differs only in some details from that described above for beta collapse in DIII–D. The high-n ballooning modes do not play a direct role but may influence the pressure and current distributions at high beta, causing the evolution toward broader profile shapes which is observed at high β_N in both Doublet III and DIII–D. A sawtooth fall provides a sudden final broadening, triggering the $n = 1$ instability which causes the disruption. This instability is probably a pressure-driven resistive mode, a hypothesis suggested by its relatively slow growth rate

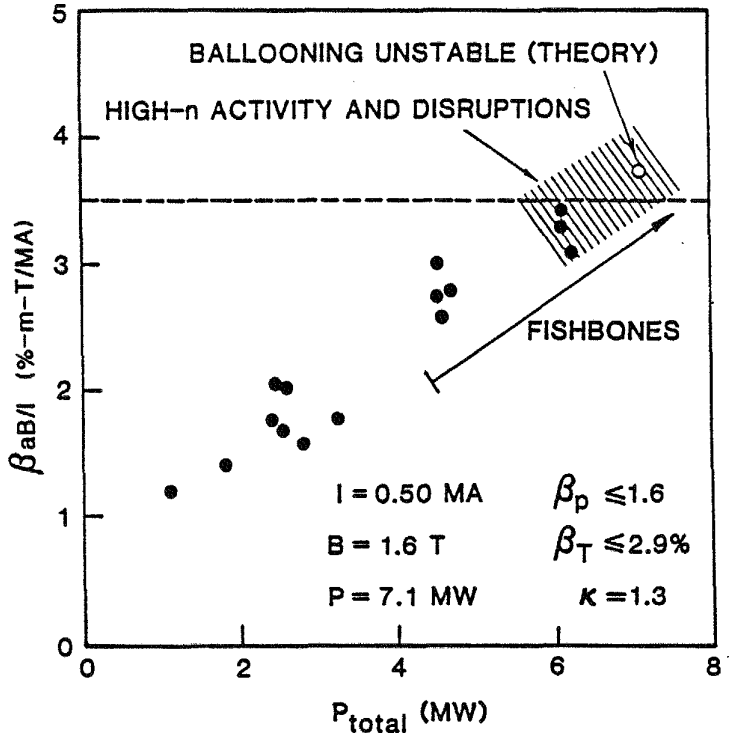

Fig. 2.3-10. Beta normalized by I/aB for a series of repeated Doublet III discharges. Several types of MHD activity are observed as beta increases, but there is no saturation of beta before the disruptive limit is reached.

and supported by good agreement between the observed mode structure and resistive MHD stability calculations [2].

Another major activity during FY85 was the design, installation, and calibration of new magnetic diagnostics and plasma control hardware for DIII–D, including nearly 200 magnetic pickup loops. These signals are used for realtime control of discharge shape and position, post-shot equilibrium calculations, and in some cases also for analysis of magnetic fluctuations. The Doublet III integrators were upgraded for the new machine, with the addition of auto-nulling circuits (required by the longer shot durations) and remotely programmable gains. A flexible analog computation system was designed and built for discharge control.

Soon after the first plasma was produced early in 1986, the capabilities of the new machine were demonstrated with the achievement of stable discharges having elongations up to 2.1 and plasma currents up to 2.5 MA. As a data base of experimental as well as theoretical equilibria was built up, more sophisticated plasma controls were developed, leading to precise and programmable control not only of the vertical and radial position of

the discharge, but also of such quantities as the vertical position of the divertor x-point, and the distances between the divertor separatrix and the various limiting surfaces in the vacuum vessel.

In FY87, after the cleaning effect of several months of plasma operation and with the availability of the full 10 to 12 MW of hydrogen neutral beam heating, the range of operating parameters of DIII–D expanded dramatically. Initial high beta experiments were begun. In addition, stable low-q operation was demonstrated, with q_{95} (safety factor at 95% of the enclosed poloidal flux) as low as 2.1 in limiter discharges and 1.9 in divertor discharges. Due to the larger inverse aspect ratio and elongation, this represents an increase of more than a factor of 2 in I/aB compared to Doublet III. Even lower values of q_{95} were obtained transiently. Some doubts had existed about the stability of the $n = 1$ kink mode in elongated discharges at q below 3, particularly in a divertor configuration, based both on theoretical calculations and on Doublet III results. DIII–D's low q results, and the ease with which they were obtained, were sufficient to dispel any such doubts.

An important aid to the operation of stable plasmas was the understanding gained during 1987 of "locked" (non-rotating) MHD modes. Non-rotating modes require detection techniques which are different from those for rotating modes; in our case (as on JET) the saddle loops on the outer surface of the vacuum vessel have proved most useful. A locked mode may occur when a rotating mode, generally with toroidal mode number $n = 1$, becomes stationary, but more often the mode grows at a locked amplitude. The locked mode may exist in a saturated state, causing degraded confinement, or it may eventually grow and lead to a disruption. Locked modes, believed to be tearing modes, can appear any time the discharge is not properly tuned, but are particularly troublesome when operating at extreme parameter values such as high current (low q) or very high or very low density. The precise cause of these modes, and the possibility of active control, are still areas of continuing investigation. However, the development of detection methods and some simple rules of thumb for avoiding locked modes has greatly increased the reliability of stable operation.

2.3.8.1. References for Subsection 2.3.8

[1] Stambaugh, R.D., R.W. Moore, L.C. Bernard, A.G. Kellman, E.J. Strait, *et al.*, in *Proc. 10th Int. Conference, Plasma Physica and Controlled Nuclear Fusion Research*, London, 1984, Vol. I, IAEA, Vienna (1985), 217.

[2] Strait, E.J., M.S. Chu, G.L. Jahns, J.S. Kim, A.G. Kellman, *et al.*, *Proc. 13th Int. Conference, Controlled Fusion and Plasma Heating*, Schliersee, 1986, Europhysics Conference Abstracts, Vol. 10C, Part I, 204.

[3] Chu, M.S., L. Lao, R.W. Moore, H. St.John, R.D. Stambaugh, E.J. Strait, and T.S. Taylor, *Nucl. Fusion* **27**, 735 (1987).

[4] Chu, M.S., J.M. Greene, J.S. Kim, L. Lao, R.T. Snider, R.D. Stambaugh, E.J. Strait, and T.S. Taylor, *Nucl. Fusion*, **28**, 399 (1988).

2.4. BOUNDARY PHYSICS

Our understanding of the physics of plasma boundary and its relation to global features of the plasma, such as H–mode, has been enhanced significantly in the last five years of operations on DIII/DIII–D. Progress in this field is described in sections on vessel conditioning, impurity and radiation studies, divertor physics, ELM behavior and long pulse H–mode plasmas.

2.4.1. VESSEL CONDITIONING

Initial conditioning of the DIII–D vacuum vessel was performed with a combination of 400°C baking, Taylor pulsed discharge cleaning (TDC), and rf-assisted glow cleaning (GDC) [1]. The bare metal vessel was baked in November 1985 at successively higher temperatures until the design specification of 400°C on the walls and 150°C on the port flanges was reached. In February 1986 – after a two-month vent during which graphite armor, a graphite-clad limiter blade and a variety of in-vessel diagnostics were installed – the vessel was baked for 40 hours and then subjected to 20 hours of GDC and four hours of TDC. Plasma initiation with low voltage (10 V/turn) startup was successful on the first attempt.

The amount of outgassing measured with a residual gas analyzer during bakeout showed a declining trend with successive vents. After the installation of the graphite armor and graphite-clad primary limiter, outgassing (primarily of water vapor) increased all the way up to the maximum bakeout temperature of 400°C before rolling over and decreasing. During the remainder of 1986 the vessel was subsequently vented five more times for hardware installation and minor vacuum repairs. After the vent of November 1986 the partial pressure of water vapor already began to decline as the vessel temperature

passed 230°C. The rapid speed with which high current tokamak operation was achieved on DIII–D (2.5 MA by September 1986) underscores the importance of high temperature bakeout in shortening the initial cleaning period for a vessel and in particular one with large amounts of graphitic armor.

In the first year of DIII–D operations the vessel was routinely conditioned with bakeout, GDC and TDC on the evening preceding the day of tokamak operations. In recent times, the DIII–D vessel is conditioned with GDC alone in the evenings.

With the introduction of extensive amounts of graphite for the inner wall and top divertor in early 1988, DIII–D now retains large amounts of hydrogen and deuterium. The release of this gas during a plasma shot causes larger than normal density rises and recycling levels and suppresses H–mode. We have developed glow discharge wall conditioning between shots (typically lasting for 5 min) using helium gas to desorb the hydrogen from the graphite [2]. This technique has been shown to be effective and necessary in obtaining H–mode.

2.4.2. IMPURITY AND RADIATIVE STUDIES

Impurities in DIII–D are monitored with two extreme ultraviolet spectrometers. A 1 m grazing incidence spectrometer equipped with an intensified, multichannel detector array which can be moved along the Rowland circle covers a bandwidth of ~100Å in the range from 50 to 600Å. A SPRED-type spectrometer with two interchangeable gratings at 450 grooves/mm and 2100 grooves/mm provides a bandwidth of 100 to 1100Å or 100 to 300Å with resolution of 2Å or 0.4Å respectively. Other diagnostics which have contributed to our understanding of impurity behavior are a bolometer array with 21 spatial channels and a visible bremsstrahlung array with 16 channels.

Observations reveal that Ni and Cr are the dominant metallic impurities in DIII–D (Inconel vessel), while oxygen and carbon are the most important low-Z ones, with Ni being the most radiative and carbon the most abundant [3]. In DIII–D plasmas we have found that radiation generally does not pose a serious problem in the overall power balance, seldom exceeding 60% of input power during neutral beam injection.

For ohmic plasmas, more than 80% of the input power can generally be accounted for using the 21-channel bolometer and divertor IR camera [Fig. 2.4-1(a)(b)]. At higher densities, radiation is the dominant loss mechanism (typically ~70% of input power, with half of the radiation from the divertor). At lower densities, power flow to the divertor tiles and total radiated power are roughly equal. The radiation profiles in ohmic plasmas are

typically flat to somewhat hollow. Most of the impurity radiation is the result of carbon and nickel contamination. Oxygen levels are usually quite low, so that oxygen emission lines are visible only very early in the shot ("burnthrough").

For steady-state neutral-beam-heated discharges, between 50 and 80% of input power is usually accounted for using the bolometer and IR camera. During steady-state L–mode discharges, power loss is typically ~33% into radiation, ~30% to the divertor tiles, and <5% to the midplane limiters. The radiation profiles in these L–mode plasmas are usually flat to slightly peaked on-axis. Spectroscopic measurements indicate that while metallic impurities (mainly Ni) do not account for more than 50% of the radiative loss, the measured $Z_{\text{eff}} < 2$ is due largely to carbon. These impurities apparently do not accumulate during the L–mode phase, because the total power remains a constant fraction of the input power after the bulk plasma density and temperature have reached steady state.

The shape of the radiation profile changes dramatically after the plasma makes a transition from the L–mode to the H–mode. Under H–mode conditions, the total radiation in the bulk plasma rises monotonically, and the radiation profile becomes increasingly hollow. Shortly before the first giant ELM, total radiated power is typically 40 to 50% of the input power. Figures 2.4-2(a) and 2.4-2(b) show the changes in the overall power balance and the bulk plasma radiation profile at different stages of a neutral beam-heated discharge.

The influence of ELMs is crucial in controlling the increase of impurities in H–mode plasmas. ELMs modulate the brightness of various impurity emission lines, as well as the radiated power. Detailed spectroscopic analyses, however, have shown a clear trend emerging in the impurity behavior during H–mode discharges with giant ELMs [4,5]. This process is due to the fact that, as plasma current is increased, impurities become more concentrated near the plasma edge. Thus, when an ELM occurs, impurities concentrated nearer the plasma edge are more likely to be expelled from the plasma bulk, in contrast to the lower current cases for which impurities are peaked more toward the plasma center.

2.4.3. DIVERTOR PHYSICS

Investigations of DIII–D divertor plasmas have been enhanced by studies of divertor-related processes, such as characteristics of heat flow into the divertor and the nature of recycling in the divertor. The main diagnostic techniques used to study the divertor are an absolutely calibrated divertor IR camera; absolutely calibrated divertor H_α TV; neutral pressure gauges; H_α photodiodes; and divertor Langmuir probes (see Fig. 2.4-3). Modeling

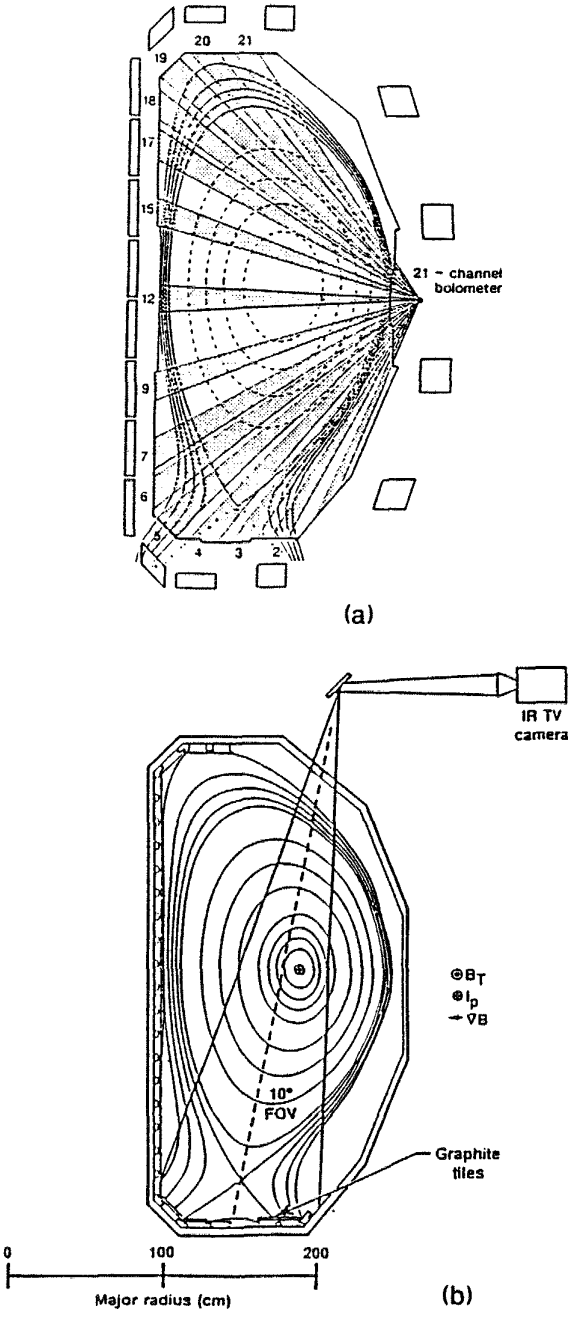

Fig. 2.4-1. (a) The poloidal cross-section of the 21-channel bolometer chord is superimposed on the cross-section of a typical single-null DIII–D divertor. The bolometer is sensitive to both particle and electromagnetic radiation (<10 keV); (b) The poloidal cross-section of the divertor IR camera is superimposed on a divertor cross-section. The camera is sensitive to 3-14 μm radiation. Heat flux to the divertor tiles is deduced from the surface temperature measurements made with the IR camera.

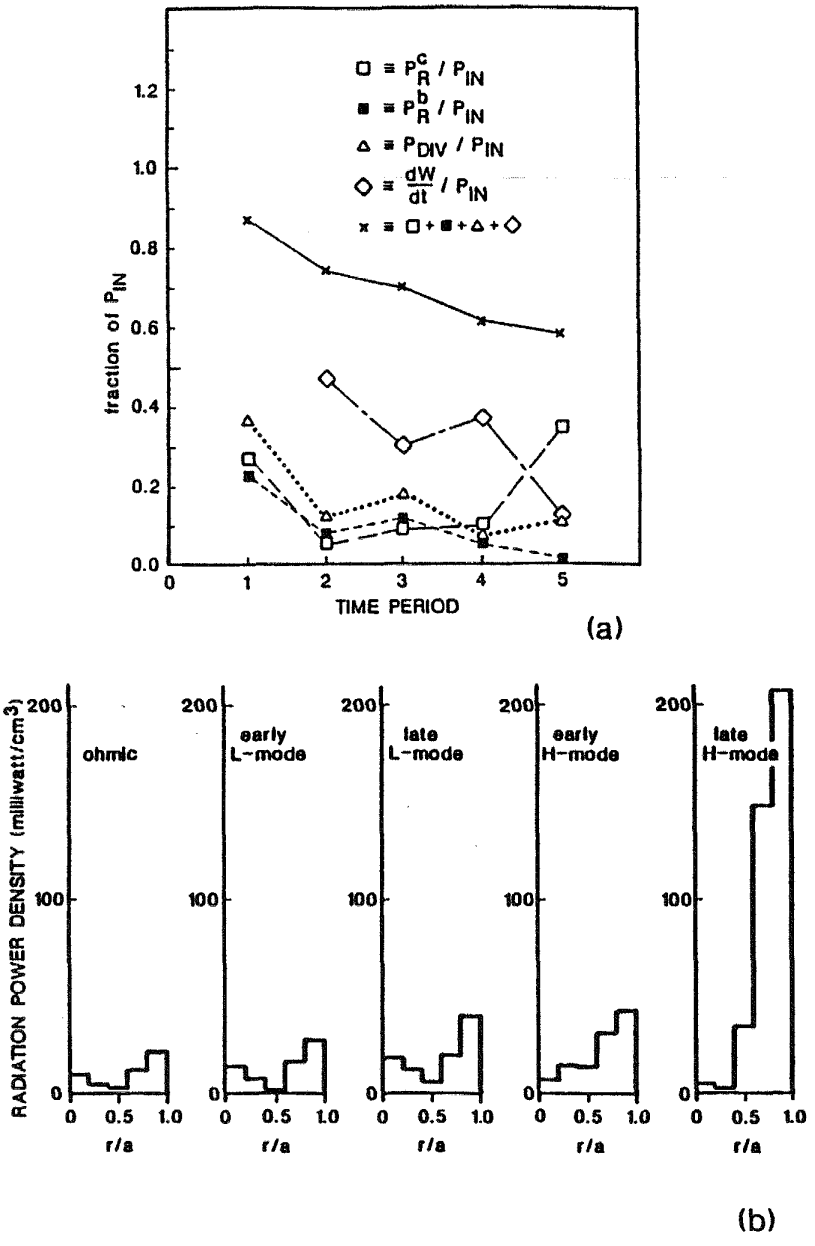

Fig. 2.4-2. (a) The evolution of the measured power balance is shown at various stages during a divertor shot (I_p = 1.25 MA, B_T = 2.1 T). The "time periods" represent (1) ohmic, (2) early L–mode, (3) late L–mode, (4) early H–mode, and (5) late H–mode(*i.e.*, shortly before the first ELM).P_r^c,P_R^b, P_{DIV}, and dW/dt represent radiated power from inside the separatrix, radiated power from outside the separatrix, power flow onto the divertor tiles, and the change in the plasma stored energy, respectively. (b) The evolution of the radiation profile is shown for the same series of shot.

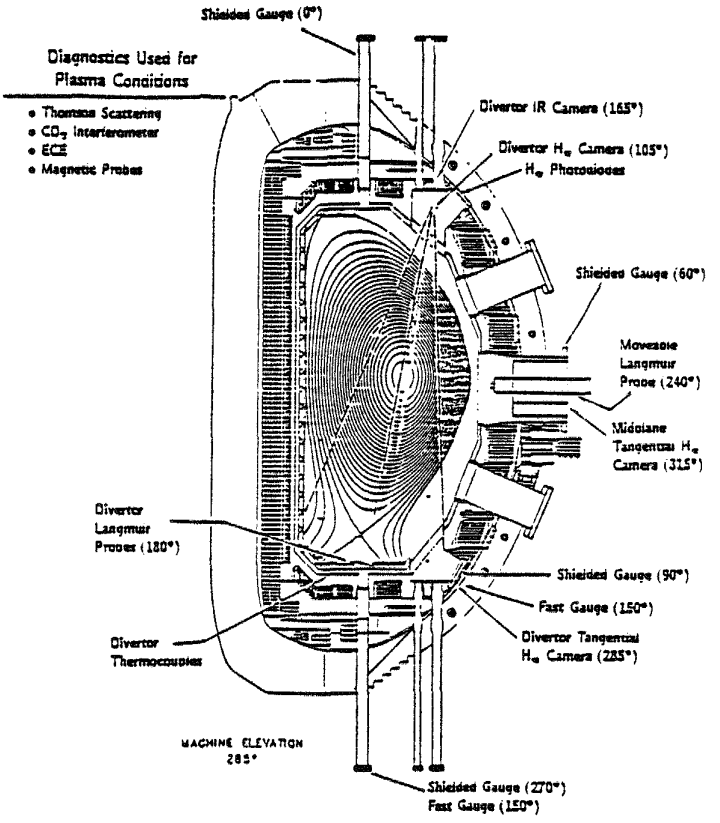

Fig. 2.4-3. Some of the recently installed or upgraded divertor diagnostics on DIII–D: a radial array of Langmuir probes spanning the divertor region, an absolutely calibrated H_α TV camera, a divertor-facing IR TV, and calibrated ionization gauges.

of the divertor recycling and neutral pressure distribution is carried out using the DEGAS Monte Carlo neutral transport code, which is benchmarked against experimental data.

Heat flux to the divertor region has been studied in considerable detail [6]. For ohmic plasmas, the power flow to the divertor decreases with increasing plasma density. In addition, the width of the heat flux at the inner and outer divertor strike points broadens with increased density. Figure 2.4-4 shows the behavior of the heat flux distribution during ohmic, L–mode, and H–mode phases of a beam-heated discharge. Typically for a DIII–D divertor discharge, (1) the heat flux into the divertor is largest during the L–mode phase, (2) the heat flux shifts closer to the separatrix and becomes more peaked during the H–mode (vis-a-vis L–mode), and (3) the power flow to the divertor tiles is somewhat above that of the ohmic phase.

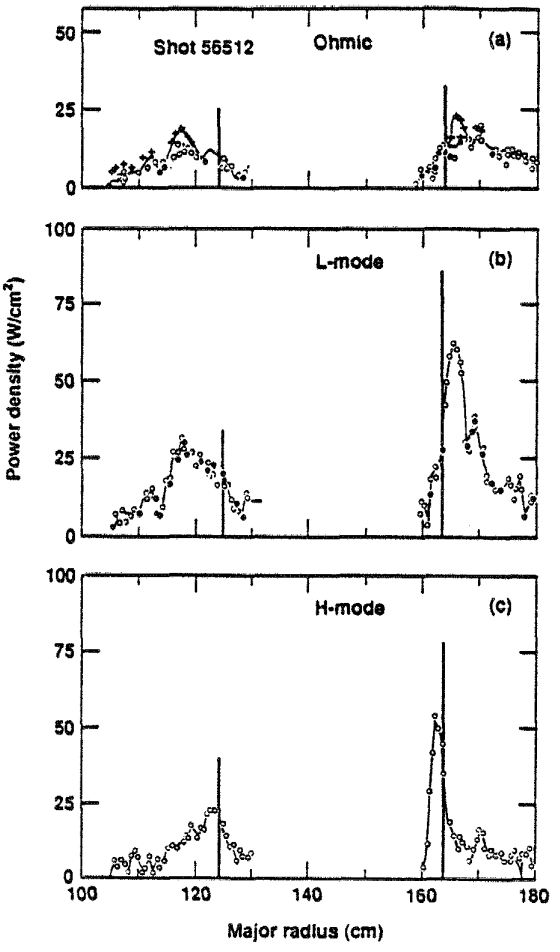

Fig. 2.4-4. The divertor tile heat flux during ohmic and neutral beam-heated plasmas is shown as a function of divertor location. The vertical bars indicate the calculated separatrix intercepts.

The peak power density along the outboard-located strike point in the divertor appears to scale linearly with beam input power during NBI L–mode operation. For an input power of 8 MW, the peak power density is found to be roughly 300 to 400 W/cm^2. On the other hand, the heat deposition profile during an ELM is broader than that of either the L–mode or quiescent H–mode. More than 50% of the energy lost during a giant ELM is deposited on the divertor tiles. During these disruptions, instantaneous peak powers as high as 6 kW/cm^2 have been observed.

Divertor recycling studies have also shown interesting results [7]. H_α measurements near the inboard and outboard intercept locations in the divertor may be highly asymmetric. Figure 2.4-5 shows that H_α emission can be much stronger near the inner peak than near the outer peak during the L–mode. Langmuir probe measurements also detect

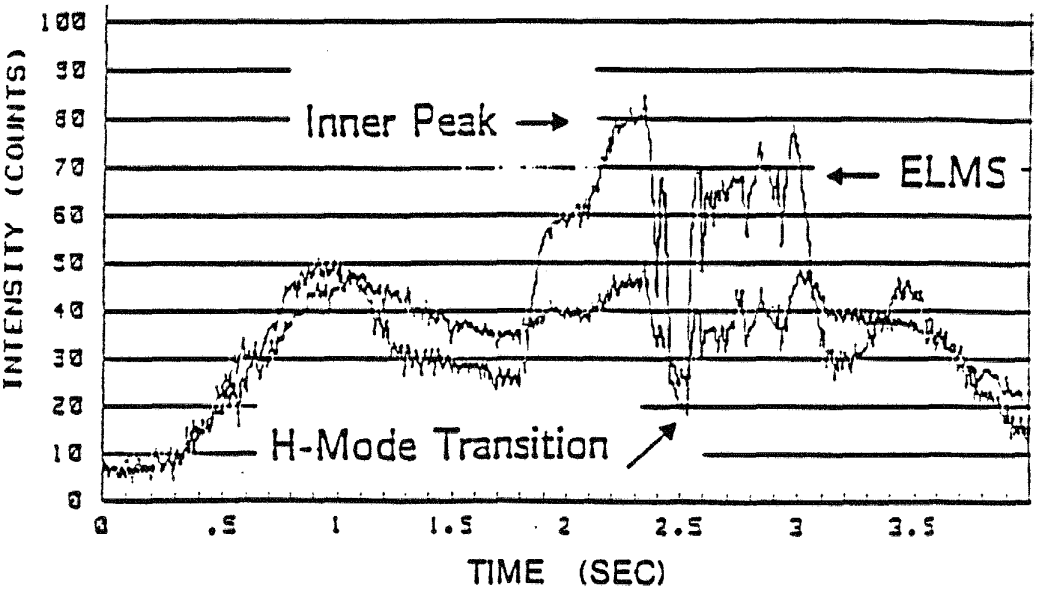

Fig. 2.4-5. The time history of the H_α intensity near the inner and outer peaks in the divertor. Note the relative strength of the inner peak during the L–mode phase of this neutral beam-heated discharge.

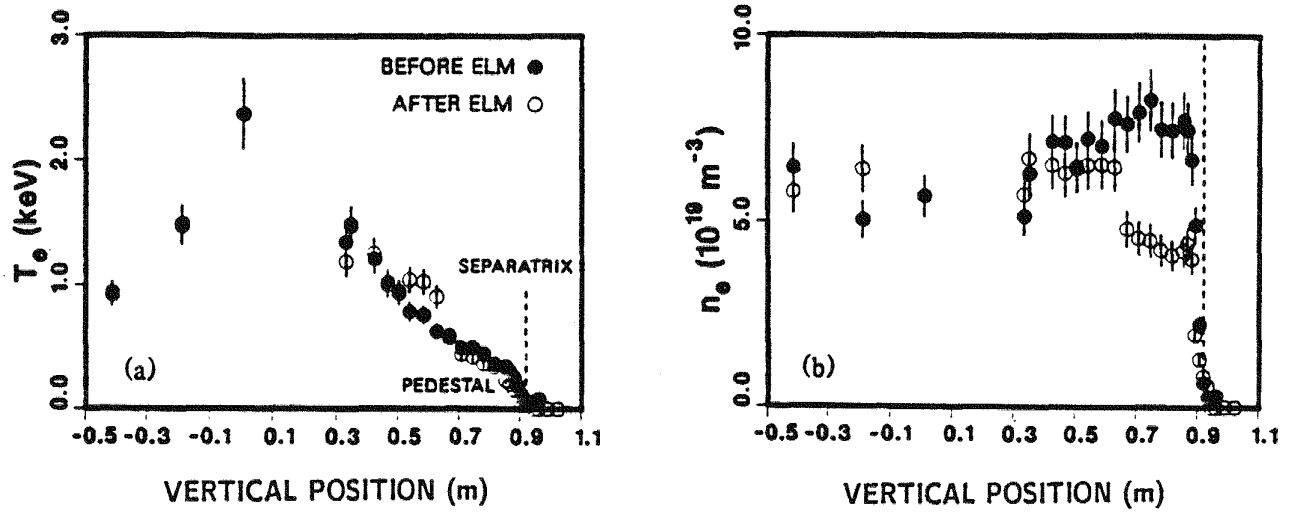

Fig. 2.4-6. (a) Electron temperature profile and (b) electron density profile 5 ms before (•) and 11 ms after (o) the start of the first giant ELM (I_p = 1.25 MA; B_T = 2.1 T; P_{BEAM} = 6.8 MW).

asymmetries between the inner and outer intercepts. In some L–mode cases, the outer intercept is roughly a factor of five lower in density.

A distinct transient increase in neutral pressure in the divertor region is observed after an ELM or an L to H transition. The edge neutral pressure is found to decrease and H–mode energy confinement is improved in divertor discharges with large limiter/separatrix gaps of approximately 10 cm. The DEGAS Monte Carlo transport code is being used in modelling neutral transport in the divertor. For example, with input data obtained from IR camera measurements of the heat flux, along with Langmuir probe data from Thomson scattering data, DEGAS-predicted H_α profiles agree to within a factor two to three with the experimentally measured H_α profiles.

2.4.4. ELM BEHAVIOR

An important contribution to the study of boundary physics and the associated influence on H–mode plasmas and impurity and density control has resulted from our greater understanding of ELMs. Detailed studies of electron density and temperature profiles indicate large amplitude modulation of steep edge electron pressure gradients during the occurrence of giant ELMs (see Fig. 2.4-6). Over a large range of plasma currents (1 to 2 MA) the experimental edge pressure gradient before a giant ELM is close to the theoretically predicted marginal stability limit for the first regime of the ideal ballooning mode (see Fig. 2.4-6). These results, together with spectroscopic observations that ELMs originate in the regime of bad curvature, strongly suggest that ELMs are triggered by ballooning mode instabilities [8]. Also, comparisons with observations of similar quantities during the transition from L–mode to H–mode indicate that an ELM may be a short transient relapse into L–mode.

The most dynamic change during an ELM is the convectional flow or ejection of particles from the plasma edge into the scrapeoff region (see Fig. 2.4-6). Consequently, frequent ELMs tend to limit the increase in electron density and impurities at the plasma edge. This behavior can hence maintain a low level of radiation from impurities as has been shown in an earlier section and hence increase the duration of the H–mode as will be discussed in the next section.

ELMs increase in frequency with increasing injected beam power and decreasing plasma current (see Fig. 2.4-7). This is consistent with ballooning theory since the ballooning limit increases with I_p^2 and so it takes longer to reach the limit after an ELM for a given beam heating rate at higher currents and for a lower beam heating rate at a

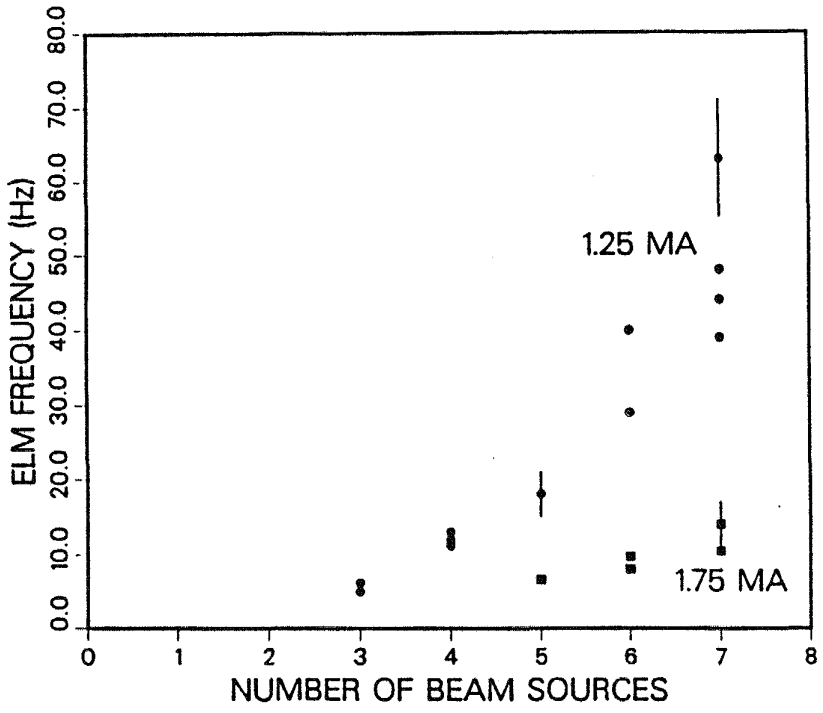

Fig. 2.4-7. The frequency of ELMs increases with increasing injected beam power.

fixed current. Further, at low neutral beam power decreasing the gap between the x-point and the divertor plates also increases the ELM frequency. In all these cases, the ELM frequency increases, the duration of each ELM decreases and the resultant effect on the decrease in edge density and stored energy is less *per ELM.*

2.4.5. LONG PULSE H–MODE PLASMAS

Our understanding of the influence of edge physics on H–mode plasmas has allowed us to produce long-duration H–mode plasmas lasting the entire length of the neutral beam-heating pulse (5 sec) and which exhibits no significant impurity accumulation or confinement degradations. These long-pulse H–mode plasmas, which have frequent (30 Hz) short duration ELMs, exhibit no significant change in plasma characteristics or profile behavior after 1 sec from the onset of the H–mode (see Fig. 2.4-8). These plasmas consisted of ≈30% deuterium and ≈70% hydrogen with I_p = 1.25 MA, B_T = 1.4 T, NBI power = 7 MW and $\bar{n}_e = 2.8 \times 10^{13}$ cm^{-3} before NBI. An important aspect of the long-pulse discharges is that the line radiation from impurities, both from the plasma core and the plasma edge, remains constant (about 20% of the total NBI power) for the duration of the H–mode after the initial rapid rise just after the L-H transition (see Fig. 2.4-9). This

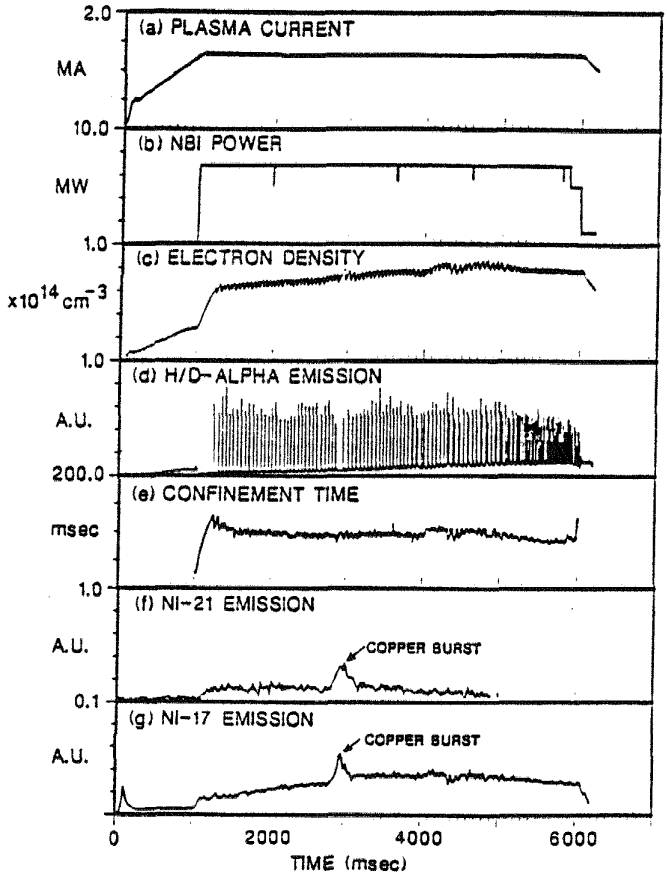

Fig. 2.4-8. Time histories of plasma parameters for quasi steady-state H–mode: (a) plasma current; (b) NBI power input; (c) line-integrated electron density; (d) H_α/D_α plasma emission from plasma divertor; (e) confinement time; (f) line emission from Ni-21 impurity near plasma center; (g) line emission from Ni-17 impurity near plasma edge.

trend is facilitated by the presence of frequent ELMs, which expel particles from the plasma edge and thereby reduce the rate of rise of density and the radiative losses from impurities. During ELM free periods, the rate of density rise is typically 2 to 3 times the sum of the external sources, whereas the averaged rate of density rise over the H–mode with ELMs is typically $\approx$10% of the beam fueling rate.

The successful long-pulse discharges require a minimum power level. Plasma discharges with lower NBI power at the same plasma current as in Figs. 2.4-8 and 2.4-9 contain fewer ELMs which result in radiation from impurities increasing to the extent of causing periodic transitions to short L–mode phases and which eventually result in a transition to steady-state L–mode behavior. In this case, impurity radiation can be up to

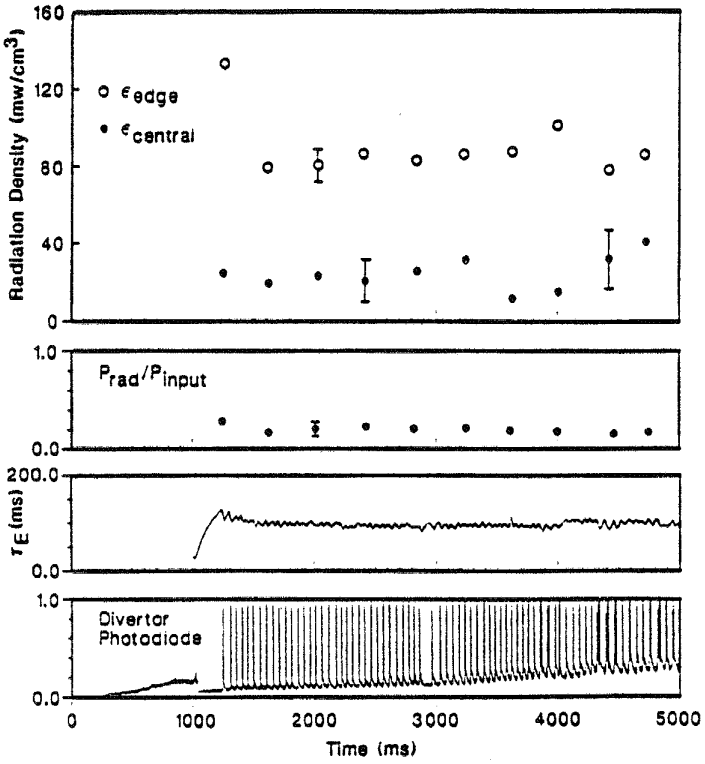

Fig. 2.4-9. Radiated power density at the plasma center and near the plasma edge change little during the long pulse H–mode plasma.

80% of the total NBI power and radiation emanates predominantly from the plasma core. This radiation from the plasma core further cools the plasma which radiates even more, further reducing the rate of pressure buildup, thus reducing the ELM frequency, which in turn results in more density and impurity increase and even greater radiative losses.

2.4.6. REFERENCES FOR SUBSECTION 2.4.

[1] Brooks, N.H. and P. Petersen, *J. Nucl. Mater.*, **145-147**, 770 (1987).

[2] Jackson, G.L., T.S. Taylor, S.L. Allen, *et al.*, "Reduction of Recyling in DIII–D by Degassing and Conditioning of the Graphite Tiles," *Proc. of the 15th European Conference on Controlled Fusion and Plasma Heating,* May 16-20, Dubrovnik, Yugoslavia, General Atomics Report GA-A19295, 1988.

[3] Content, D., H.W. Moos, M.E. Perry, *et al.*, "Impurity Profile Analysis in DIII–D H–mode Discharges," General Atomics Report GA-A19288, submitted to *Nucl. Fusion*, 1988.

[4] Brooks, N., M. Perry, S. Allen, *et al.*, "Regulative Effect on Impurities of Recurring ELMs in H–mode Discharges on the DIII–D Tokamak, General Atomics Report GA-A19108, submitted to *Phys. Rev. Lett.*, (1988).

[5] Mahdavi, M.A., D. Hill, S. Allen, *et al.*, "Modification of the Scrape-Off Layer By Edge Plasma Modes," *Proc. of the 8th International Conference on Plasma Surface Interactions,* May 2-6, 1988, Jülich, Federal Republic of Germany, General Atomics Report GA-A19291, 1988

[6] Hill, D., T. Petrie, M. Ali Mahdavi, *et al.*, *Nucl. Fusion*, **28**, 902 (1988).

[7] Allen, S.L., M. Rensink, D.N. Hill, *et al.*, "Recycling and Neutral Transport in the DIII–D Tokamak," *Proc. of the 8th International Conference on Plasma Surface Interactions*, May 2-6, 1988, Jülich, Federal Republic of Germany, General Atomics Report GA-A19292, 1988.

[8] Gohil, P., M. Ali Mahdavi, L. Lao, *et al.*, *Phys. Rev. Lett.*, **61**, 1603 (1988).

2.5. RF HEATING

2.5.1. FY88 HIGHLIGHTS

2.5.1.1. Electron Cyclotron Heating

Electron cyclotron heating (ECH) in tokamaks is an effective means of heating plasma to high temperature, and ECH has been assigned an important role in heating plasma in CIT to ignition and in ITER startup. Experiments on DIII–D have provided a significant part of the basis for confidence in ECH for reactors. All of the principal modes of heating have been studied in experiments on DIII–D, including outside launch of the ordinary mode (O–mode) at the fundamental frequency (the mode chosen for CIT) and the extraordinary mode (X–mode) at the fundamental and second harmonic, and inside launch of the fundamental X–mode. Central electron temperatures above 5 keV have been achieved with 1 MW of ECH in DIII–D.

In addition to bulk heating, ECH has potential applications affecting confinement and stability. In DIII–D experiments, central application of ECH has been shown to generate the H–mode of improved confinement [1,2]; heating near the $q = 1$ surface has suppressed sawteeth [3]; and applying ECH with the resonance near the edge has stabilized the edge localized modes (ELMs), leading to improved energy confinement for plasmas in which the H–mode was generated by neutral injection [4].

These ECH experiments at 60 GHz have used two antenna systems. For the outside launch, a system of eight antennas is located on the outer wall near the plasma midplane. For inside launch, ten antennas have been placed on the inboard wall of the vacuum vessel near the plasma midplane. Since the vacuum barrier windows are placed outside the vacuum vessel, which reduces constraints on the size of the windows and facilitates the cooling of the windows, the fundamental resonance lies in the evacuated waveguide at the top of the vessel. Breakdown in the waveguide at the location of the fundamental cyclotron resonance has been successfully suppressed by splitting the waveguides longitudinally and electrostatically biasing the halves in order to sweep out rapidly electrons which may start a breakdown [5].

In the experiments described here, the DIII–D tokamak was run in the divertor configuration, with major radius 1.68 m, minor radius 0.62 m, and elongation 1.7 (volume 21 m^3). In most cases, the working gas was deuterium. Plasma energy W was determined from a full MHD equilibrium analysis using magnetic measurements as input, or from measurements of plasma diamagnetism.

As expected from theoretical considerations, Fig. 2.5-1(a), the measurements shown in Fig. 2.5-1(b) indicate that the central heating extends to highest line-averaged density, above 4×10^{19} m^{-3}, by use of the inside launch of the X–mode. For outside launch of the O–mode, the peak in central heating is at slightly lower density than expected, about 1.5×10^{19} m^{-3}, but the heating extends slightly above the expected cutoff. For X–mode heating at the second harmonic [6], the falloff with density is about as predicted by theory.

For the ECH discharges, $T_e(0)$ is larger at low densities, reflecting the very weak dependence of confinement time on density in the L–mode. Figure 2.5-2 shows this behavior for fundamental heating with the O–mode. Central temperatures above 5 keV are observed at low density, 1×10^{19} m^{-3}.

Confinement in the L–mode discharges using O–mode heating tends to be better than the Kaye-Goldston scaling. In Fig. 2.5-3, τ_e is plotted as a function of τ_e^{KG}. Although τ_e does decrease from ohmic levels during ECH, τ_e remains about a factor of 2 above L–mode scaling. This is similar to results from outside launch of the fundamental X–mode [7], in which case the heating is believed to be due to O–mode heating also. Here, $\tau_e = W/(P_\Omega + P_{ECH})$, where P_{ECH} is the total ECH power incident on the plasma.

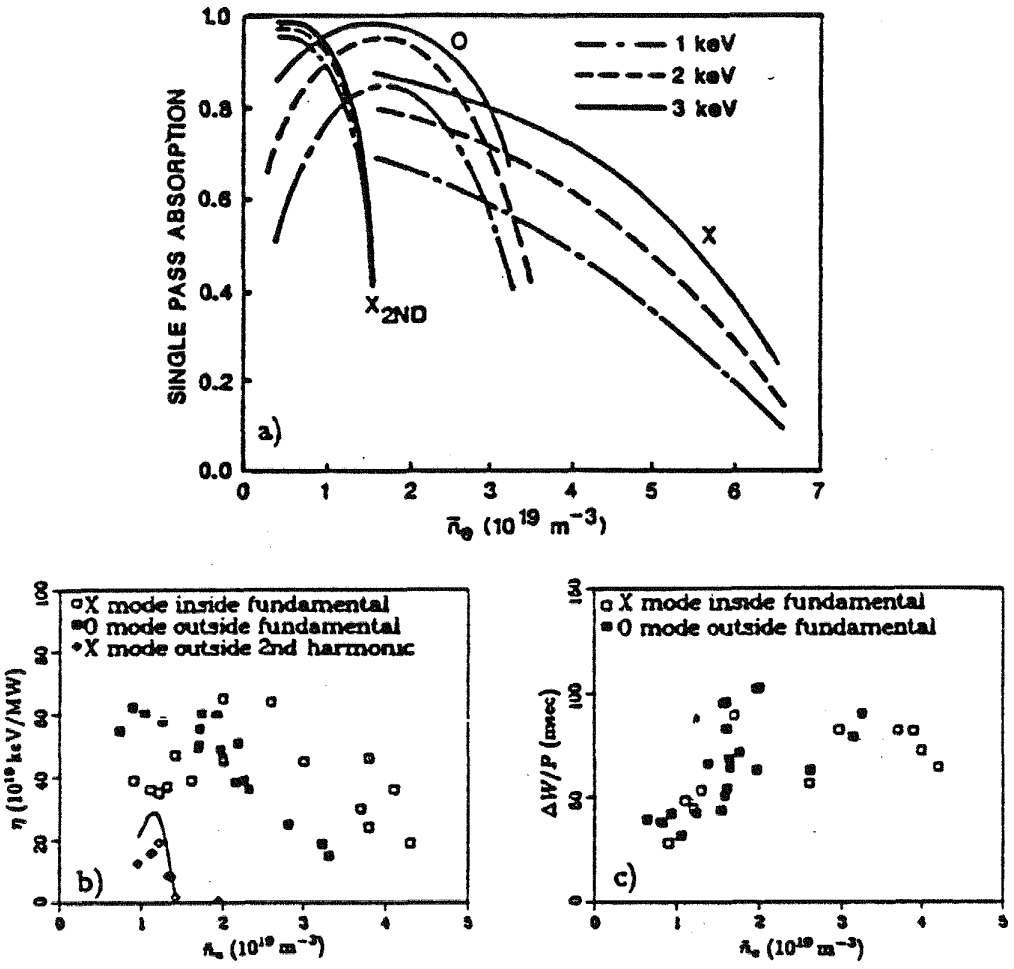

Fig. 2.5-1. (a) First pass absorption calculations from the TORAY ray tracing code; (b) Heating efficiency $\eta = \bar{n}_e \Delta T_e(0) V / P_{ECH}$ as a function of line-averaged density. Here, $T_e(0)$ is the central electron temperature measured by ECE. Data for the fundamental X–mode (inside launch), fundamental O–mode (outside launch), and second harmonic X–mode (outside launch) are presented. (c) Increase in plasma energy W, $\Delta W/P_{ECH}$ as a function of $\bar{n}_e$ for the O–mode and the inside launch X–mode.

MHD activity is known to reduce confinement or lead to disruptions in tokamak plasmas. The effect of the internal disruption associated with the sawtooth crash is to limit the attainable central electron temperature and to increase the energy and particle transport in the central region of the plasma. Activity with $m = 2$ is believed to lead to disruptions, and in H–mode discharges the Edge Localized Modes (ELMs) reduce confinement and decrease the quality of the H–mode. Because of its localized absorption, ECH can be used to affect these phenomena with relatively little power.

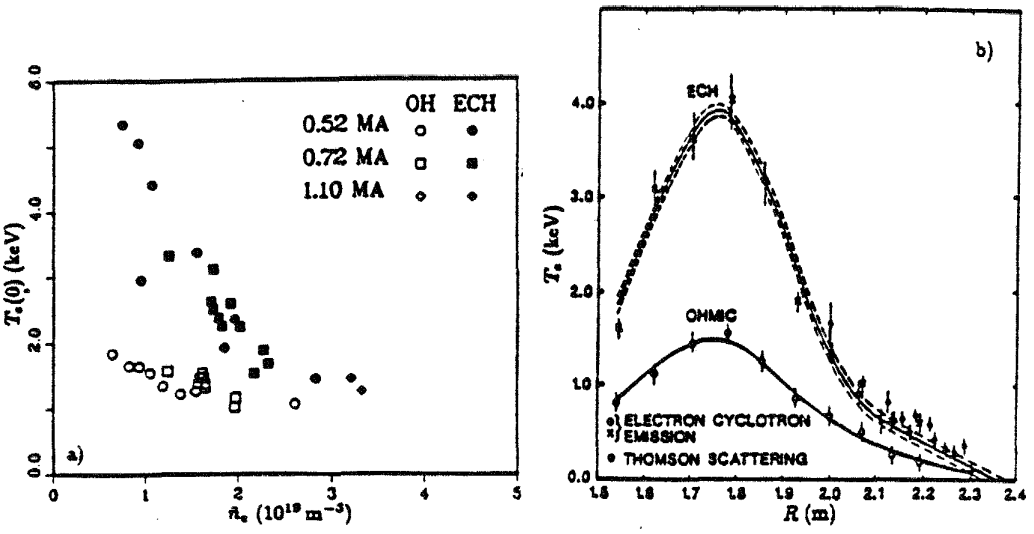

Fig. 2.5-2. (a) Central electron temperature from ECE as a function of $\bar{n}_e$, for central heating (B_t = 2.14 T) with the O–mode. ECH power was 0.9 to 1.1 MW, and I_p was varied from 0.52 to 1.1 MA; (b) Electron temperature profile from ECE and Thomson scattering for the 1.2×10^{19} m^{-3} case of Fig. 2(a).

In order to investigate the effect of the heating location on sawteeth in DIII–D, a detailed scan of toroidal field was performed using the second harmonic X–mode launched from the outside, with 0.85 MW of ECH power. A maximum was found in both the sawtooth period and amplitude when the ECH resonance was placed near the sawtooth inversion surface, with the effect sensitive to the resonance placement near that location. A shift of 3 cm in resonance location changed the sawtooth period by a factor of three, from 25 msec to 80 msec. In general the sawtooth period was still evolving to longer periods when the 500 msec ECH pulse ended. We speculate that the sawtooth period extension is due to an effect on the sawtooth trigger mechanism. Support for this idea is found in the sharp peak in the effect with the heating at the sawtooth inversion radius, where, for example, the $m = 1$, $n = 1$ instability is thought to originate. Depending on the form of the instability, changes in the local parameters or gradients (current or pressure) can change the growth rates of the modes or saturate them.

Suppression of ELMs by application of ECH has also been demonstrated in DIII–D [4]. In the first experiments, the second harmonic resonance was placed near the outboard edge of the plasma by reducing the toroidal field to 1.4 T. Waves were launched in the X–mode polarization from the outside antennas into a divertor plasma with 2.8 to 4.3 MW of neutral injection. Without ECH these plasmas were in the H–mode, but the ELMs were present during the entire H–mode period. When ECH was applied, the ELMs disappeared, and τ_e increased by over 50%. The rate of rise of the density also increased when the ELMs

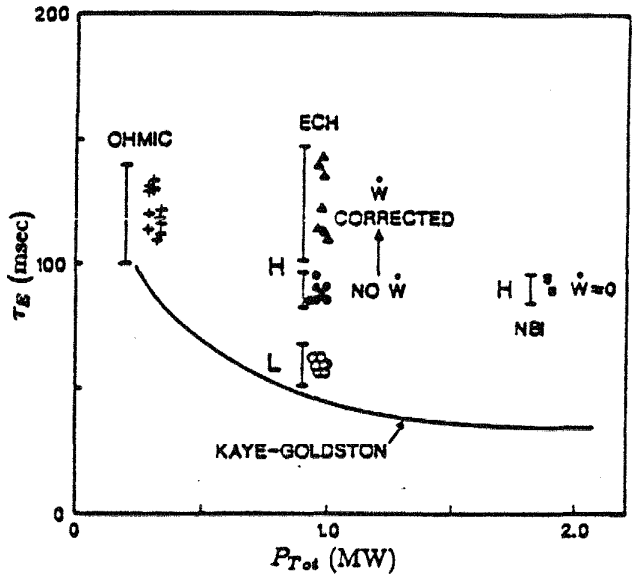

Fig. 2.5-3. (a) Global energy confinement time, derived from magnetic determinations of W, as a function of the Kaye-Goldston confinement time for central heating using the fundamental O–mode; (b) Energy confinement time as a function of total input power for central heating using the second harmonic X–mode. Plasma current is 0.48 MA and toroidal field is 1.07 T. This figure includes H–mode data for which the density was rising during the H–mode phase, so that a dW/dt correction is needed to account for the changing ECH power absorption.

disappeared, and after about 200 msec the density even at the plasma edge was above the cutoff density. After this time, the suppression of ELMs ended, and confinement time dropped.

The ELM-free period is characterized by improved confinement of electron heat as well as density. Figure 2.5-4 shows profiles of electron temperature for the ohmic, NBI L–mode, NBI plus ECH H–mode, and ELM-free H–mode phases of a discharge. These profiles show that the effect of ELMs is not just on the density, but that by suppression of ELMs the electron temperature may be increased.

2.5.1.2. Ion Cyclotron Heating Fast Wave Coupling Studies

The coupling of the ICH fast wave prototype antenna to H-mode plasmas was improved by modifying the antenna geometry in order to increase the linkage of rf magnetic flux to the plasma. By deepening the antenna cavity, moving the current strap closer to

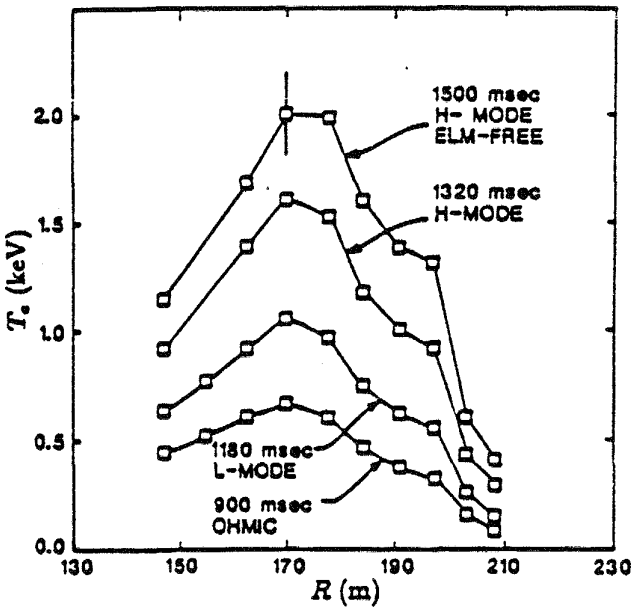

Fig. 2.5-4. Electron temperature profiles from ECE for a discharge with ECH suppression of ELMs.

the Faraday shield (and hence the plasma), and eliminating one tier of the Faraday shield, the antenna loading resistance was doubled, in agreement with theoretical predictions (see Fig. 2.5-5).

2.5.1.3. IBW Heating System

During FY88, a toroidal loop antenna for use in ion Bernstein wave (IBW) heating experiments was designed [8], built, and installed on the DIII-D tokamak (see Fig. 2.5-6). The antenna, which consists of two colinear conducting straps oriented in the toroidal direction, located in a large recessed port area, 1 m long in the toroidal direction. The current straps are fed at the ends of the antenna, grounded electrically at the center, and contained within box-like enclosures. Each half of the antenna is moveable over a distance of 5 cm in the radial direction. By feeding the antenna at both ends, a means is provided for varying the $k_{||}$ spectrum of the antenna by adjusting the relative phase between the two feeds.

A Faraday shield consisting of a single tier of vertically oriented molybdenum rods is located in front of the current strap. The rods are covered on the plasma side with a layer of graphite to reduce the input of high Z impurities to the plasma. The antenna is designed to operate at the 2 MW level for pulse lengths up to two seconds. Cooling occurs by radiation only as there are no provisions for active cooling. RF dissipation within the antenna structure has been minimized by coating all conducting surfaces with 0.065 mm

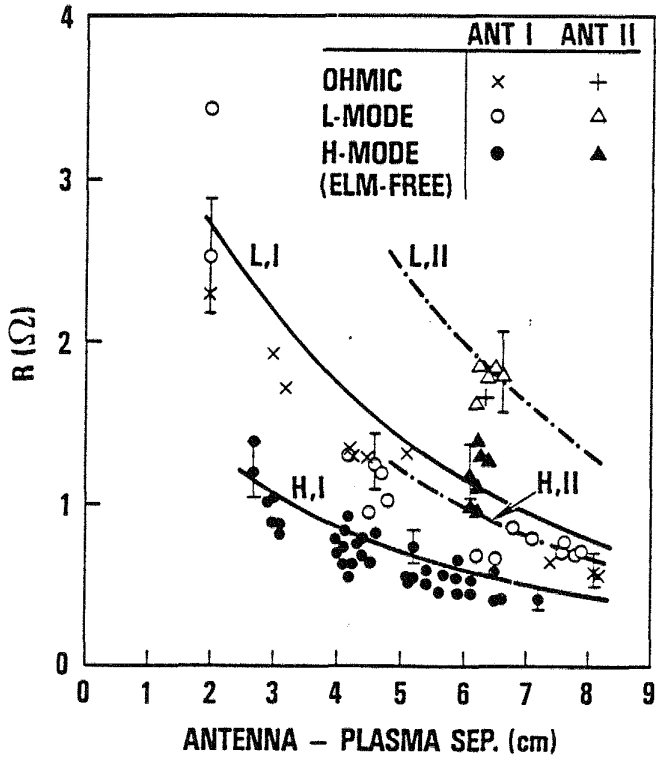

Fig. 2.5-5. Fast wave antenna loading resistance for the original geometry (Ant I) and the modified antenna geometry (Ant II) plotted versus the distance between the plasma separatrix and the antenna face.

of copper using a plasma spray process. The antenna is also protected from the plasma heat flux with an array of graphite bumper tiles.

The completed IBW antenna was installed on DIII-D in June, 1988. During the remainder of FY88, the 2 MW, 30 – 60 MHz IBW heating system was fully assembled, tested, and made ready for initial plasma heating experiments beginning in FY89. Initial RF conditioning of the IBW antenna in vacuum proceeded rapidly. With less than 5 hours of conditioning time, a power level of 160 kW was achieved with no limit apparent. In terms of antenna and transmission line voltages, this power level was equivalent to 1.3 MW with plasma.

2.5.2. SUMMARY OF FY84 TO FY87 PROGRAM

2.5.2.1. Electron Cyclotron Heating

In FY87, second harmonic heating using outside launch of the X–mode at a toroidal field of 1.07 T was found to be effective at generating a transition to H–mode at power levels

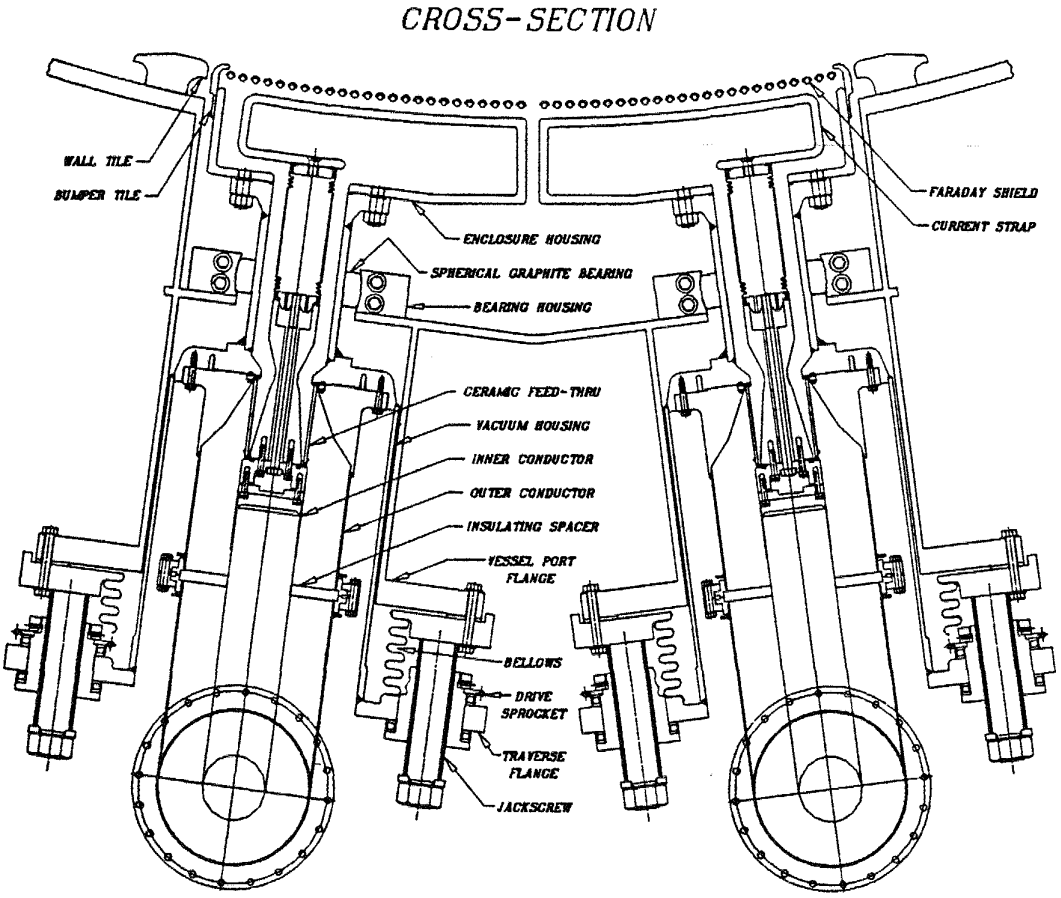

Fig. 2.5-6. Diagram of the toroidal loop antenna installed in DIII-D for high power ion Bernstein wave (IBW) heating experiments.

above 0.75 MW. This was the first demonstration of the H–mode using ECH, which does not generate an ion tail as the previous heating methods attaining the H–mode (neutral injection and ICRF) do. The H–mode so generated demonstrated the characteristics of the H–mode generated by neutral injection in DIII–D: an increase in plasma energy, signifying an improvement in τ_e; an increase in $\bar{n}_e$ and a decrease in the D_α emission, signifying an improvement in particle confinement time τ_p; and a broadening of the pressure profile and development of a very steep density gradient at the plasma edge. The improvement in τ_e, from values near the Kaye-Goldston level to the ohmic value, is shown in Fig. 2.5-3.

The H–mode is exhibited in the discharge of Fig. 2.5-7. This discharge went through two complete cycles. In the first, it remained in the H–mode for about 150 ms and then reverted to L–mode. Ray tracing calculations show that the reverse transition from H- to L–mode occurred when the density had risen to levels for which the absorption of the ECH power in a single pass had dropped to less than 0.5 MW due to refraction, and the plasma

center was cut off for most rays. Although after the first H–mode phase the density had returned to a value below cutoff, the second transition to the H–mode did not occur until the radiated power dropped to near its L–mode level of 0.3 MW.

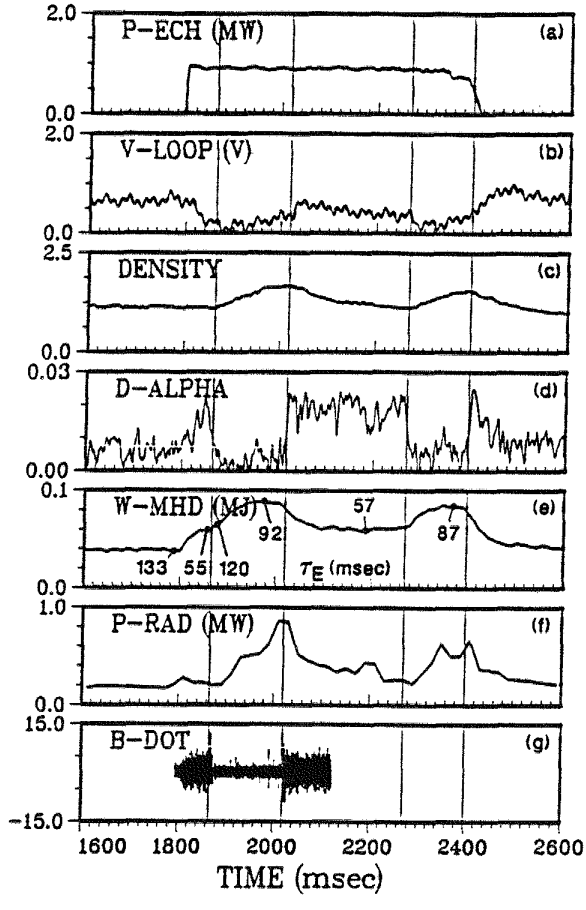

Fig. 2.5-7. Data from discharge #56360 with 0.48 MA plasma current, toroidal field of 1.07 T, and incident ECH power of 0.90 MW. (a) ECH power, (b) loop voltage, (c) line-averaged density, (d) central soft x-ray emission, (e) D_α light emission from the plasma midplane, (f) plasma stored energy from MHD analysis, (g) ultra-soft x-ray emission from the plasma midplane, and (h) total radiated power from the plasma within the separatrix flux surface, as a function of time. Traces labeled A.U. are in arbitrary units. This discharge is in the divertor configuration, in deuterium gas.

In FY86, ECH efforts concentrated on the analysis of data from Doublet III. Of particular interest was the analysis of heating at densities above twice the cutoff density, using inside launch of the extraordinary mode [9]. For these shots, it was determined that the heating was taking place at a minor radius in excess of 70% of the minor radius of the plasma, yet the confinement time did not decrease, and in fact the global energy confinement time increased above that of the ohmic discharges when the ECH was applied. An explanation of this observation has not been developed.

In FY84-85, experiments were performed on Doublet III. These experiments treated the heating efficiency and wave absorption as a function of density; the extension of the sawtooth period by the localized heating of ECH; and the study of the propagation of pulses of heat generated by ECH in the interior of the plasma, as a means of studying the local electron heat transport. Also studied was a correlation of high heating efficiency of ECH with the state of plasma rotation in the toroidal direction. It was found that plasmas with no rotation during the ohmic phase preceding the ECH were poorly heated by ECH, but that plasmas which were rotating at even a small fraction of the ion sound speed were very effectively heated [10]. Possible explanations include magnetic field errors or locked MHD modes.

2.5.2.2. ICRF

According to ICRF coupling theory [11], the weak antenna coupling to H-mode plasmas could be due to a steepening of the edge density gradient near the separatrix or to a density reduction in front of the antenna. Experiments in FY87 were aimed at a better understanding of the ICRF coupling behavior during the H-mode through detailed measurements of the edge plasma density profile. These measurements were carried out using the Thomson profile diagnostic and a newly installed Langmuir probe diagnostic. The Langmuir probe, which was installed on a midplane port adjacent to the antenna, was moveable on a shot-to-shot basis, and could be positioned up to 2 cm beyond the limiter radius during divertor discharges.

The Thomson scattering diagnostic showed that a very sharp density gradient developed near the separatrix during the H-mode. This was accompanied by a factor-of-two drop in density in the scrape-off layer as measured by the Langmuir probe. Both effects contributed to the drop in loading resistance at the H-mode transition. During giant ELMs, the density profile broadened as plasma particles were expelled from the edge region into the scrape-off layer, and the ICRF coupling improved.

A comparison of the experimental coupling results with theory was carried out using a modified version of the Brambilla ICRF coupling code [12]. In this analysis, the measured density profiles were used, and the image currents associated with the side walls of the antenna enclosure were taken into account. Excellent agreement between the theoretical predictions and the experimental results was obtained.

Preparations were also begun for 2 MW ion Bernstein wave (IBW) heating experiments. Work this year included the conceptual design of the IBW toroidal loop antenna, modifications to the FMIT transmitter by Continental Electronics to permit $30 - 60$ MHz operation, and procurement of transmission line components.

Low power coupling measurements were the primary focus of the ICRF program on DIII-D during FY86. The compact loop antenna used for these studies was developed jointly by GA and Oak Ridge National Laboratory with funding from the D&T Division of DOE/OFE. Of particular interest was the antenna coupling to H-mode divertor discharges in DIII-D heated with up to 6 MW of neutral beam injection (NBI). During these discharges, the ICRF antenna loading resistance dropped typically by a factor of two at the H-mode transition [13]. When giant edge localized modes (ELMs) occurred during the H-mode, the loading resistance typically increased transiently by a factor of four. While the antenna coupling to L-mode and Ohmic discharges increased linearly with the line-averaged density, the H-mode coupling was nearly independent of density. These results showed how changes in the edge density profile brought about by the H-mode greatly affected the coupling properties of the fast wave antenna.

2.5.3. REFERENCES FOR SUBSECTION 2.5.

[1] Lohr, J.M., *et al.*, "Observation of H–mode Confinement in the DIII–D Tokamak with Electron Cyclotron Heating," *Phys. Rev. Letters* **60**, 2630 (1988).

[2] Prater, R., *et al.*, "Confinement in H–mode Discharges in the DIII–D Tokamak with Electron Cyclotron Heating," *Proc. of the EC-6 Sixth Joint Workshop on Electron Cyclotron Emission and Electron Cyclotron Resonance Heating*, Oxford, Culham Report CLM-ECR (1987), p. 195.

[3] Snider, R.T., *et al.*, "Modification of Sawteeth by Second Harmonic Electron Cyclotron Heating in a Tokamak," General Atomics Report GA-A19057 (1988); accepted for publication in *Phys. Fluids.*

[4] Prater, R., *et al.*, "Electron Cyclotron Heating Experiments in the DIII–D Tokamak," General Atomics Report GA-A19448 (1988); to be published in the *Proc. of the 12th International Conference on Plasma Physics and Controlled Nuclear Fusion Research* 1988 (Nice, France).

[5] Moeller, C.P., *et al.*, "A High Field Launch for Electron Cyclotron Heating using an External Window," *Proc. of the EC-6 Sixth Joint Workshop on Electron Cyclotron Emission and Electron Cyclotron Resonance Heating*, Oxford, Culham Report CLM-ECR (1987), p. 325.

[6] Stallard, B.W., *et al.*, "Heating and Confinement in H–mode and L–mode Plasmas Using Outside Launch ECH," General Atomics Report GA-A19349 (1988).

[7] Prater, R., *et al.*, "Electron Cyclotron Heating using the Fundamental Extraordinary Mode Launched from the Low Field Side on DIII–D," in *Applications of Radio-Frequency Power to Plasmas* (Seventh Topical Conf., Kissimmee, Florida, 1987), S. Bernabei and R.W. Motley, Eds., New York: Amer. Inst. of Physics, 1987, p. 9.

[8] Phelps, R.D., M.J. Mayberry, and R.I. Pinsker, "Ion Bernstein Wave Antenna Design for DIII-D," GA Report No. GA-A19435, 1988, to be published in *Proc. of 15th Symposium on Fusion Technology* (Ultrect, 1988).

[9] Ejima, S. and R. Prater, "Interpretation of Electron Cyclotron Heating Results in Overdense Plasma in Doublet III," *Nucl. Fusion* **27**, 1135 (1987).

[10] Prater, R. and A.J. Lieber, "Heating Effectiveness in Electron Cyclotron Heating Experiments in the Doublet III Tokamak," *Proc. of the EC-5 Fifth International Workshop on Electron Cyclotron Emission and Electron Cyclotron Heating*, General Atomics Report GA-A18294 (1985), p. 56.

[11] Mau, T.K., S.C. Chiu, and D.R. Baker, *IEEE Trans. on Plasma Sci.*, **PS-12**, 273 (1987).

[12] Brambilla, M. *Nucl. Fusion* **28**, 549 (1988).

[13] Mayberry M.J., *et al.*, "Coupling of an ICRF Compact Loop Antenna to H-mode Plasmas in DIII–D," in *Applications of Radio-Frequency Power to Plasmas* (Seventh Topical Conf., Kissimmee, Florida, 1987), S. Bernabei and R.W. Motley, Eds., New York: Amer. Inst. of Physics, 1987, p. 278.

2.6. CURRENT DRIVE

2.6.1. INTRODUCTION

The development of methods for noninductive current drive has become a major focus of the DIII–D research program. During the initial period of operations (FY84-86), current drive was not a primary goal. However, with realization of the significant advantages of truly steady-state tokamak operation, much more attention has been devoted to this issue. Work on neutral beam current drive and AC helicity injection (oscillating fluxes current drive) was initiated in FY87 continued and expanded in FY88. In addition, preparatory work was undertaken in FY88 for experiments on current drive using fast waves, electron cyclotron waves, and DC helicity injection.

The present DIII–D long-range program plan has a primary goal of achievement of a high β plasma with full noninductive current drive (the target is 2 MA at 5% by 1993). The current drive program also supports the efforts in confinement improvement (through the development of current profile control) and development of efficient techniques for next generation devices. The current drive effort has benefited greatly from the participation of the LLNL and JAERI groups at GA, as well as many other individuals.

2.6.2. NEUTRAL BEAM CURRENT DRIVE

Experiments in neutral beam current drive (NBCD) began in late 1987 and continued through 1988. The outstanding result was the sustainment of a steady plasma current of approximately 340 kA, for almost 1 second, with no inductive voltage (Fig. 2.6-1). The current drive efficiency for this experiment was $n_{20}IR/P \simeq 0.01$ at $T_e \simeq 2$ keV.

Another feature of these discharges is the very high value of β_p obtained (up to 4.5). In addition values of $\epsilon\beta_p$ up to 1.5 were reached. These discharges showed some indications of approaching equilibrium β limits, with the motion of the x-points of the separatrix toward the inner surface of the plasma. The high values of β_p also suggested the possibility that these plasmas may be entering the second stability regime for ballooning modes. Stability analysis of the high β_p shots shows that they lie just at the transition between first and second stability regimes (Fig. 2.6-2).

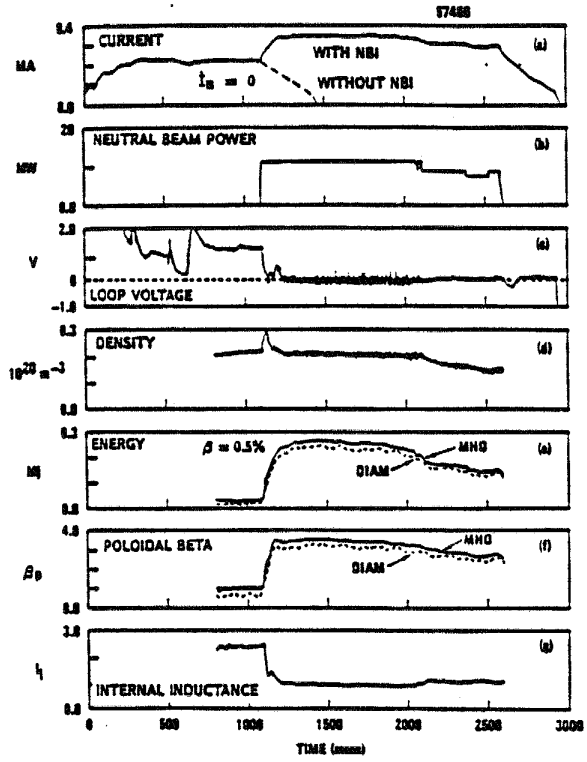

Fig. 2.6-1. NBCD discharge at 340 kA. A stationary state is maintained for over 0.8 seconds, until two NB sources are lost.

In these studies we found that the maintenance of a steady-state current by NBCD depends sensitively on plasma conditions. The range of experimental conditions studied include electron temperature up to 3 keV, density up to 4×10^{19} m^{-3}, and plasma current up to 500 kA. Discharges were run with helium and deuterium, and up to 1.5 MW of ECH power was used to control the initial electron temperature.

The experimental discharges were in the single-null divertor configuration, initiated with standard ohmic operation. After establishment of a stationary ohmic plasma, the transformer (E-coil) current was clamped at a fixed value, and the beams (up to seven sources) were turned on. Typically, there was a fast increase in the total plasma current, on an energy confinement time scale. This was followed by a stationary (or very slowly decaying) phase, with little or no loop voltage, lasting up to 1 second, but more typically a few tenths of a second. Subsequently, there was a transition to a second phase of slow decay (characteristic time $\sim$ 5–10 seconds). The transition to the second phase was generally accompanied by a transient increase in loop voltage, and was often accompanied by a brief contact between the plasma and the limiter.

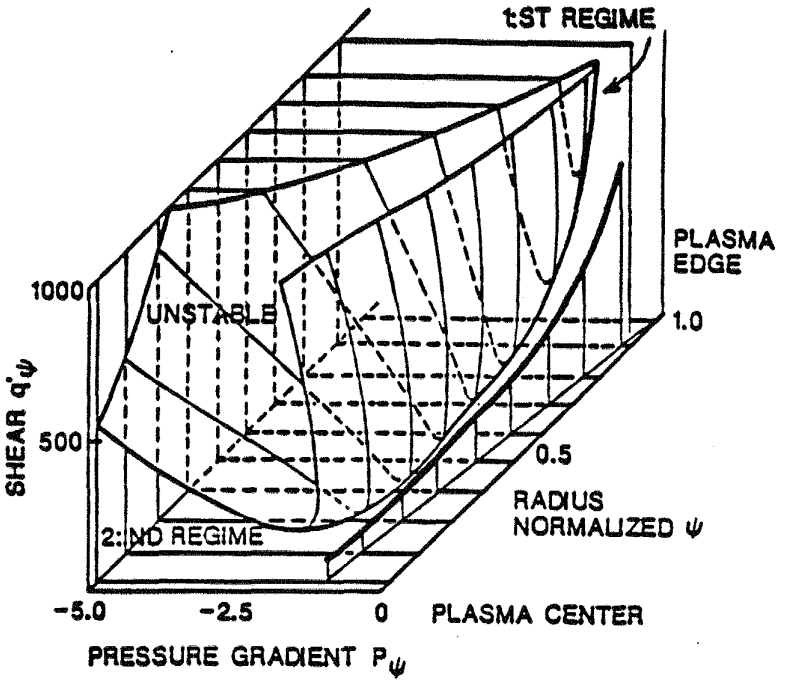

Fig. 2.6-2. Diagram of ballooning stability for the discharge shown in Fig. 2.6-1. The shear versus pressure gradient stability curve is calculated for each magnetic surface. The line corresponding to the actual value of p′ and q′ lies between the first and second stability regions, for an assumed $q_0 = 3$.

The sensitivity of the quasi-stationary state to plasma conditions appears to result from the close coupling between current drive efficiency, total current, energy confinement, and electron temperature. The energy confinement time was about 60 msec per MA of plasma current in this state, typical of H-mode confinement, and decreased by 10–20% during the decay phase. Even slight injection of impurity, due to contact with the limiter as the plasma shape changes, is sufficient to decrease the temperature and trigger the decay. Estimates of the current drive efficiency (nIR/P) indicate that it ranges from 0.01 at low I_p, T_e and τ_E to 0.05 at higher values.

2.6.3. AC AND DC HELICITY INJECTION

Preliminary tests of AC helicity injection oscillating flux current drive (OFCD) were carried out on DIII–D in 1987 and 1988. For closed, nested toroidal magnetic surfaces, evolution of helicity is given by $dH/dt = -\chi\,(d\psi/dt) + \int \eta J \cdot B d^3x$, where ψ and $\chi(\psi)$ are poloidal and toroidal fluxes, the helicity is $H = \int \chi\, d\psi$, and $-d\psi/dt$ is the loop voltage, V_ℓ. In steady-state, the loss of helicity through dissipation can be balanced by a non-zero

time average: $\langle \tilde{\chi}\, \tilde{V}_\ell \rangle \neq 0$, where $\chi = \langle \chi \rangle + \tilde{\chi}$, etc. The dissipation of helicity, due to resistivity, can be estimated from the ohmic case, $\dot{H} \simeq \langle \chi \rangle V_o$, where V_o is the ohmic loop voltage.

In the OFCD experiments, the toroidal flux variation has been produced by variation of the plasma cross-section area in a fixed toroidal field. The loop voltage variation results from modulation of the plasma current. The clearest result is obtained by modulation of the major radius, with the plasma bounded by the outer limiter. The change in loop voltage is dependent on the relative phase of the two flux modulations. A reduction in voltage of up to 0.09 V is seen (Fig. 2.6-3). On the basis of the flux modulation, the expected reduction is about 0.33 V, indicating an "efficiency" of 25–30%. The oscillating state is stationary, with clean and reproducible plasmas. There is no impurity accumulation and only a minor change in energy confinement. Further interpretation of these observations will require direct measurement of changes in the plasma current density, particularly near the edge.

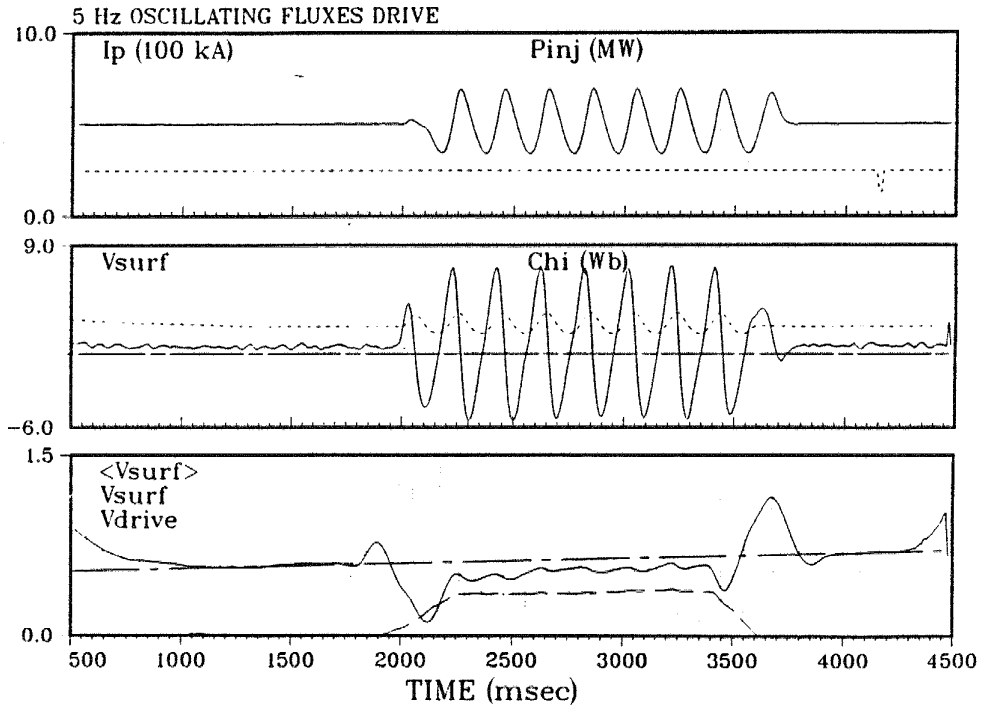

Fig. 2.6-3. OFCD at 5 Hz; (a) Plasma current (solid) and heating power (NBI) versus time; (b) Loop voltage at the plasma surface (solid) and toroidal flux within the plasma (dashed); (c) Time average of the surface voltage (solid) showing a 0.09 V reduction during the OFCD phase, and the OFCD voltage ($= \langle \tilde{\chi}\, \tilde{V}_\ell \rangle / \langle \chi \rangle$) of 0.33 V. For this experiment $I_p = 0.5$ MA, $P_{NB} = 2.5$ MW, $\tilde{I}_p \leq 0.2$ MA, and $\tilde{\chi}/\langle \chi \rangle \simeq 0.3$.

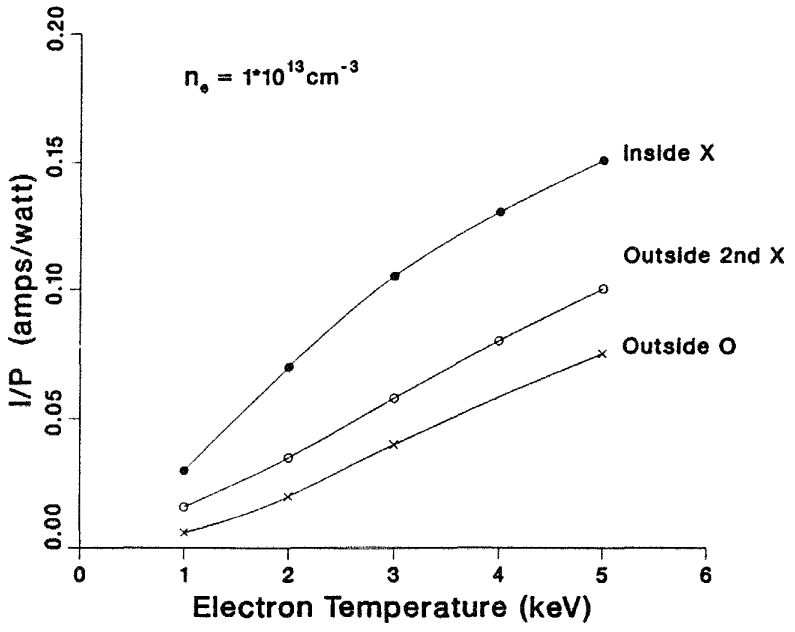

Fig. 2.6-4. ECCD versus central electron temperature. The plasma profiles are modelled by $n_e = n_0(1-(r/a)^2)^{0.6}$ and $T_e = T_0(1-(r/a)^2)^{1.5}$. Thirty rays with a spread of ~20° (FWHM) are used to model the antenna. For inside launch the centerline is 30° from perpendicular; for outside launch the angle is 17°.

Preparatory work for a DC helicity injection (DCHI) experiment was carried out in 1988. Current drive by DCHI is based on the helicity equation for open magnetic surfaces, $dH/dt = \sum \phi_i \Psi_i - \dot{H}$. The new term is the sum over flux tubes (each with flux Ψ_i) touching the wall, where ϕ_i is the wall potential at the end of the flux tube. The OFCD term, $\chi\, d\psi/dt$, does not appear because the loop voltage is assumed to be zero. For a single-null divertor, there is one flux tube (the scrape-off layer) which touches the wall in two places (the inner and outer legs of the divertor). Thus $\Psi_1 = \Psi_2 = \Psi$ and $\phi_1 - \phi_2 = U$, where U is the voltage difference applied between the inner and outer contact points. In steady-state the helicity source, ΨU must balance the helicity dissipation, which can be estimated as before from the ohmic case: $\dot{H} \simeq \chi V_o$. For DIII–D, the toroidal flux is $\chi \simeq 2$ Wb, the scrape-off layer flux is $\Psi \simeq 0.04$ Wb, and the loop voltage is $V_o \simeq 1$ V. Thus the electrode voltage should be about $U \simeq \chi V_o/\Psi \simeq 50$ V. The estimated electrode current is 10 kA for a plasma current of 1 MA. The electrodes needed for this experiment are scheduled to be installed in 1990, as part of the Advanced Divertor Project.

2.6.4. ELECTRON CYCLOTRON CURRENT DRIVE

Work in ECCD through 1988 concentrated on the development of theoretical models and on the use of these models for prediction of results of planned experiments. The TORAY code calculates three-dimensional rays in exact plasma equilibria on the basis of cold plasma dispersion. It incorporates a fully relativistic damping calculation, and includes relativistic and trapping effects in the current drive calculation. Proposed inside and outside launch experiments are compared in Fig. 2.6-4.

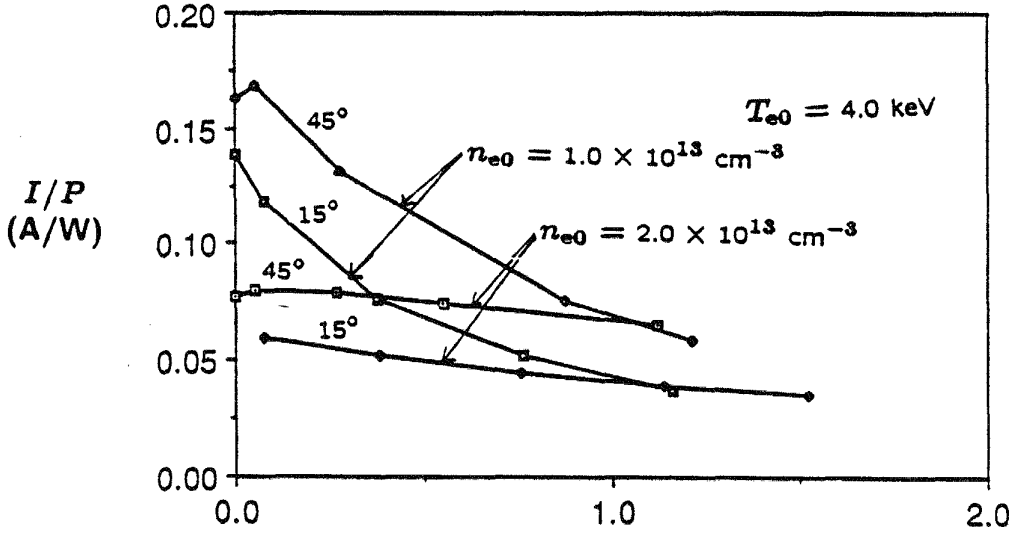

Fig. 2.6-5. ECCD versus RF power for inside launch, predicted with CQL3D. Relativistic modification of the resonance curve and enhancement of quasilinear diffusion at high power lead to a reduction in ECCD efficiency. The effect of increasing power on outside launch efficiency is much smaller.

A fully 3-D, bounce-averaged Fokker-Planck code for ECH and ECCD analysis (CQL3D) has been developed in collaboration with LLNL. This simultaneously solves the quasilinear Fokker-Planck equation and the RF energy transport equation in a non-circular plasma. It provides information on the wave amplitude and the evolution of the electron distribution function. It can also predict the resulting SXR and ECE spectra that would be observed. Applying this analysis to the proposed ECCD experiments indicates that the inside launch configuration may have a reduction in efficiency of a factor of 2–3 as the power is increased to ~1 MW (Fig. 2.6-5). Experiments to test ECCD and measure the power-dependence are planned for the coming year.

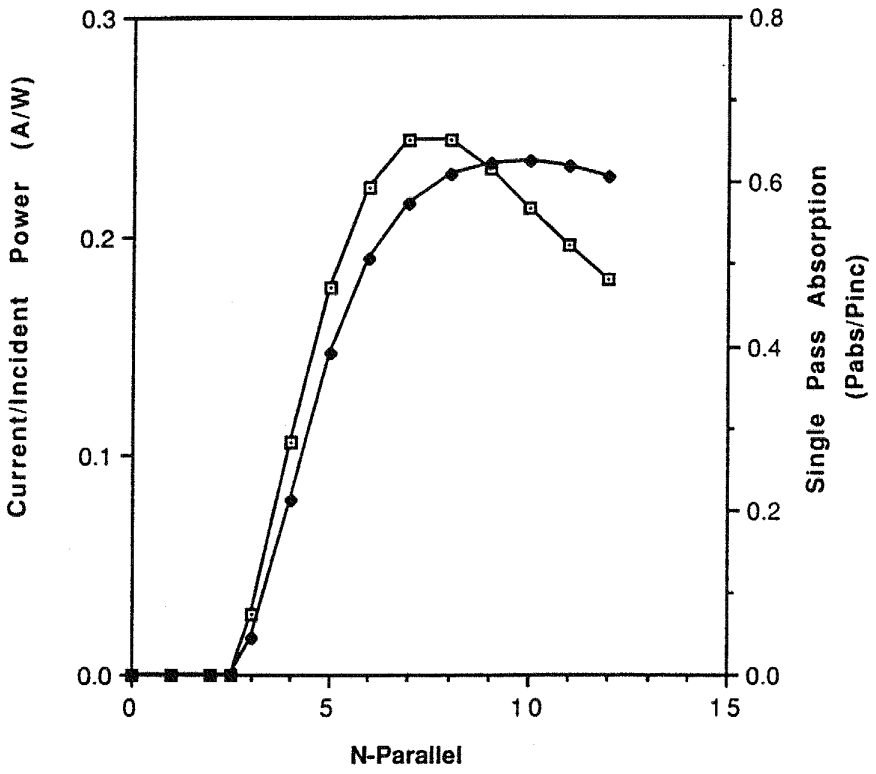

Fig. 2.6-6. Single pass absorption (solid dots) and current (hollow squares) versus $n_{||}$ at $T_{e0} = 7$ keV. The current is normalized to the incident power.

2.6.5. FAST WAVE CURRENT DRIVE

Fast wave current drive (FWCD) is predicted to combine high efficiency and good penetration of the plasma. Work in 1988 concentrated on developing theoretical analyses of the characteristics of FWCD in DIII–D, and on preliminary designs for a fast wave antenna. A test of FWCD on DIII–D is planned for 1990. The present antenna design is a four-strap, independently phased configuration. This will fit into the large, 1 m wide $\times$ 0.5 m high, RF port. For 0–$\pi/2$ phasing, the radiated spectrum peaks at $n_{||} \simeq 5$. This should be sufficient to give more than 50% absorption at a central electron temperature of 7 keV (Fig. 2.6-6). The high electron temperature can be provided by the present DIII–D ECH system. Unless T_e exceeds about 3 keV, the absorption and current drive are essentially zero (Fig. 2.6-7). These analyses indicate that, with sufficient directivity ($P_-/P_+ < 1/3$), the present 2 MW system at 60 MHz should be able to sustain more than 0.5 MA.

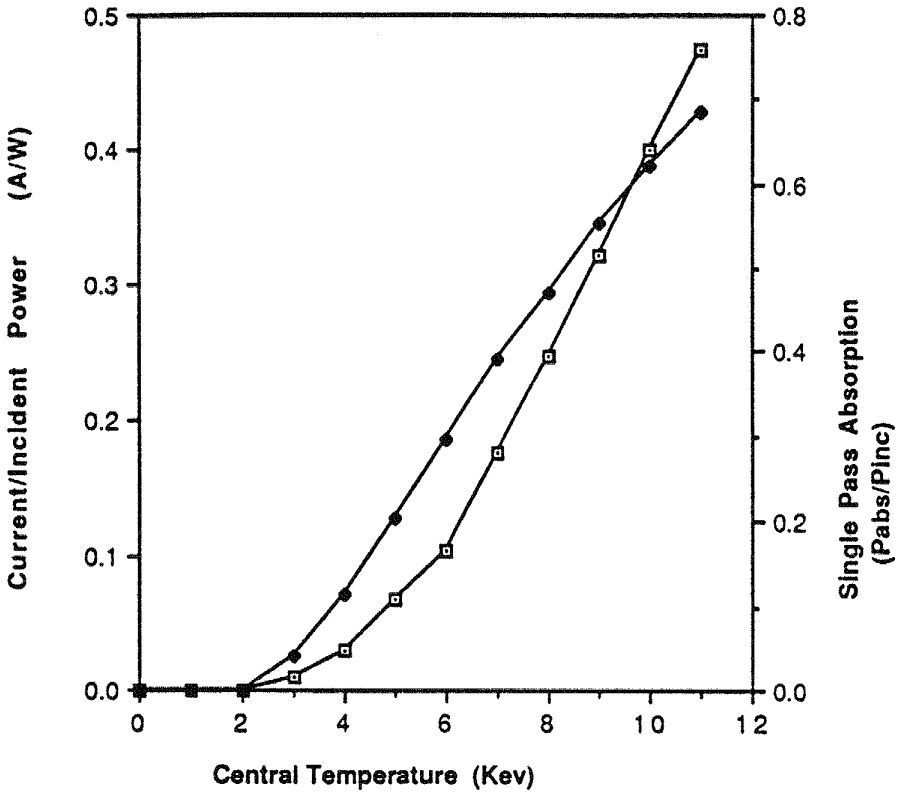

Fig. 2.6-7. Single pass absorption and current versus electron temperature for $n_{||} = 5$.

2.6.6. NONRESONANT RF CURRENT DRIVE

It is well known, but worth recalling, that the current drive efficiency for schemes that interact with the bulk of the electrons and do not distort the electron distribution is much higher than for strongly resonant current drive schemes. Furthermore, for nonresonant schemes, the efficiency (J/P) can be independent of density whereas for resonant current drive the reciprocal density dependence makes current drive difficult at reactor-like densities. The best example of a nonresonant scheme is DC induction, which has an efficiency $n_{20}IR/P \simeq 200$ for a reactor-like device such as ITER (or $I/P \simeq 30$ A/W). Thus, it is important to look for noninductive schemes with some of these properties. During 1988 we started an effort, primarily theoretical, to further the understanding of such schemes and to define possible experimental parameters.

A particularly elegant approach is to note that a photon with energy $\hbar\omega$ also carries helicity $\mu_0\hbar\omega/k$. Thus, when radiation is absorbed by a plasma, the helicity deposition is related to the absorbed power: $(k/\mu_0)\, dH/dt = P_d$. The dissipation of helicity in the plasma due to resistivity is $dH/dt = 2\eta JB$. Balancing these rates gives the power

needed to drive the current J with photon helicity: $P_d = 2k\eta JB/\mu_0$, or $J/P_d = \mu_0/2k\eta B$. Comparing the RF power to the ohmic power gives $P_d/P_{OH} = qkR$, where $kR = n$ is the toroidal mode number and q is the safety factor.

The same result can be obtained by two other different analyses. One way is to note that conservation of canonical momentum when a wave is introduced into a plasma leads to an average current. Since the wave carries momentum, there must be a corresponding kinetic momentum in the plasma electrons. The other analysis considers the response of a single, magnetized charged particle to a low frequency electromagnetic wave. For a damped, circularly polarized wave there is a net force along the confining magnetic field proportional to the damping rate: $\langle F \rangle = \pm(q/B_0)(\mu_0 P_d/2k)$. In steady-state, the force is balanced by resistive drag, leading to a net current flow. Consideration of a circularly polarized wave, with frequency below the ion cyclotron frequency (damped on a heavy minority ion species) leads to the result that the current is $(J/P_d) = (2/\sqrt{\pi})(ev_{te}/\nu_{ei}T_e)(\Omega_i/kv_A)(v_{te}/v_A)$. For DIII–D conditions ($T_e = 2$ keV, $B = 1$ T, $m_i = 5$) this analysis predicts $I/P \simeq 0.35$ A/W. For next generation devices (e.g., STE: $T_e = 10$ keV, $B = 5$ T), the efficiency improves to 0.8 A/W.

The important issues to be addressed next are the effects of propagation across the magnetic field, the effects of inhomogeneous fields, and the selection of suitable modes for experimental tests in tokamak plasmas.

2.7. DIAGNOSTICS

2.7.1. DIAGNOSTIC ADDITIONS AND PROGRESS IN 1988

With the basic plasma diagnostics well established on DIII–D, we concentrated in 1988 on improving our ability to diagnose plasma parameters that are related to stability issues. Our goal was to improve our understanding of the physics associated with both the beta limit instabilities and instabilities that limit confinement.

A toroidal soft X–ray array was installed to determine toroidal mode numbers of internal fluctuations. Poloidal cameras of 12 detectors each were installed at four different toroidal locations on DIII–D and have high spatial resolution near the outside edge of the plasma. The toroidal spacing was chosen to allow toroidal mode number identification of up to 24. During high beta operation, toroidal mode numbers of up to 4 were identified and were well correlated to magnetic measurements.

A narrow band microwave reflectometer was installed and operated under a collaborative effort with UCLA. The 7-channel system has provided both density profile and fluctuation data although the profiles have not been inverted. A new broadband system is being installed and should be operational in 1989.

One of the charge exchange particle analyzers used on Doublet III has been improved and modified for use on DIII–D. The spectrometer was calibrated and installed and operated during 1988. The diagnostic has been used to measure the spatial distribution of beam ions and fast ion losses during neutral beam injection. Particle spectral measurements during ion wave heating will be another important application of this diagnostic.

Forty-four new magnetic probes were installed including a new complete poloidal array.

A vertical-viewing electron cyclotron emission diagnostic was installed and used during ECH experiments to assess the nonthermal electron distributions. This system used a fast-scanning Michelson interferometer to detect emission between the 2nd and 10th harmonics. LLNL and University of Maryland installed this diagnostic as part of an ongoing collaborative effort.

A new set of IR cameras was built to view the new inside carbon tiles and upper divertor tiles installed on the DIII–D vacuum vessel.

2.7.2. SUMMARY OF DIAGNOSTIC CAPABILITIES ON DIII–D

In FY84 the plans were completed for the conversion for use on DIII–D of many of the diagnostics that were operating at that time on Doublet III. The essential diagnostics for operating the tokamak were available early in 1986. In Table 2.6.1-2 we list the operating diagnostics on DIII–D. The basic diagnostics planned for the first phase of DIII–D operation have been completed. Collaborative efforts with other institutions have contributed greatly to our ability to properly diagnose DIII–D plasmas.

DIII–D diagnostic construction resources were focused on the systems for n_e, T_e, and T_i profile measurements that we felt would yield the highest quality data. Our Thomson scattering system, grating ECE radiometer system, CO_2 interferometer system and charge exchange recombination (CER) system are all the products of careful and innovative design. They are performing very reliably and are yielding excellent, complete profile measurements being used for transport analysis.

TABLE 2.7-1
DIAGNOSTICS FOR DIII-D

Operations-Related Diagnostics	Quantity Measured	Comments	Installation and First Data Date
Magnetics	$\dot{B}$, Magnetic flux contours, I_p	2 poloidal (58), 1 toroidal (8) mag. probe arrays; 4 div. Rogowskis, 41 flux loops, 9 diamagnetic loops, 30 saddle loops, 3 I_p Rogowskis	1986
Hard X–rays		2 toroidal locations, 4 detectors	1986
Plasma TV	Visible TV	1 tangential, 180° limiter, divertor	1986
IR cameras	Heat load to armored surfaces	180° limiter, upper divertor; 0° limiter, divertor (LLNL)	1986
Photodiodes	H_α radiation, recycling	H_α filtered, 16 locations	1986
Neutron detectors	Fusion and photo-neutrons	3 toroidal locations	
Soft X–ray arrays	Internal fluctuations	1 vertical, 1 horizontal, 32 ch. ea.	1986
		4 toroidal locations, 12 ch. ea.	1988
Ultrasoft XRD	Edge fluctuations	1 location, 3 detectors	1987
H_2 gas injection		Main system, 2 locations	1986
		At divertor X–point, 1 location	
ECE grating radiometer	T_e (r, t)	Radial profile, 10 ch., 0.1 msec	1986
ECE Michelson	T_e (r, t)	Radial profile, each 25 msec	1989
Thomson Profile	T_e (r), n_e (r)	Vertical profile, 28 pts.	1987
CO_2 interferometers	$\bar{n}_e$	Vertical, 1 chord	1986
		Radial, 1 chord	1988
		an additional vertical	
Microwave reflectometer	n_e (r), density fluctuations	UCLA collaboration	1988

TABLE 2.7-1. (Continued)

Electron Temperature and Density	Quantity Measured	Comments	Installation Date
Ion temperature and rotation			
Charge exchange recombination	T_i (r, t), v_ϕ	Vertical, 8 ch. radial profile Tangential, 8 ch. radial profile	1986
UV doppler and UV profile	T_i edge	Radial profile, 1 pt. per discharge	1988
Impurities and boundary parameters			
Visible bremsstrahlung	Z_{eff} (r,t)	Radial profile, 16 chords	1986
Bolometer array	Radiated power	Radial profile, 21 ch.	1986
Multichannel VUV spectrometers	Impurity concentrations	Single chord, 100-600 Å, 80 Å view	1986
SPRED	Impurity concentrations	100-1700 Å, 800 Å view (LLNL)	1987
H_α TV	Divertor H_α	LLNL	1988
Divertor IR camera	Heat load to divertor	LLNL loan	1986
Thermocouples and Langmuir Probes	Edge T_e (t), n_e (t)	On divertor tiles and pumped limiters	1986
Laser blowoff system			1987
Probe carriage	Edge T_e (t), n_e (t)	Long stroke carriage with Lang probes and high frequency probes	1987
Fast pressure gauges	Neutral pressure	Near divertor region (ASDEX, LLNL)	1987

TABLE 2.7-1. (Continued)

Impurities and Boundary Parameters (Continued)	Quantity Measured	Comments	Installation Date
Fast Ion Diagnostics			
Scintillator	Neutron fluctuations		1987
E‖B charge exchange, H_α profile	Beam-Ion density profile	Conventional charge exchange analyzer coupled with H_α detectors used to measure beam neutral density profile	1988
Current Drive Diagnostics			
ECE Michelson	Microwave emission	Detects tail population in the electron distribution function (LLNL and Maryland)	1988

SECTION 3

OPERATIONS AND HARDWARE SUPPORT

3. OPERATIONS AND HARDWARE SUPPORT

In this section we describe: (1) the vessel modification to DIII–D (1984-85), (2) commissioning of DIII–D (1986), (3) hardware development (1987-88), and (4) FY88 operations.

3.1. VESSEL MODIFICATION (FY84 – FY85)

Fiscal year 1985 was a year of transition in the Doublet III program. The year began with the complete disassembly of the Doublet III tokamak until only the toroidal field coil centerpost was left standing in the machine pit. The year ended with the first vacuum vessel pumpdown and bakeout operations on the completely assembled new tokamak, DIII–D. With this new machine, the General Atomics tokamak program has advanced from the previous generation of 40 cm minor radius devices (PLT, PDX, ASDEX, Doublet III) to the current generation of large multimegampere machines (TFTR, JET, JT-60, DIII–D).

The task required the construction and assembly of a new vacuum vessel, some new poloidal coils, new coil and vessel support structures, a new in-vessel protection system, and new ancillary fluid, power, instrumentation, and computer systems. All tasks were completed on schedule to bring the machine into operation for the initial plasma cleaning operation milestone in November 1985.

The reconstruction resulted in a device capable of plasma currents up to 5 MA, limited initially by available power supplies to 3.5 MA, (2.5 MA divertor) and energy throughputs of up to 200 MJ per discharge, limited initially to 40 MJ per discharge by the fact that only a fraction of the ultimate vessel protection has been installed. The high-temperature baking and high-efficiency discharge cleaning produced a device with rapid cleanup and short turn around times. A cross-section of DIII–D is shown in Fig. 3.1-1.

A more complete discription of the DIII–D vessel modification project is given in References 1 and 2.

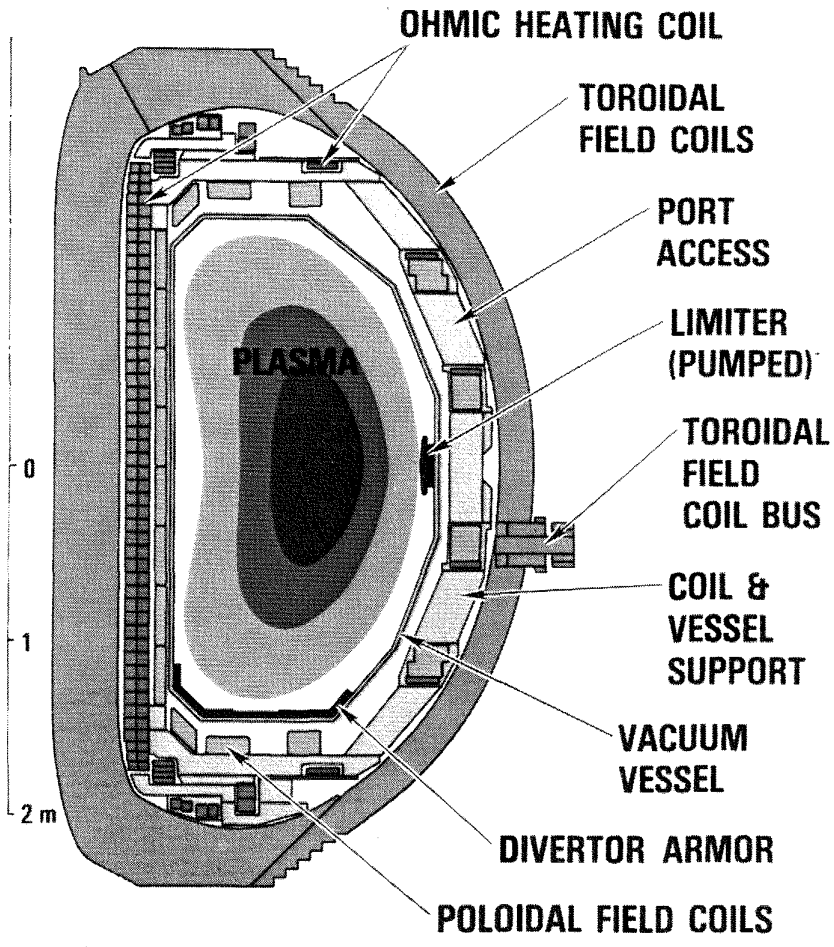

Fig. 3.1-1. DIII–D cross section.

3.1.1. DISASSEMBLY OF DIII–D

The Doublet III experimental program was completed in mid-September 1984, at which time disassembly began. The disassembly of Doublet III required the removal of all components down to the E–coil solenoid. The E–coil solenoid and the B–coil inner turns are contained in a bonded monolithic structure resting on the machine.

The major disassembly steps of Doublet III were: (1) removal of neutral beams and diagnostic hardware, (2) removal of the space frame, (3) removal of the B–coil prestress rings, (4) removal of the outer B–coil, (5) removal of the vessel, and (6) removal of the inner F–coil stack (see Fig. 3.1-2). The disassembly proceeded on schedule; the only unexpected

discovery was the full loss of the vertical clamping preload which had been applied to the studs on the inner F–coil stack located inside the Doublet III vessel bore. It was determined that during discharge cleaning the heat from the vacuum vessel had reduced the creep properties of the epoxy, and creep occurred in the epoxy-filled spaces between the F–coils. The coil stack was removed for rework since the DIII–D design required that the preload be doubled to about 500,000 lb. total. Pockets were machined in the epoxy joints between the coils within the stack and fiberglass/epoxy G10 laminate shins were bonded in these joints to produce a stable compressive load path. The stack was preloaded to design value and thermally cycled over the design temperature range to remove any residual creep of the repaired system. During the test the localized primary creep occurred until the stack became stabilized on its hard shins, as designed.

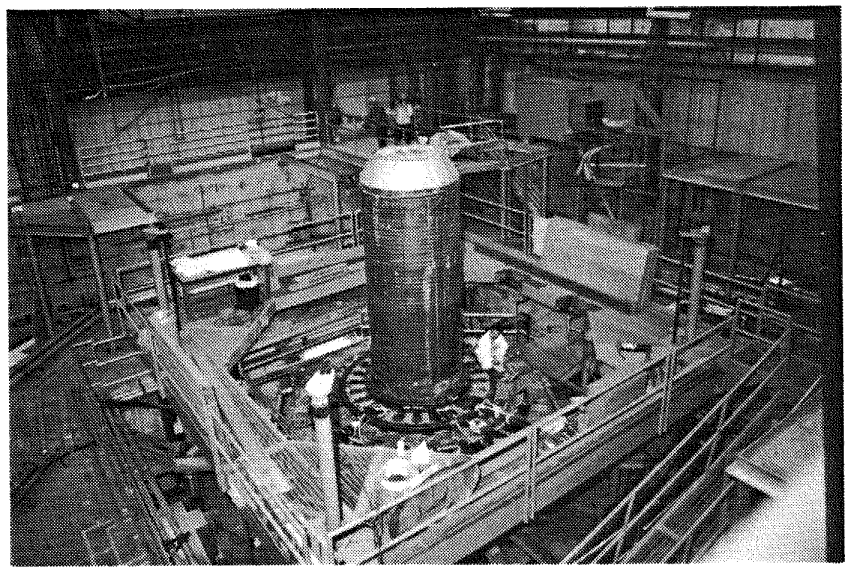

Fig. 3.1-2. Doublet III disassembled, ready for DIII–D construction.

3.1.2. DIII–D COMPONENT MANUFACTURE

The corrugated wall design of the vacuum vessel is similar to that used on Doublet III. The only solid wall is the outer midplane band, which is fabricated from 1 in.-thick Inconel 625 plate with heating/cooling flow channels externally mounted. The remainder of the vessel is 1.5 in.-thick construction with the corrugated wall sections being reinforced with 0.090 in.-thick Inconel sheet corrugations and 0.125 in.-thick solid sheets on the inside and the outside. This construction contains 120 poloidal heating/cooling channels connected into 60 parallel circuits entering and exiting at the base of the vessel. The water coolant or bakeout air is routed round port cutouts through port stubs on the vessel. The vessel

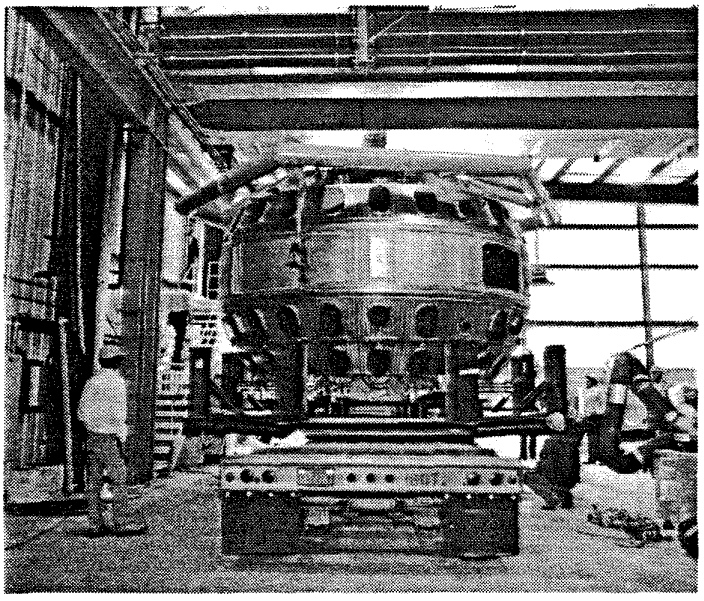

Fig. 3.1-3. Vessel arrived at GA.

walls were constructed by Toshiba International Corporation in Yokahama, Japan. The vacuum vessel as delivered from Toshiba is shown in Fig. 3.1-3.

In order to minimize assembly time, a maximum amount of subassembly work was completed on the vessel prior to its installation over the inner F–coil stack and B–coil centerpost. This work took place over 12 weeks beginning in April 1985, and was done with the vessel mounted in a subassembly stand. The subassembly began with leak testing of the vessel and port stubs with closure plates. Approximately 100 ports were then welded onto the vessel in five levels. After leak testing of the ports and coolant circuits, the following equipment was then installed: approximately 300 thermocouples, vessel magnetic diagnostics, F6A- and F6B-coils, four vessel support trunions and 14 midplane structure columns. Fiberglass-covered Kaowool insulation was then installed over the entire vessel and port assembly.

Six new field shaping F–coil assemblies were required and are referred to as F6A, F6B, F7A, F7B, F9A, and F9B; all are multiple turns of Kapton-insulated hollow rectangular copper conductor. The F9-coil turns are overwrapped with Kapton and fiberglass and vacuum encapsulated with epoxy inside a removable case form. The F6- and F7-coil assemblies are similar in construction to the F9, but were vacuum encapsulated along with a single E–coil turn inside a permanent case of stainless steel. The stainless steel coil cases form an integral part of the structural support system, which is the top-to-bottom load

path around the vacuum vessel. They support the vessel weight and applied vessel forces through four trunions located on the vessel midplane. The coil cases were manufactured by Votaw Precision Tool Co. in Los Angeles. The coil winding and encapsulating was done at GA Technologies' coil facility in San Diego.

Plasma disruptions can generate high induced voltages to these coils. The design requirement of 1000 v per turn during disruptions necessitated a coil insulation and test requirement of 60 kV terminal to terminal. The coils were tested to full voltage periodically during construction to prevent future need of repair to the encapsulated and encased coils, which is extremely difficult. Full insulation capability was demonstrated with dry Kapton prior to the epoxy encapsulation. Thus, weak areas of insulation were detected and repaired, and there were no coil turn faults when the coils were tested to 1000 v per turn after encapsulation.

Each of the 24 B–coil outer bundles is composed of six turns of water-cooled copper conductor. Machining was required on 20 of the 24 bundles to provide clearance for the new vessel ports. The belt bus components were assembled onto each of the B–coil subassemblies prior to installation onto DIII–D.

The subassemblies were installed in the following order. First the inner F–coil stack was installed, followed by the E–coil solenoid lower support beams, the F7B–coil assembly, the vacuum vessel subassembly, and the vessel insulation. Then the F7A–coil subassembly was installed, followed by the upper beam and coil subassembly, E–coil solenoid upper support beams, and the top E–coils. Next were the Upper B–coil subassemblies, the Outer B–coil subassemblies, the upper prestress ring and the lower prestress ring. Final installations were the vessel port extensions, the anti-torque structure, the neutral beam stands and isolation valves, and the vessel vacuum pumping station. The assembled tokamak prior to prestress ring attachment is shown in Fig. 3.1-4.

3.1.3. REFERENCES FOR SUBSECTION 3.1

[1] Davis, L., J. Luxon, P. Anderson, R. Callis, A. Colleraine, P. Rock and R. Stambaugh, "DIII–D Vessel Modification Project, Final Report for the Period FY83 through FY86," General Atomics Report GA-A19327, June 1988.

[2] Program Staff, "System Design Description of DIII–D," General Atomics Report GA-A19264, 1989.

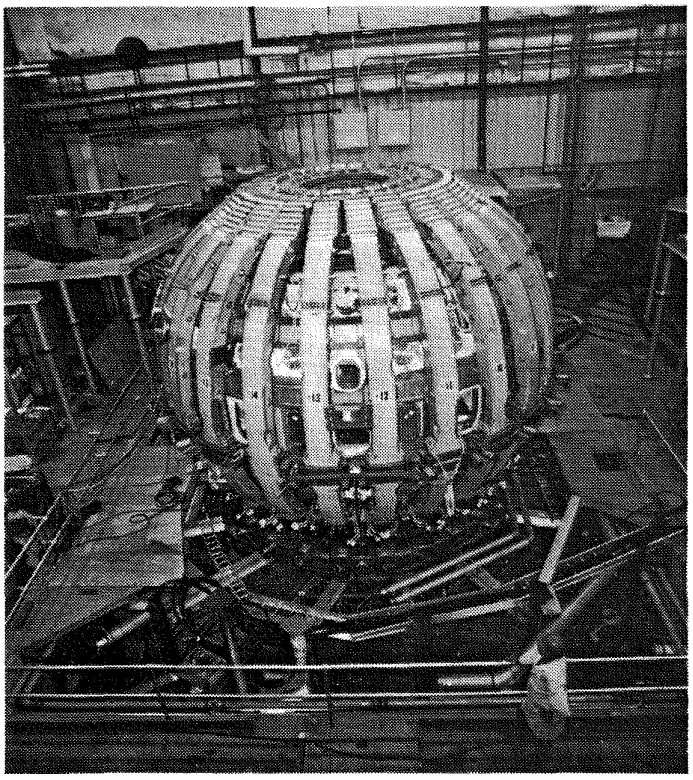

Fig. 3.1-4. DIII–D with toroidal field coils installed.

3.2. COMMISSIONING OF DIII–D (FY86)

3.2.1. SUMMARY

The Doublet III tokamak was shut down in September 1984 after six years of experimental operation that produced over 50,000 plasma discharges in a variety of shapes — doublets, circles, dees, and single null divertors. Record values of beta (4.5%) were attained along with demonstrating the importance of elongated high-current plasmas in improving beta and energy confinement time. It was also demonstrated that coils outside the vacuum vessel could produce divertor configurations whose confinement time was a factor of two longer than in limited discharges.

Recognizing that present scalings indicate that higher plasma current leads to improved plasma performance, a self-consistent design was developed (Table 3.2-1) that improved the capability of Doublet III within the structural limitations of the basic core of the machine. The design allowed for the reuse of the toroidal field coil and the innermost ohmic heating and poloidal field shaping coils and required replacement of the vacuum vessel and the outer poloidal coils and their supporting structure (Fig. 3.2-1). The coil

TABLE 3.2-1
DIII-D DESIGN PARAMETERS

Parameter	Anticipated First Year Capability	Ultimate Design Capability
Major radius	1.67 m	1.67 m
Minor radius	0.67 m	0.67 m
Vessel elongation	2:1	2:1
Aspect ratio	2.5	2.5
Plasma area	3 m^2	3 m^2
Plasma volume	30 m^3	30 m^3
Max. plasma current, limiter	3.5 MA	5 MA
Max. plasma current, divertor	2.5 MA	3.5 MA
Nominal discharge duration	6 sec	6 sec
Nominal flattop duration	1.5 sec	1.5 sec
Max. toroidal field on axis	2.2 T	2.2 T
Flux swing	9 V-sec	12 V-sec
Generator stored energy	3 GJ	3 GJ
Vessel protection energy handling capability	40 MJ	200 MJ
Neutral beam power	12 MW	14 MW
Neutral beam pulse length	0.7 sec	5 sec
ICRH power at 30 to 60 MHz	—	20 MW
ECH power at 60 GHz	1.4 MW	10 MW

design allows for a plasma current of 5 MA (3.5 MA diverted) for up to 5 sec with adequate access for 20 MW of auxiliary power.

The capability of the device was developed in stages. Presently, there is an ohmic and poloidal coil power supply capacity to drive 3.5 MA (2.5 MA diverted) plasma for 1.5 sec which is consistent with the vessel thermal handling capability of 40 MJ. Initially, the bulk of the auxiliary power capability (14 MW) was provided by four existing 80 kV neutral beam injectors which have been modified to use long-pulse ion sources (5 sec). The remainder of the auxiliary power come from electron cyclotron heating (2 MW) and ion cyclotron heating (9 MW). As the vessel's thermal protection and limiter systems are upgraded to their maximum design values of 200 MJ, the duration of the energy input of the heating systems can be extended from 2 sec to a full 10 sec plasma duration (maximum plasma current for a 10 sec pulse is limited to 4.0 MA).

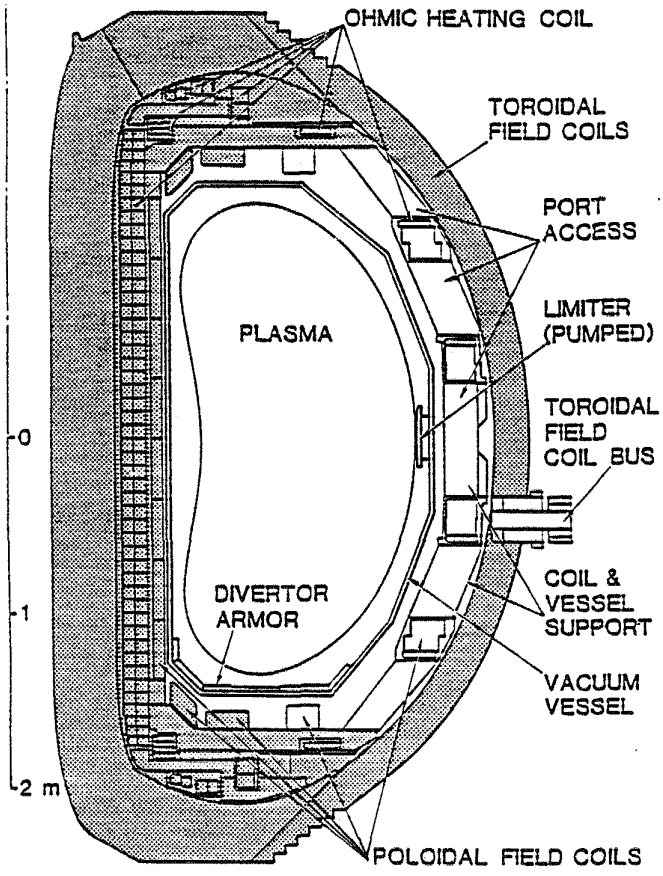

Fig. 3.2-1. Cross section of Doublet III. Reused Doublet III components shown shaded.

Progress in establishing machine operation was rapid. Baking to 400°C along with rf-assisted glow- and pulsed-discharge cleaning resulted in rapid cleanup of the vessel.

3.2.2. VESSEL COMMISSIONING

Prior to the first pumpdown of the fully assembled vessel in October 1985, the vessel interior was washed with hot deionized water and Alconox detergent using a high-pressure jet-spray apparatus. The wash was followed by a rinse with pure deionized water. After evacuation and leak-checking, the vessel was vented briefly for the installation of an initial set of internal magnetics probes. In November, the vessel was evacuated for commissioning of the bakeout and discharge cleaning systems. The vessel was baked at successively higher temperatures until the design temperatures of 400°C on the walls and 150°C on the port flanges were reached. The discharge cleaning systems were run only long enough to demonstrate their operational status.

In early December, the machine was opened for a seven-week period to install limiters, thermal armor, Langmuir probes, thermocouples, and the remaining sets of magnetic probes. The thermal armor alone doubled the surface area of Inconel in the vessel and added $\sim$10 m^2 of graphite to the previously all-metal vessel. In addition, many diagnostics were attached from the outside to ports with demountable flange seals. After pumpdown in late January, the vessel was conditioned with bakeout ($T \leq 350°$C) for 40 hr, rf-assisted glow-discharge cleaning ($T = 250°$C) for 20 hr, and pulsed-discharge cleaning ($T = 350°$C) for 4 hr. Plasma initiation with low voltage (10 V/turn) startup was successful on the first attempt.

3.2.3. PLASMA OPERATIONS

The construction of DIII–D was completed in February of 1986 at which time conditioning of the vacuum vessel commenced [1]. After about 100 hours of baking, rf assisted glow discharge cleaning, and Taylor pulse discharge cleaning, plasma operations were begun. On February 25, 1986, a plasma was successfully made on the first attempt, producing over 350 kA of plasma current (Fig. 3.2-2). By the end of the first day plasma currents of 0.5 MA with a flattop time 300 MA had been produced. The performance of DIII–D improved at a steady rate, with 2.5 MA plasmas limited, and 1.3 MA diverted, being produced by late June. During this same period a full range of plasma cross sections were investigated (Fig. 3.2-3); these included circles, dees with elongation up to 2.2, double and single null divertors. Discharges were maintained for more than 3 sec. No stability problems were observed in elongated plasmas, even at elongations as high as 2:1 in dees and 1.6:1 in divertor-shaped plasmas [2].

3.2.4. ECH SYSTEM

During a vent in July 1986, eight Electron Cyclotron Heating (ECH) antennas were installed on the outer vessel wall (low magnetic field side) of the DIII–D tokamak, with each antenna connected to a single 0.2 MW gyrotron. The antennas are distributed vertically over a height of 0.36 m centered on the midplane, and they are directed $\pm 17°$ with respect to the radial direction. The antenna consists of a vacuum barrier window of fused quartz with a diameter of 3.8 cm, which carries the TE_{01} mode, followed on the vacuum side of a taper to 1.9 cm, a mode converter to the TE_{11} mode, and a second converter to the HE_{11} (See Fig. 3.2-4 for a simplified schematic of the ECH waveguide system). The HE_{11} waveguide radiates with an approximately gaussian radiation pattern of characteristic angular half width 11°. The output is linearly polarized with the electric field in the

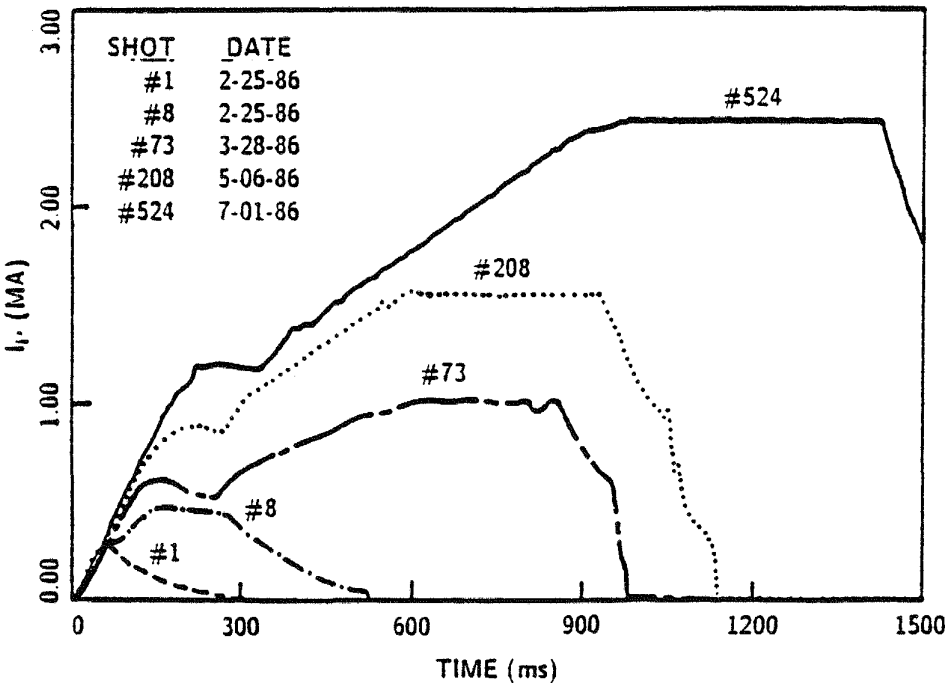

Fig. 3.2-2. DIII–D plasma current history for five discharges illustrating the progress in attaining high constant plasma currents over the first several months.

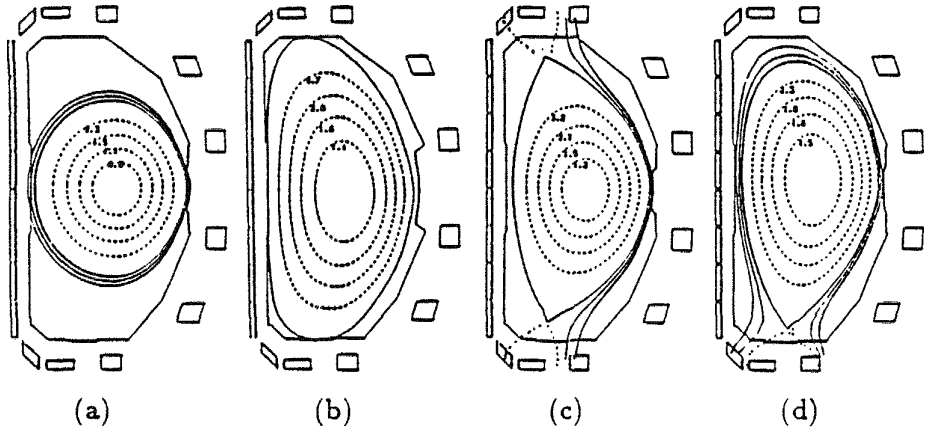

Fig. 3.2-3. MHD equilibrium cross sections for ohmic discharges produced in DIII–D. (a) $\kappa = 1.2$ limiter discharge, (b) $\kappa = 2.1$ dee-shaped discharge, (c) double null divertor, (d) single null divertor.

vertical direction; for the 17° orientation this provides over 90% of the incident power in the X–mode. About 68 ± 5% of the generated power is launched as a pure X–mode and 8% is launched as an O–Mode. The remainder is dissipated in waveguide losses.

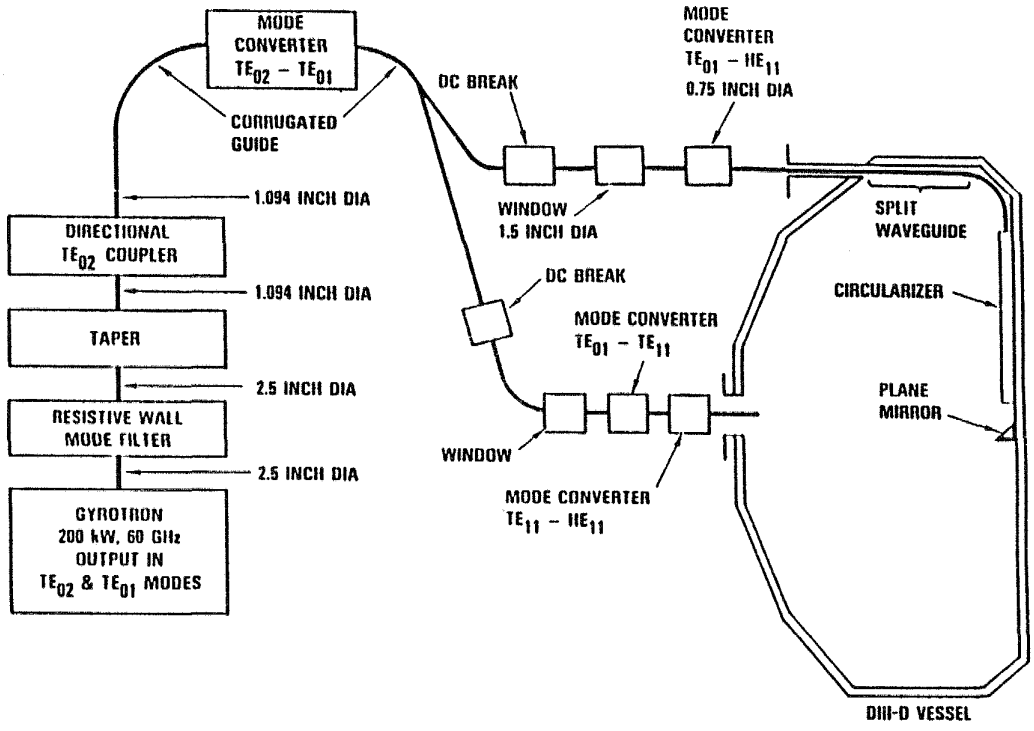

Fig. 3.2-4. Schematic of the inside launch and outside launch for ECH system.

ECH experiments during FY86 using outside launch of the extraordinary mode showed effective heating at the fundamental resonance, in apparent contradiction of the theory of wave propagation. This result is explained by an efficient process of mode conversion from the extraordinary mode to the ordinary mode upon reflection at the vessel wall of waves reflected from the right hand cutoff in the plasma. The resulting heating has the characteristics expected for heating with ordinary mode.

3.2.5. REFERENCES FOR SUBSECTION 3.2.

[1] Luxon, J., P. Anderson, F. Baity, C. Baxi, G. Bramson *et al.*, in Plasma Physics and Controlled Nuclear Fusion Research, Kyoto, 1986 (IAEA, Vienna, 1987).

[2] Kellman, A.G., N.H. Brooks, L. Davis, J. Luxon, M. Ali Mahdavi, T.S. Taylor, and the DIII–D Physics Group, *Bull. Amer. Phys. Soc.* **31** (1986) 1502.

3.3. HARDWARE DEVELOPMENT (FY87 – FY88)

Following the commissioning phase of DIII–D (see Subsection 3.2), the experimental program initiated dual tasks of developing an understanding of the physical limits for high beta plasmas, and exploring the phenomena at the plasma edge with the goal of improving the energy confinement time. As with most experimental devices hardware must be changed or modified to adjust to the changes in the experimental program and to new technological developments. Along these lines several hardware changes were made to DIII–D. These changes included the addition of eight long pulse ion sources, 10 inside launch ECH antennas, new graphite armor for the vacuum vessel floor, inner wall, and ceiling, a new magnetic probe array, 2 MW of ICH power, neutron shielding and many new diagnostics. Besides new hardware there is a constant effort to improve and update all the existing support systems such as power supplies, computers and other auxiliary support systems.

3.3.1. NEUTRAL BEAM LONG PULSE ION SOURCES

The neutral beam system had been completely reconstructed during the vessel modification project of 1985/86 to provide for multi-second operation when long pulse ion sources became available. Commissioning of this heating system proceeded in parallel with the tokamak start-up using the vintage short pulse ion sources, leading to the first observation of H–mode discharges in an open divertor configuration. As a consequence of these significant results, installation of the new long pulse neutral beam sources was accelerated in order to yield more pulse length and heating power so that the range and nature of the experiments could be extended. Completion of this effort was marked by the injection of 10 MW of power for 2 sec in May 1987, more than one month ahead of schedule.

Since that time, the delivered power levels and pulse lengths have been increased and routine operation with both hydrogen and deuterium has been possible for five second pulses. A new technique of regulating the arc power has been tried and this enables an ion source to run stably at a higher than anticipated perveance. When hydrogen is used as the fueling gas, the neutral power delivered to the plasma by each source at 80 kV is approximately 1.5 MW (*i.e.*, $\approx$ 12 MW for the four beamlines). The equivalent number

with deuterium fueling is about 2 MW/source and, although all beamlines have not been run simultaneously in this mode, a possible 16 MW of delivered power is available.

3.3.2. VESSEL ARMOR

During FY87, a design for an upgrade of the vacuum vessel protection system for DIII–D was completed. The ceiling, floor, and inner wall of the vessel was completely armored with over 1500 graphite tiles which will enable plasma operation with double null diverted plasmas and allow the use of the inner wall as a limiting surface (Fig. 3.3-1). Prior to late CY87, the vessel wall was partially covered with cast Inconel tiles and Inconel castings with Poco graphite brazed to the top surface. The broad graphite tiles proved not to have the thermal ruggedness demanded by divertor operation. A new design concept was needed that could survive the higher thermal loadings and still meet the cool down requirements.

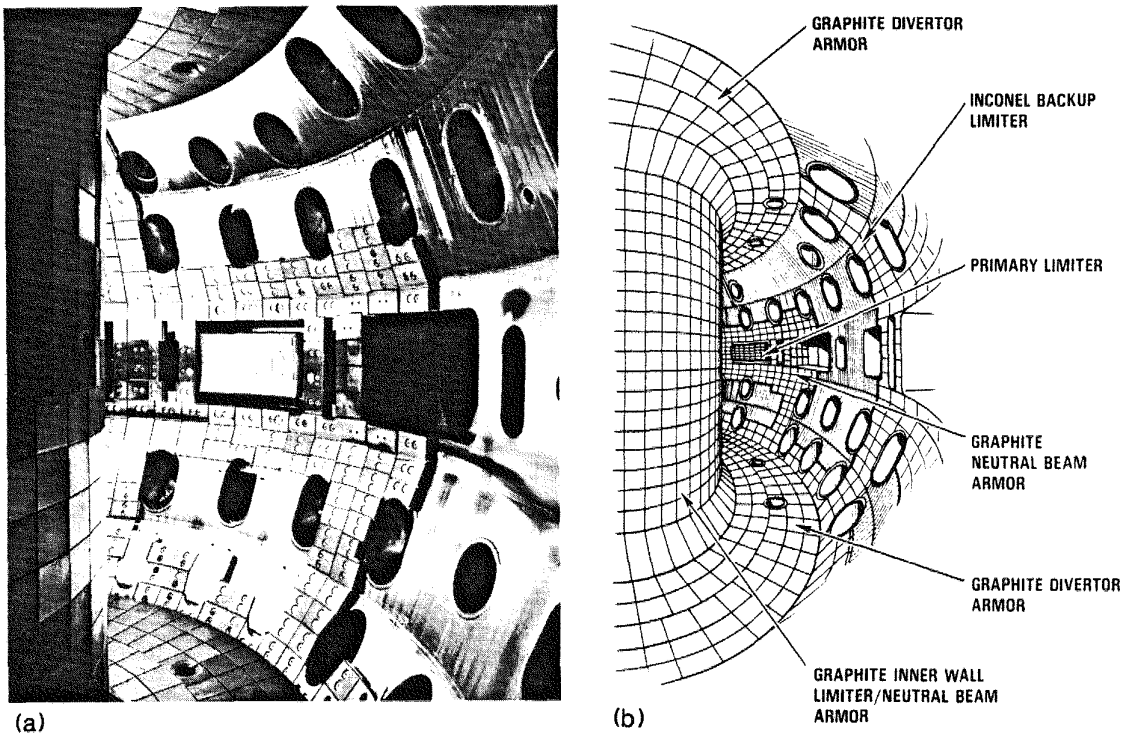

Fig. 3.3-1. (a) Actual view of DIII–D vessel protection, and (b) artist's conception of DIII–D interior.

Two design concepts were developed along with a review of graphite materials available. Two-dimensional thermal/stress analysis was performed on each of the two design concepts to optimize the designs. A three-dimensional analysis was then performed on each.

The three-dimensional analysis showed significantly lower thermal stresses in one design, the edge clamped concept (Fig. 3.3-2). Especially important was the lower stress in the critical area around the hold-down point. There were also other advantages to this design, such as the absence of through holes acting as sharp stress concentrators which could lead to failure. After a complete evaluation of the two designs, the edge clamped concept was chosen.

A parallel study to the design effort was undertaken to evaluate the material for the tiles. Research and analysis were performed to screen the list of approximately 45 candidate graphites. Using calculated parameters and other criteria such as cost and availability, the list was reduced to six. A testing program was implemented in conjunction with Sandia National Laboratory, Albuquerque (SNLA). Prototype tiles were manufactured from the candidate materials and tested in the ion beam facility at SNLA. Conclusions from the testing program were that Union Carbide TS-1792 graphite was the most suitable material and that the tile design could survive the design heat fluxes without failure.

3.3.3. ECH INSIDE LAUNCH SYSTEM

An ECH inside launch system consists of a gyrotron for microwave generation, oversized waveguide transmission line ending at a vacuum window interface followed by mode converters, internal waveguides, a split waveguide, a circularizer waveguide, and a launching antenna in the form of a copper mirror plus the required support structure. Figure 3.3-3 shows a schematic of these components inside the DIII–D vacuum vessel.

The work was split into two subtasks: (1) waveguides outside DIII–D, including the vacuum boundary waveguides up to the flanges on the machine, and (2) the waveguide runs through the tubular port, across the top of the vacuum chamber, and down the centerpost, terminating in the mirror assembly at the centerpost midplane.

The inside launch concept required the development of a new waveguide component, a split waveguide which carries the microwaves across the ceiling of the vacuum vessel. This section of waveguide is split to prevent breakdown of the vessel gas in the waveguide, as the vacuum window is outside the vessel. The brazing and subsequent splitting of the waveguide was important and time consuming. A brazing technique was developed

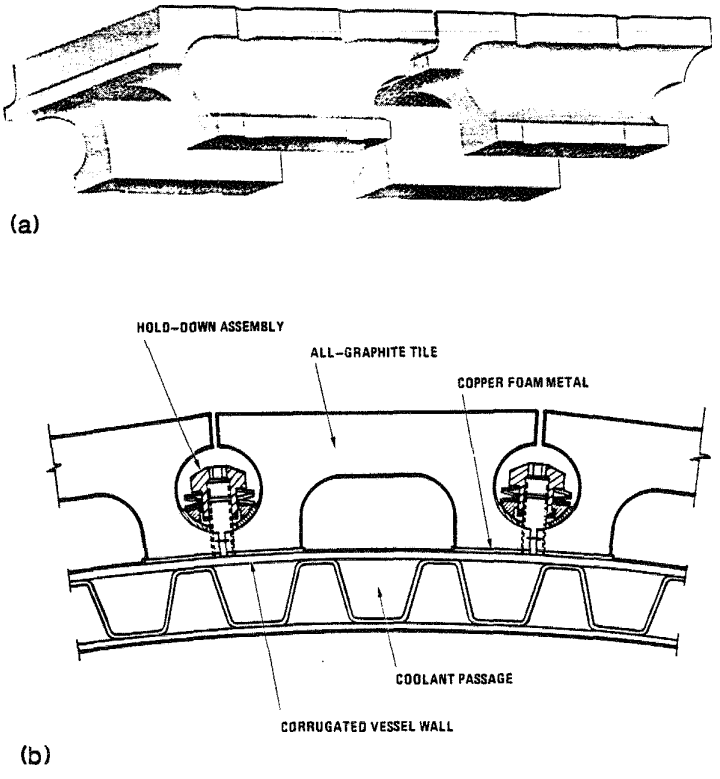

Fig. 3.3-2. (a) CAD conception of DIII–D armor tiles, and (b) cross section of vessel wall showing tiles and hold-down components.

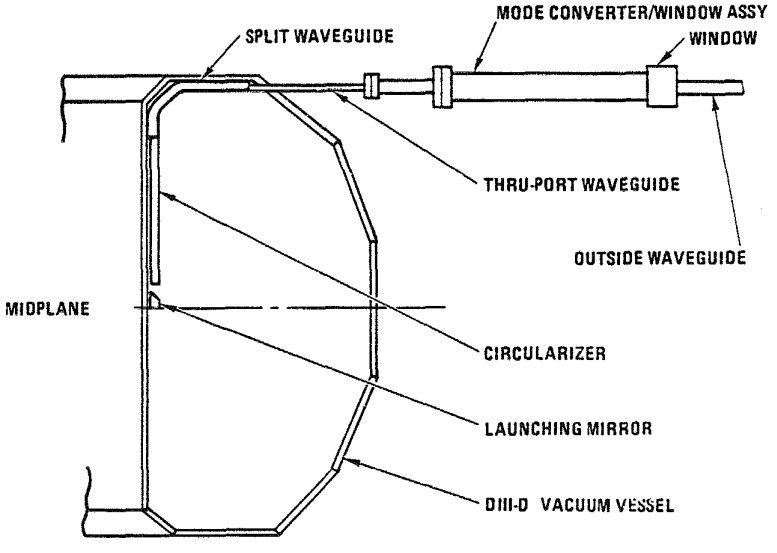

Fig. 3.3-3. Inside launch waveguides in the DIII–D vacuum vessel.

that satisfied design requirements. The design required that a convoluted waveguide be brazed into a precise cavity formed between the halves of the split supports. The brazed assembly was split using a wire EDM process to achieve a clean and precise cut across the convolutions.

The electrodeposit plating process for manufacturing the corrugated waveguides presented many challenges for the designer and for the plater. The waveguide material is plated over machined aluminium mandrels, and after plating, the mandrel is caustic-etched away. The thickness of the plating critical to achieve the best compromise between strength, flexibility, leak tightness, and the capacity to stay round. Waveguides that needed bending were plated from copper with a nickel strike on the outer diameter wherever a brazing operation was necessary. Waveguides that had to remain straight were plated from bronze. All waveguide runs in air were plated from copper.

All hardware to complete that part of the waveguide system located inside the vacuum vessel was installed during the December 1987 machine vent. Two of the required ten waveguide assemblies, located at 45°, which consist of a mode converter and window assembly were also installed during the vent. The other eight assemblies at 240° and 255° were installed during the May 1988 machine vent.

3.3.4. ICH 2 MW SYSTEM

The ICH program at DIII–D started with low power coupling tests of a fast wave ICRF antenna design and built by ORNL. Measurements indicated that the coupling changed dramatically when the plasma reached H–mode conditions. It was determined that the coupling of this antenna would not be appropriate for H–mode plasmas and changes were proposed. The antenna was modified by ORNL in order to improve the coupling to DIII–D H–mode plasmas. Based on theoretical modeling, the antenna geometry was modified in order to increase the amount of rf magnetic flux linked to the plasma. The changes include (1) removal of the back tier of the Faraday shield, (2) moving the current strap closer to the plasma, and (3) increasing the depth of the antenna in order to reduce the cancellation effect of image currents flowing in the backwall. These modifications are increased the antenna loading.

The original ICH 2 MW system design was modified to achieve operation at frequencies below 31 MHz, 2.25 MW pulses (1 sec) at 45 MHz, and 1.9 MW pulses (10 sec) at 60 MHz have been obtained. Harmonic content in the output waveform became apparent at the lower frequencies, and necessitated the addition of stub tuners to the driver and final power amplifier outputs to bring these harmonics down to acceptable levels.

Final acceptance tests of the ICH 2 MW system took place in May 1988, and the system was shipped and installed at GA. In the 4th quarter FY88, RF power testing into dummy load was completed with an early version of X2242 final amplifier tetrode (as delivered by Continental Electronics). Power levels of 500 kW or 500 msec and 250 kW for 10 sec were achieved. The original X2242 tetrode was repaired at Varian, and was then reinstalled and tested to the same power levels. Testing at higher power levels will begin following the completion of new protection circuits recommended by Varian.

RF leakage from the dc breaks between the DIII–D and transmission line grounds was corrected by installing additional shielding. Antenna conditioning and rf leakage measurements continues at increasing power levels at the close of FY88.

3.3.5. MAGNETIC PROBE ARRAY

A magnetic diagnostic system is required in the DIII–D vessel to provide voltage signals for feedback control of the plasma current and plasma position and shape, as well as to acquire data which can be used to analyze machine performance.

A number of the individual magnetic probes comprising the two poloidal arrays originally installed in the vessel had failed over the first two years of machine operation. A new more robust, but simple, magnetic probe design has been developed to eliminate the problems which contributed to the failures experienced with the original design. The new probes exhibit essentially the same signal strength as the original probes, along with a frequency response on the order of 50 kHz.

A total of 44 magnetic probes were fabricated for installation in the vessel during the December 1987 machine vent.

3.3.6. NEW SHIELDING FOR DIII–D

3.3.6.1. Introduction

A neutron shielding system is being prepared for the DIII–D facility to allow a full program of experiments in deuterium while limiting the radiation at the site boundary to 20 mRem per year. The goal of the shielding effort for the DIII–D facility is to provide a shielding enclosure (walls and roof) which reduces the radiation at the site boundary by a factor of two by the end of 1988 (roof alone), and which reduces the radiation at the site boundary by a factor of 300 when complete in April 1989.

It is desirable to minimize the interference of the shielding system with the existing diagnostic and other devices. It is also necessary to maintain access to the torus hall using the existing overhead 20-ton bridge cranes in order to handle heavy equipment and machinery. The weight of the added shielding system must be kept to a minimum since it will increase soil bearing pressures that can produce differential settlement in the DIII–D facility.

3.3.6.2. Design Description

Several concepts were evaluated to provide the required supplemental shielding to the DIII–D facility. The conclusion of the engineering study is that the Translating Overhead Protective System (TOPS) concept best meets the design requirements since it provides minimal experimental interference, maintains access to the machine pit area and minimizes additional structural and foundation work, if any, that may have to be performed on the building.

Figure 3.3-4 shows the chosen TOPS concept, which consists of a fixed roof, translating roof, and side walls. Figure 3.3-5 shows a CAD isometric projection of the roof.

Table 3.3-1 presents the basic specifications for the TOPS system. Water in the form of gel was used as the shielding material for the roof because of its availability, low cost and ease of installation. The gel is packed in fiberglass boxes which are placed over the roof supporting structure. The gel, though more expensive than water, has the following advantages: it has little water-sloshing effect during possible seismic activities; it keeps boron uniformly distributed; it is leak resistant against small holes or punctures.

Since building settlement can occur due to the added weight of the shielding, a soil study was performed to determine the load-settlement curve for the soil under the building. The variation in settlement due to the increase weight is not significant. Major components of the TOPS system are briefly described below.

3.3.6.3. Fixed Roof

The fixed roof located at the northern end of the DIII–D facility is supported by the existing crane structure. The roof structure is made of supporting steel structure framing with built-up plate girders and 1-3/8-in. corrugated metal decking for support of the selected shielding material. In order to provide access to the 20-ton cranes, the existing 20-ton north crane will be parked over the fixed roof when the translating roof is closed over the pit. Also, to access the machinery underneath the fixed roof, such as the neutral

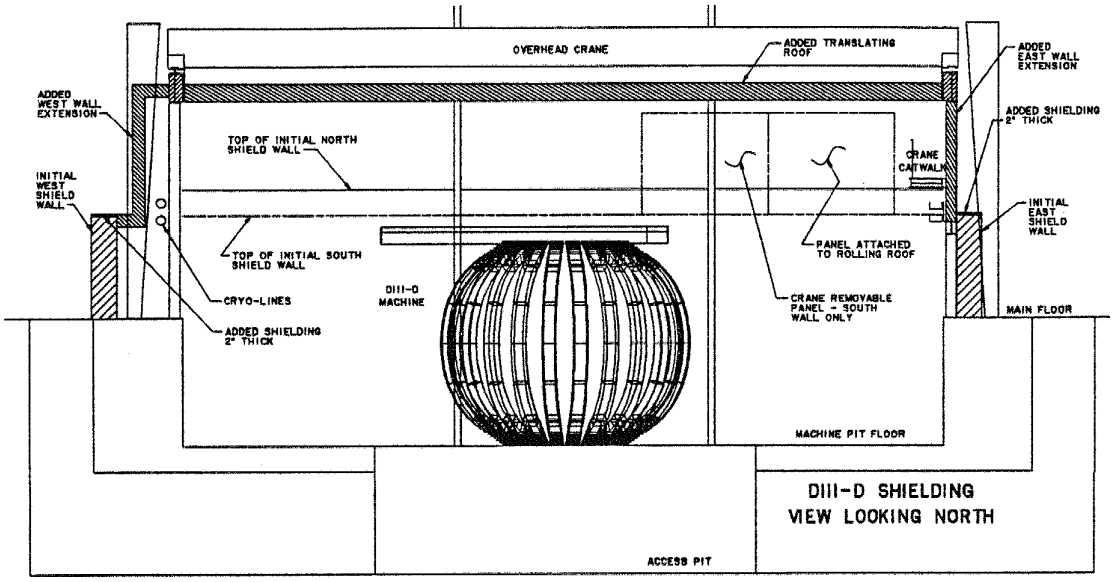

(a)

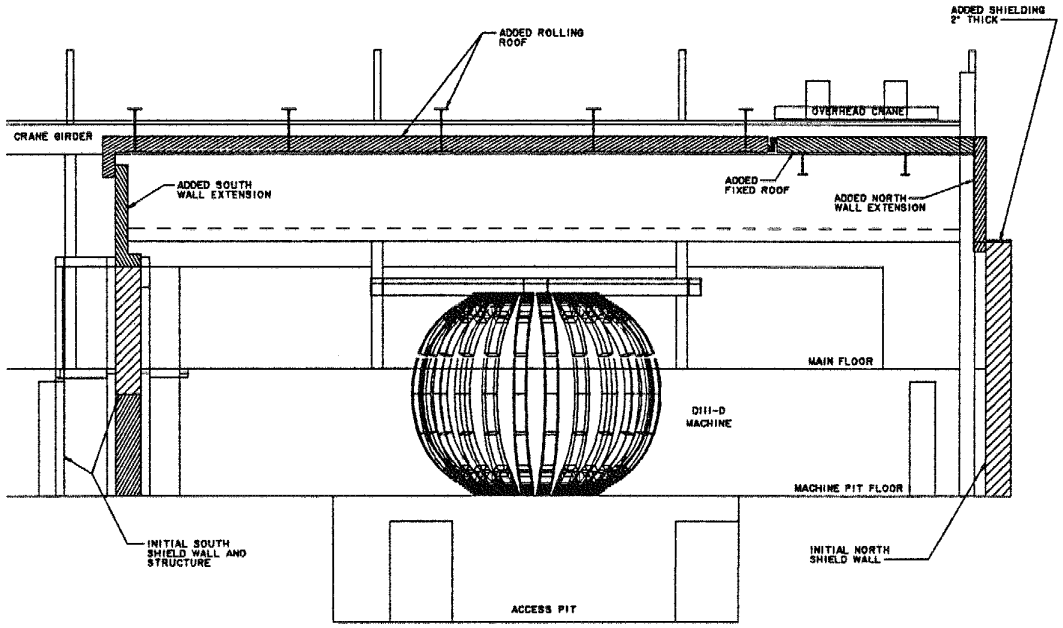

(b)

Fig. 3.3-4. Overall shielding geometry of DIII–D; (a) viewing looking north; (b) view looking west.

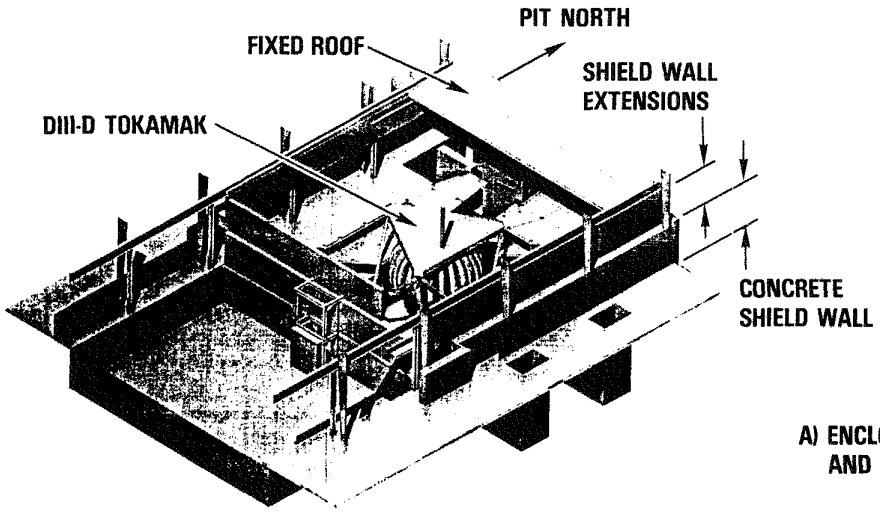

A) ENCLOSURE ROOF OPEN (MOVING ROOF AND CRANES OUT OF PICTURE AT LEFT)

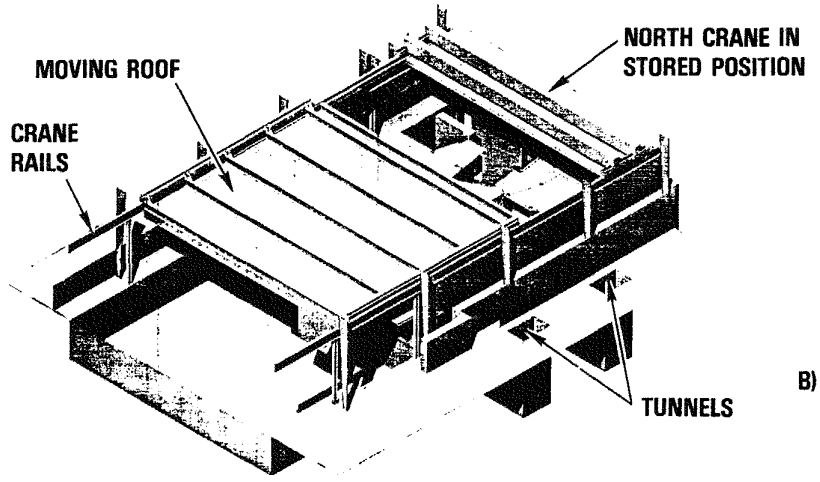

B) ENCLOSURE ROOF PARTIALLY OPEN SOUTH CRANE OUT OF PICTURE AT LEFT (AVAILABLE FOR SERVICE)

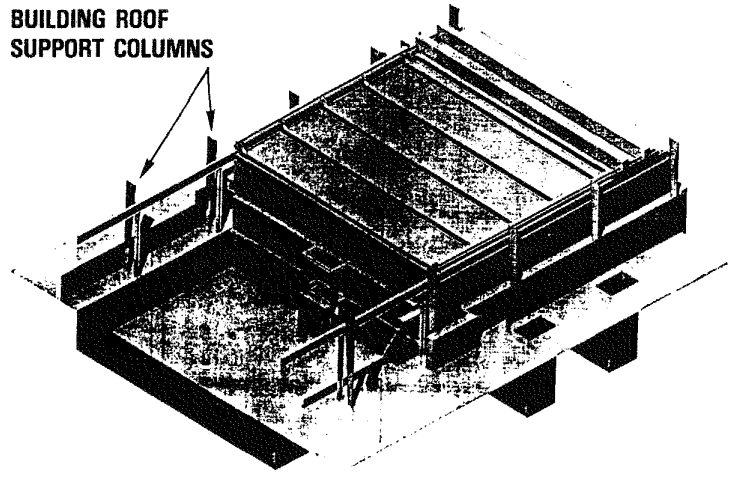

C) SHIELD ENCLOSURE CLOSED

DIII-D RADIATION SHIELD CONCEPT. THE SHIELDING ENCLOSURE IS COMPLETELY WITHIN THE DIII-D BUILDING. THE ENCLOSURE ROOF OPENS TO ALLOW CRANE ACCESS TO THE TOKAMAK AND SURROUNDING EQUIPMENT.

Fig. 3.3-5. Roof design.

Table 3.3-1.
Basic Specifications of the TOPS System

Shielding Materials	
Roof	13 in. of borated water in gel form packed in fiberglass boxes.
Walls	Pourable shielding materials or poly/boron sheets equivalent to 12-in. B-poly. Flexible hydrogeneous foam is considered in penetrations and embedments where conduits and pipes have to be moved.
Dimensions	
Fixed roof	14 ft × 61 ft
Translating roof	54.5 ft × 61 ft
Fill-in walls	
North	61 ft × 7 ft
South	61 ft × 9 ft [a]
East	68.5 ft × 10.5 ft
West	68.5 ft × 12.5 ft [b]
Environmental Control Systems	
Heat removal	A new ventilation system to be installed in the torus hall area in order to regulate the temperature inside.
Fire protection	A fire-suppression sprinkler system along with smoke and fire alarm will be provided.
Lighting	A lighting system will be attached to the translating roof, and sufficient lighting underneath the fixed roof.

[a] Includes 2-ft overhang attached to translating roof.

[b] Includes 3-ft, 10-in. horizontal slab wall.

beam source housings, etc., a 4-ton underhung bridge crane will ride on the east-west spanning girders and will be able to move objects at least 6 feet from the southern end of the fixed roof.

3.3.6.4. Translating Roof

The translating roof structure rides on the existing crane support structure and can be moved in or out of the machine pit area. This permits easy access to the torus hall area and allows installation and maintenance of the moving portion of the roof to be performed in the high bay area away from the DIII–D machine, thus minimizing interference with the experimental work. The translating roof structure consists of a similar supporting structure framing with tapered built-up steel girders with preset camber spanning the east-west direction across the machine pit. A 1-3/8-in. corrugated metal decking supports the shielding materials between the girders.

3.3.6.5. Side Walls

The side walls fill the space between the existing concrete shield walls and the roof shielding. The shielding material is a castable material in a hydrogenous binder placed in fireproof plywood forms.

3.3.6.6. Penetration Management

There exist a multitude of openings (or penetrations) on the shielding enclosure. The important penetrations include eight openings for high-voltage cables leading to eight ion sources, four openings for cable trays for the torus, two for ECH waveguides, one for the ICH transmission lines, one for cryogenic lines, and two long-slot openings (13 cm by 1680 cm, each) along the roof by the East and West wall. The last slot openings correspond about 65% of the total penetration area, although not direct line-of-the-sight.

In addition to these penetrations, there are four entries and five underground tunnels. The entry ways will be provided with sliding shield doors with equivalent shielding effectiveness as the existing concrete wall. The effect of the tunnels appear to be of minor concern in terms of radiation leakage, since they are located roughly 4.3 meters below the torus median plane or nearly the ground level, and extend horizontally some 20 meters before turning upward to the ground level (about $z = 0.6$ m).

3.3.7. POWER SYSTEM OPTIMIZATION

The power system for the DIII–D experiment increases in size and complexity with each upgrade. The purpose of the ohmic heating (E) power system is to drive poloidal E–coil current and to induce plasma current into the tokamak machine. The toroidal (B) power system energizes the B-coil and produces a magnetic field for plasma confinement.

The plasma shape control system or field (F) shaping system, provides fine tuning of plasma position and shape during operation. The F system is made up of seven medium-sized power supplies and 36 high-speed SCR switching regulators called "choppers" which control individual poloidal coil currents. There are 20 low voltage (600 V dc) and 16 high voltage (1200 V dc) choppers. The vertical field power supplies are called V and HV power supplies. The divertor power supplies are called D supplies. T (tweaker) supplies provide additional fine tuning of the magnetic field. The low voltage choppers are called X choppers and the high voltage choppers are called the HX choppers. Experimental flexibility is achieved with an elaborate high current patch panel where all tokamak field coils, power supplies, and choppers can be interconnected. Multiple coils can be driven from one F power supply. Choppers are usually connected in parallel to drive current in one coil.

DIII–D experiments have required higher operating power levels from the power conversion system. Demands for longer pulse lengths and higher coil currents resulted in new power system challenges in 1988. Most of the original power supplies were specified for shorter pulse operation. Component aging increases when the power supplies are operated at their peak power design levels, and this has resulted in some system failures.

Improved system availability at the new energy levels was in FY88 was achieved by upgrading the existing power supplies and solving recurring operational problems. An expanded effort to identify and correct potential problems was started.

In an integrated systems effort, the Electrical Engineering group reviewed the original specifications and actual component configurations. Marginal components were identified, evaluated, and replaced. A review of SCRs, fuses, interphase reactors, and transformers was made for the line-commutated converters. New SCRs and fuses were installed on the HV1 supply to bring it up to the same performance level as that of the newer HV2 supply. These new components have higher thermal capacity and higher current ratings. Water cooling lines were cleared, water flow was adjusted, and water flow monitors were installed in critical areas.

Power systems schematic diagrams were updated in an ongoing effort. Documentation was upgraded to actual as-built configurations on water flow interlocks, power supply fault interlocks, and power supply access interlocks. The discharge cleaning system was also upgraded to a higher performance Taylor discharge cleaning method. Modifications to the poloidal E-coil system pulse current shaping circuit were made.

The D1 and V1 power supplies had experienced repeated down time due to failures of the main circuit breaker failures, which were mechanically fatigued. New vacuum circuit breakers were installed to correct that problem. T1, T2, and HV1 circuit breakers are also being refurbished and replaced.

Critical field shaping control chopper equipment was modified to provide better current sharing when driving the F-coils. The current sharing resistor and reset inductor modification improved chopper availability. A chopper paralleling control selection panel was installed in the control room annex to allow operators to reduce chopper-to-field coil connection errors and lost time. Additional choppers were needed for for the higher coil currents, so two new HX choppers were fabricated and four U choppers were converted to the improved X version. New higher energy coil current discharge resistors were installed on the HX choppers. Current monitoring circuits using LEM devices were installed on all choppers for longer pulse requirements. A new chopper test facility was constructed.

Current versus temperature measurements were conducted on the poloidal field high current switch contacts. These measurements indicate that the switch contacts are being operated well within a thermally safe region.

An I^2T energy calculator was designed to allow higher utilization of power converters. A prototype calculator was installed in HV1 for evaluation. Production units are expected to be in place in all of the power converters by the end of FY89. The I^2T calculators will maintain power supply operation within design limits independently of operator actions.

An internal test circuit was designed and incorporated in three of the F power supplies. This circuit provides an independent 3-phase signal source for troubleshooting power supply control circuits without using the primary power source, and it is available at the flip of a switch. The amount of setup time required for troubleshooting is greatly reduced. This test circuit will be installed in all of the F power supplies by the end of FY89.

A recording system was designed and installed in the control room annex to digitize and store the voltage and current waveforms from each of the power supplies and choppers. These waveforms are invaluable in analyzing performance of the power converters. Under specific predetermined circumstances, the waveforms can be stored in the permanent computer data base.

The numerous changes made during FY88 included several other tasks. Bench test equipment was fabricated for repair and calibration of E and B power supply circuit boards. Control systems were calibrated and realigned. Also, B power supply module output current balance was greatly improved.

3.3.8. NEUTRAL BEAM POWER SYSTEM CONVERSION FOR ECH

Two of the eight neutral beam power systems (NBPS) installed at GA were procured with dual polarity crowbar assemblies, and are convertible to negative polarity high voltage output for use in electron cyclotron heating (ECH) experiments. One of the convertible NBPSs was delivered in the negative polarity configuration from the factory, and was used in ECH experiments until October of 1987. It was then converted to the positive polarity output configuration for use in neutral beam injection (NBI) experiments with the new common long pulse ion sources. Modifications were made to simplify future polarity changes so that the setup for either ECH or NBI use can be accomplished with minimum down time.

The conversion from NBI to ECH configuration was accomplished by reversing the polarity of the rectifier stacks in the transformer/rectifier, the polarity of the connections to the crowbar, the polarity of the connections to the modulator/regulator, and connecting the ECH control system to the modulator/regulator.

A change from one configuration to another can be achieved in three days, and thus, can be accomplished over a weekend in conjunction with a following maintenance day.

3.3.9. TOKAMAK AND NEUTRAL BEAM CONTROL SYSTEM

The tokamak control system has been functioning since prior to the startup of the Doublet III fusion device in 1978. The system consists of one MODCOMP 16-bit Classic II/25 cpu and one CAMAC serial highway connected to hardware throughout the complex. The system controls and monitors approximately 1,800 discrete points relating to power supplies, vessel temperatures, timing synchronization, thermocouples, and so on.

During FY87, the tokamak control system hardware was upgraded by replacing the disk drive with a larger, faster drive, which also is compatible with the other drives at the installation. The memory was doubled to 1 Mb. The operating system was brought up to current levels, and new features were incorporated into the system. Considerable work was done on the residual gas analyzer system. Two more mass peaks were added to the display. A second RGA unit was added, and the accompanying control software was installed. Data acquisition was modified to acquire spectrum just before and after a tokamak shot, incorporating this data into the shot data file. Additional checks were built into the system to ensure reliability. The software, which monitors the San Diego Gas & Electric power loads, was redone to add functionality and to be more user friendly.

There are four neutral beam injectors, consisting of two sources in each beam unit. Four MODCOMP 16-bit computers (two model 7870s and two Classic II/75s) control, monitor, and acquire data. Each cpu is responsible for one injector. The cpu's are networked together and also are networked to a central PC console. Each cpu controls similar equipment (although there are two types of power supplies used by the beam injectors) and run nearly identical software. Each system monitors approximately 1,500 distinct digital points per second, and approximately 150 Kb of data is collected with each neutral beam shot. The beamlines can be run in several modes: test stand, calorimeter shots, source conditioning, and DIII–D plasma injection.

Changes were made to several elements of the neutral beam systems to accommodate the use of the long pulse sources. This included changes to digitizer initialization and acquisition software to handle the new dual clock rates for the slow digitizers. The data base was modified for the new clock rates, and plotting of waveforms was also modified. New hardware and software was put in place to be used with thermocouple groups. Changes were made for data acquisition and alarming functions. Some changes were made in sending the neutral beam data to the data acquisition computers when the beams are running synchronously with DIII–D. This aspect of communications has been extremely successful and also very important to the physics analysis, since this is the only mechanism for having beam power included in the shot data base. Procedures were automated which send the historical data from the beam computers to the User Service Center VAX cluster. this data is used for long-term trending and other studies. An IBM PC was installed, and software development is proceeding. This PC will be a central console to display summary information from all four neutral beam computers. Successful transfer of data from one MODCOMP to the PC has been accomplished.

3.3.10. DATA ACQUISITION SYSTEM

The DIII–D data acquisition system consists of three MODCOMP mini-computers (two 7870s and one Classic 32/85), two VAX 11/785s, and one MicroVAX II. The MODCOMP computers are responsible for initializing all equipment for data acquisition (clocks, digitizers, memory modules), for reading, checking, and formatting all data just after a tokamak discharge; and for archiving this data to tape and to one of the VAX 11/785s. One VAX 11/785 is used to receive data from the MODCOMP system and archive it in a format which is used on all the VAX computers at GA. This VAX also receives data from other VAXes on the network for inclusion in the shot data file. Data from calculations is generated between shots, and this VAX also archives the calculated results. The second

VAX is used to do calculations needed to examine the tokamak discharge. This is primarily MHD analysis. Some other analysis programs are run on both VAXes if CPU cycles are available. The MicroVAX is used to do analysis and generate data for inclusion in the shot data file.

During FY87, the total DIII–D acquired data size grew from 11 Mb per shot to over 17 Mb per shot as new diagnostics were installed on the tokamak and added to the computer systems. The bulk semiconductor memory on the MODCOMP was expanded to 24 Mb to handle the increased data size. Incompatibility problems between the MODCOMP 32/85 and CAMAC were resolved by some software changes to the CAMAC driver and firmware changes to the hardware device driver. The computer was then installed for routine data acquisition, doubling the amount of data which can be handled for a shot. The digitizer timing capability to use asynchronous triggers and both pre- and post-trigger sampling was installed. Software and hardware were developed and installed to perform automatic digitizer calibration on the MODCOMP systems. A spare MODCOMP system was purchased to provide hardware redundancy. A change in the MODCOMP-to-VAX archiving code resulted in data arriving on the VAX sooner.

The capability for revising shot data header parameters was developed and implemented on the VAX systems. The data interface software (PTDATA) was modified to run on MicroVAX or other satellite systems and access data from either the DIII–D VAX cluster or the User Service Center VAX cluster. Mechanisms were developed to acquire data from MicroVAX and PDP11 based systems directly over DECnet. This is now being done routinely for several diagnostics such as Thomson profile. The MFIT MHD analysis code is run automatically every shot and computes numerous parameters for 50 time slices which are added to the shot data file. A MicroVAX II was purchased and installed to perform analysis for several diagnostics between shots and to add calculated results to the shot data file. A MicroVAX 3500 has been ordered which will be used to do substantially more MFIT calculations between shots. Most real time data analysis codes have been examined and modified for efficiency. A substantial amount of cpu time has been saved thus freeing time for other calculations. Disk defragmentation software was installed thereby eliminating a number of problems that had resulted from fragmented disks. System time has been synchronized on all VAX and MODCOMP computer systems. Shot data compression now runs on both members of the DIII–D cluster. Installation began on a new ethernet link between the DIII–D cluster and the User Service Center cluster. Measures were implemented to improve the VAX system security.

3.4. FY88 OPERATIONS

3.4.1. TOKAMAK OPERATIONS

During FY88 the DIII–D facility operations ran very smoothly. The availability increased to 78%, the highest achieved including Doublet III. This high availability led to the productive scientific program described in Section 3.

The DIII–D tokamak operation schedule is shown in Fig. 3.4-1. Typically operation was 4 to 5 days of 10 hours per week. The normal operation periods were two weeks in a row, separated by a maintenance period of one or two weeks duration. A total of 2971 plasma attempts were made, producing 2522 successful experimental shots. More detailed statistics are listed in Table 3.4-1.

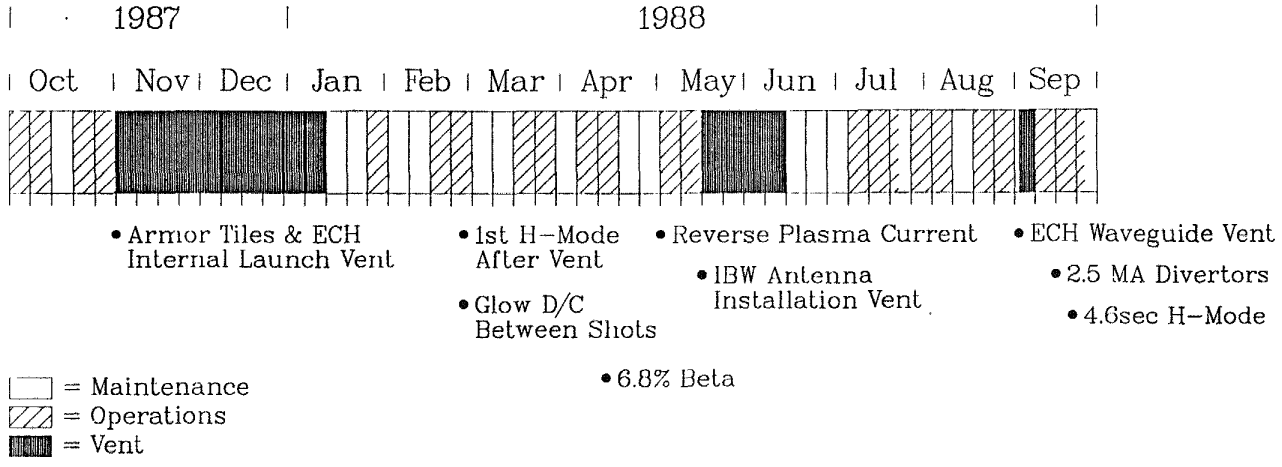

Fig. 3.4-1. DIII–D FY88 weekly operations schedule.

The remaining time was used for maintenance of the equipment, new construction and vents. There were three vents during the year, which together extended over 15 weeks. The first major vent in FY88 lasted 10 weeks. This vent was for installation of additional armor tiles and 10 inside launch ECH antenna and waveguide systems and an all graphite armor tile design to go over the waveguides. The wall coverage with graphite tiles was increased from 7.5 to 31 m^2.

TABLE 3.4-1.
FY88 DIII-D SHOT SUMMARY

	Shots	Percentage
Successful Plasma Attempts:		
Ohmic Heating Only	934	31.4%
Ohmic + NBI	1376	46.3%
Ohmic + ECH	165	5.6%
Ohmic + NBI + ECH	47	1.6%
Unsuccessful Plasma Attempts	149	5.0%
Test Shots	300	10.1%
Total	2971	100%

The addition of a significant amount of graphite inside the vessel lead to an increase in the recovery time following the vent. Efforts to overcome this problem lead to the need to perform glow discharge cleaning between shots. An automatic glow discharge cleaning system was installed on the machine first using one of the primary limiters as an anode, and later using two dedicated carbon anodes, which were installed during the second vent. The system is completely automated and computer controlled, such that it can be used between shots without increasing the time between shots. The Glow discharge cleaning improves the vessel condition, such that plasma operation can be initiated earlier after a vent and fewer recovery shots are needed after a disruption.

In the beginning of the third quarter the direction of the plasma current was changed, by changing some of the E–coil bus work. This allowed plasma confinement studies with counter injection of the neutral beams, unfortunately no improvement in the confinement time was found in this mode.

During the second major vent the several major tasks were completed. The external windows for the ECH inside launch system were installed during the vent, while the external waveguides were installed later and the system was then tested up to full power for 0.5 sec in air. The prototype fast wave low power antenna was taken out and a

new IBW antenna was completed and installed. Low power coupling test with the new IBW antenna indicated good coupling, but no heating was observed even at higher power levels. The Thompson scattering system group installed additional light baffles, which dramatically reduced the stray light. The toroidal SXR arrays and the UCLA reflectometer were installed and a substantial number of additional task repairs and refurbishments were also carried out.

The third machine vent was needed to inspect and subsequently remove the ECH inside launch vacuum assemblies. The mode converters housed in these sections had shown signs of overheating and degradation during the checkout phase of the inside launch hardware. In order to continue progress in the ECH program while the problems with the mode converters were resolved, the antenna for the outside launch system were rotated 90° to the O–mode configuration. In early FY89 an instrumented window assembly was installed on the machine which helped pinpoint the overheating problem. A modified assembly has been installed and successfully tested. Fabrication of nine more units is in progress with installation scheduled by mid FY89.

Construction of a movable neutron shielding roof and preparation for the neutron shielding walls were started in the second quarter. The roof was used for the first time over the machine during the first quarter of FY89. The shielding attenuation factor of the roof was measured to be a factor of 2, in agreement with the theoretical calculations. The need for neutron shielding is driven by two compelling desires. First it has been shown that the energy confinement time is strongly dependent upon the species mass and in order to perform reactor relevant experiments, deuterium plasmas must be run. The need for deuterium also couples well with the neutral beam program, since more energy can be injected when the ion sources run in deuterium. The addition of neutron shielding will allow the DIII–D program to explore these reactor relevant regimes in deuterium without increasing the radiation exposure to the public and to the General Atomics personnel from the extensively higher number of neutrons which are produced from these experiments.

3.4.2. NEUTRAL BEAM OPERATIONS

During the 1988 fiscal year, the neutral beam system has been a very reliable source of auxiliary heating of the DIII–D tokamak plasmas. A total of over 1400 neutral beam injection (NBI) shots were made in achieving various milestones, including the record high beta value and the quasi-steady-state H–mode. A demonstrated neutral power delivery of 3 MW H°, 4 MW D°, or 3 MW He° per beamline is available at an operating acceleration voltage of 80 kV. A demonstration of the capability of the neutral beam systems is shown

in the monthly statistics of the injected power are shown in Fig. 3.4-2. The lower end of the injected power does not indicate low power availability, but rather reflects an experimental plan requiring a lower power NBI.

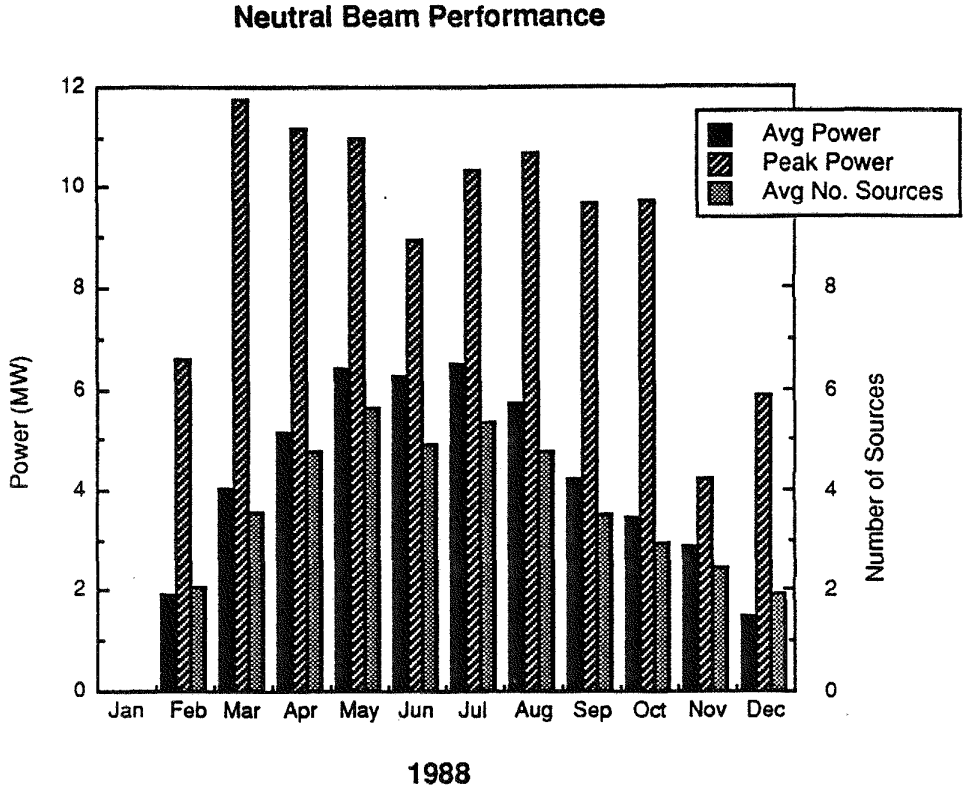

Fig. 3.4-2. Monthly neutral beam injection record.

The full operational capability of 80 keV, 5 sec hydrogen and deuterium beams was initially demonstrated on the 30° beamline with a repetition rate of one pulse per 12 minutes. No significant damage to the beamline components was observed apart from a slight melt mark on the return-ion baffle collimator in front of the ion dump. Although this melt mark was not serious, additional careful monitoring of the critical beam-absorbing components was implemented. Quasi steady-state H–mode plasmas were obtained by high power NBI with 7 beams at 5 sec pulse lengths. Long pulse NBI (in excess of 3 sec) was also important in carrying out the neutral beam current drive experiments.

As an experimental variation, helium beams were produced by all eight ion sources for 0.5 sec pulse lengths by using the volume pumping capability of the beamlines. This experimental flexibility yielded an important data point in terms of the plasma ion species. A delivered helium neutral power of 1.5 MW per source was obtained at 80 keV. In anticipation of longer pulse He° injection experiments, a demonstration of helium gas pumping by means of argon frosting on the 4.2 K cryopanels was successfully carried out. Although multisecond He° beam injection has not yet been attempted, this cryotrapping technique appears to be very promising for future NBI operation.

Improvement of the extracted beam quality has been made by feedback control of the arc power based on the ion source discharge plasma density monitored by a Langmuir probe. This technique maintains the beam current constant throughout a pulse, resulting in an overall extracted power increase of 10%. Also, good ion beam optics can be maintained over the entire pulse length and this enhances the beam transmission efficiency to the torus entrance. In a related effort, automation needs for beam system control and operation have been defined. This task is being integrated into the job to replace obsolete control and instrumentation systems over the next few years.

Beamline physics studies further improved the accuracy of the injected power delivered to the plasma. In particular, the water flow calorimetry system can account for 90% of the accelerator power since arc regulation has been adopted. The beam intensity profiling technique based on the matrix of thermocouples embedded in the calorimeter was improved with the implementation of a new algorithm suitable for the Long Pulse Ion Source beams. From the profile algorithm, beamlet divergences are obtained routinely for every calorimeter-shot. Figure 3.4-3 illustrates a "perveance scan" of the 330° right beam, showing (i) the transmission efficiency reaching a maximum at the optimum perveance ($IV^{3/2}$) and (ii) the beamline divergence angle minimum.

Since the residual stray magnetic field within the DIII–D vessel is in the order of few Gauss, any measurement using the charged particle beam is affected by it. Determination of the ion-to-neutral conversion efficiency of the neutralizer and calibration of the armor tile thermocouple signals are particularly hampered by this effect. Toward the end of the year, experiments were performed to improve the accuracy of such measurements by an iterative analysis. The neutralizer efficiency has been shown to be close to the theoretical expectations; tile-thermocouple calibration has been satisfactorily made to give the shine-through power on a shot-by-shot basis.

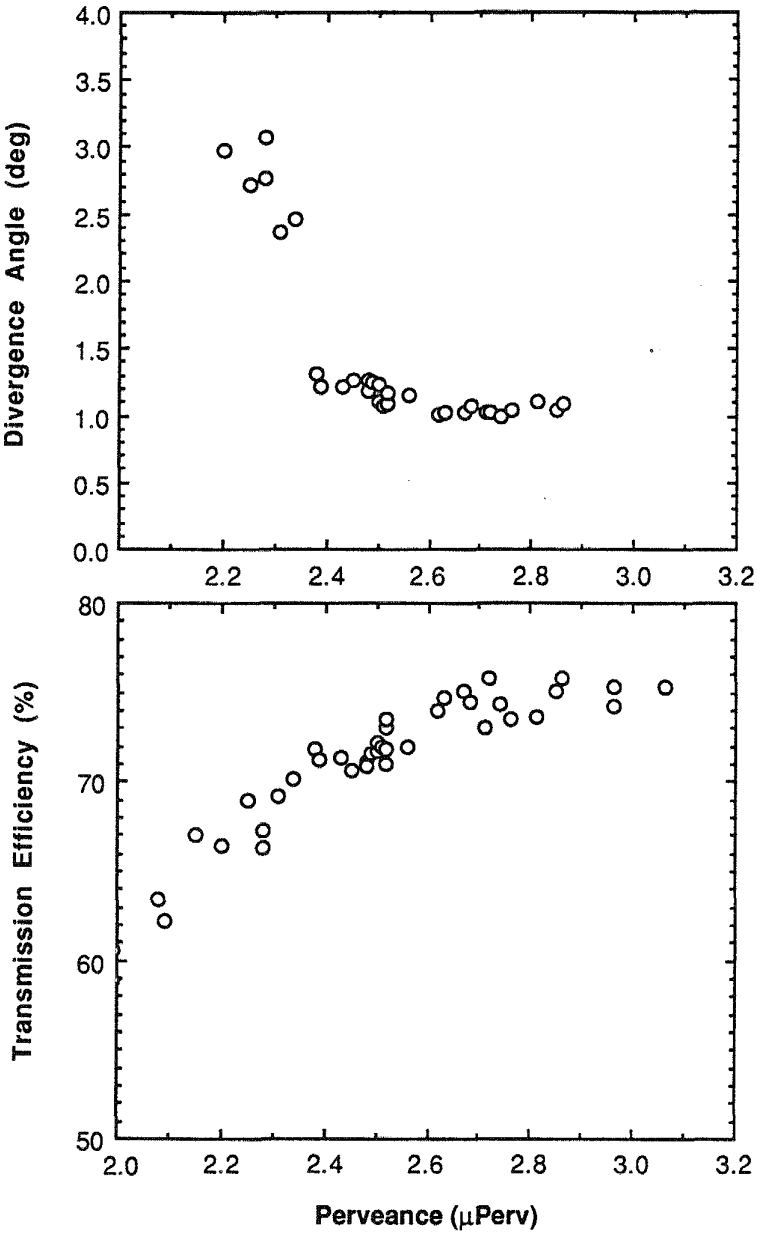

Fig. 3.4-3. Deuterium beam quality versus beam perveance.

In conclusion, the neutral beam systems have been performing extremely well. Many improvements have been made to the system to enhance reliability. The U.S. Common Long Pulse Source has shown excellent reliability overall; only minor problems with breakdowns across the mylar-insulated electrodes have occurred. It is also noteworthy that while some subcomponents of the neutral beam system have started to exhibit lifetime-related failures, (since most of these subsystems have been in continuous operation since 1980) a vigorous program to replace them has been instituted and an aggressive preventative maintenance program is now underway.

3.4.3. ECH/ICH OPERATIONS

The upgrade of the timing and control circuits for the 2 MW 60 GHz gyrotron system which was started in October 1987 was completed in the first quarter. Instrumentation for the inside launch waveguides was also completed, and waveguides from two gyrotrons to two launchers at 45 degrees were installed. Operational tests with the 45 degree system were initiated using a high voltage test power supply.

In the second quarter, the #7 neutral beam power system was converted back to negative polarity for gyrotron conditioning in preparation for inside launch ECH operation. Installation of the waveguide runs from the gyrotrons to the inside launch ports were completed during the third quarter, and conditioning of nine inside launch systems with toroidal field was completed. Experiments with these launchers showed promising results in terms of transmitting power to the plasma from a few antennas, but a problem with overheating in some of the waveguide microwave transmission systems was identified.

Because of the overheating problems, parts of the inside launch hardware were removed for modifications. The outside launch antennas were rotated 90° to the O–mode direction to allow the ECH group to continue with its experimental program. The eight outside launch antennas were operated for the balance of the year. Successful tests of modifications to the inside launch transmission system were also made, and an upgrade of the waveguide system will be completed early in 1989.

There were six days of plasma operations with ECH (as scheduled) in the last quarter of 1988. Eight of nine available gyrotron systems were used in outside launch experiments. Rf power levels up to 1.4 MW with 150 ms duration were achieved during these operations, with a total system availability of 84%. Electron temperatures up to 5 keV were produced.

3.4.4. ICH OPERATIONS

Modifications to the FMIT unit continued through January at Continental Electronics in Dallas. Testing with the rf power system commenced in February with a developmental X2242 tube serial no. CGN25 in the final power amplifier (FPA). This tube failed during power tests and was replaced with an earlier low gain version X2242 prior to the final acceptance tests at Continental Electronics. The acceptance tests were completed at a reduced power level of 1.4 MW with 1 s pulses at a frequency of 38 MHz, and the system was shipped to GA in June.

The installation of the FMIT system at GA was completed in July and rf testing into a dummy load with 0.5 MW, 0.5 s pulses was achieved the same month. The transmission line between the FPA and the antenna was completed in August. Initial antenna conditioning tests revealed rf interference problems with other systems at DIII–D. These interference problems were reduced to acceptable levels through the addition of rf shielding of the 30 kV insulating breaks between the DIII–D machine and the coaxial transmission lines leaving the machine area. The original tetrode X2242 meanwhile had been repaired at Varian, and was reinstalled in September. This tube conditioned up quickly to 1.3 MW rf output pulses of 1 sec pulse duration into dummy load. No difficulty is expected with transmitter operation at 2 MW.

IBW heating experiments were begun in October, four months ahead of the target date for this milestone. There were 6 days of vacuum conditioning of the antenna, and 12 days of plasma operations with IBW in the last quarter of 1988. A system availability of 95% was achieved with typical shots in the range of 500 to 600 kW for 1 sec duration, with peak power levels of 800 kW. Antenna arcs limited the power levels to about 0.6 MW when operating with plasma in the tokamak. This power limit has prevented coupling/heating studies at rf power levels comparable to or greater than the ohmic heating power. To date, no signs of central heating have been observed, at rf power levels of slightly less than the ohmic heating power. One possible mechanism for "parasitic" loading is plasma formation or local heating of electrons due to the fringing fields directly in front of the Faraday shield. Another possible mechanism is absorption of the IBW by partially stripped carbon ions at high cyclotron harmonics. To test these hypotheses, a new Faraday shield has two offset layers of closely spaced titanium carbide coated rods, such that the shield is completely opaque. The upcoming experiment will be the first in which the performance of open and opaque shields in IBW experiments will be compared.

SECTION 4

COLLABORATIVE PROGRAMS

4. COLLABORATIVE PROGRAMS

4.1. INTRODUCTION

A series of collaborative efforts both national and international are a key ingredient in GA's role in the worldwide fusion program. These programs enable GA to interact with the broad spectrum of the international community and allow the efficient use of resources worldwide. Through this program: (1) the cooperative efforts of many scientists throughout the world are brought to bear on the experiments undertaken on the DIII–D device, (2) the results obtained are integrated into the worldwide knowledge base, (3) GA scientists gain ready access to this knowledge base, (4) GA scientists contribute to the work done at other laboratories, and finally, (5) graduate students are trained. In addition to the efforts described here, additional programs funded by the APP and D&T Divisions of the Office of Fusion Energy are important in maintaining these interactions.

In the past, these programs have taken many forms, and we plan to continue a vigorous program of national and international cooperation throughout the duration of this contract. We intend to continue the cooperation with the Japan Atomic Energy Research Institute (JAERI) via the Doublet III U.S./Japan agreement. This agreement has increased the capability of the DIII–D facility, added breadth to our program, and JAERI personnel have contributed significantly to our research. The cooperative program with Lawrence Livermore National Laboratory has become a substantial and very productive effort. Several LLNL scientists and support people are participating in a wide range of topics with particular focus on boundary physics and ECH current drive and heating. This cooperative effort allows people from each institution participating in experiments, in order to obtain optimal efficiency in understanding and the use of equipment. We also have cooperative programs with the following institutions: UCLA, ORNL, Sandia, Johns Hopkins University, University of Maryland, U.C. Irvine, JAERI, Max-Plank Institute for Plasma Physics, Culham, and JET. In addition, the DIII–D program continues to provide training for graduate students from Princeton University, UCLA, the University of Maryland, Johns Hopkins University, and the University of Illinois.

4.2. U.S. COOPERATIVE PROGRAMS

LLNL

LLNL began a significant collaboration with GA on DIII–D in FY86 with 14 FTEs on site at GA and additional support at LLNL. LLNL personnel are assisting in the DIII–D research program in the following areas: (1) ECH and current drive, (2) boundary physics, and (3) tokamak and neutral beam operations. The mix of personnel includes scientific staff, mechanical and electrical engineering support, and technicians. LLNL mounted several diagnostics on DIII–D: (1) an IR camera which views the divertor region, (2) a SPRED survey spectrometer for impurity studies, (3) an absolutely calibrated vertical and tangential H_α TV for divertor studies, (4) pressure gauges, (5) an edge ECE measurement, (6) a vertical viewing ECE diagnostic, and (7) assistance with the DIII–D charge exchange analyzer. Future plans include a Zeeman current profile diagnostic system for current drive studies. We expect this cooperation to continue at roughly the same level. LLNL is also assisting in the 110 GHz ECH project by helping with the relocation of MFTF 80 kV power supplies.

The LLNL team carried out measurements of divertor neutral pressure and H_α emissions and made comparisons with the DEGAS computer model of neutral transport; factor of two agreement between the model and the data has been obtained. This code was used to predict the effect of baffles on the neutral transport in the plasma. Divertor power flow measurements were also coupled to a 2D transport code obtained from Princeton.

Livermore personnel contributed to a neutral beam current drive experiment. The unique feature of this experiment was that the plasma current of 0.34 MA was sustained by beam injection. The energy confinement was of H–mode quality, and the poloidal beta value of 3.5 was exceptionally high.

Livermore personnel contributed to a CIT-relevant experiment to sweep the x-point position during a shot. This experiment was done to evaluate the feasibility of using this technique to reduce the heat load on the divertor tiles in CIT. It was demonstrated that the strike point on the tiles could be moved radially by about 25 cm, thus reducing the power load by about a factor of three. In H-mode operation, the nature of the ELM activity, and hence the quality of the confinement, depended on the position of the x-point. This effect has also been observed in experiments in which the position of the x-point was varied between shots.

Livermore personnel contributed to the STE study by developing an operating scenario for the divertor/edge. The study concluded that control of the electron temperature at the divertor will require significantly greater recycling on STE than on DIII–D. This control is necessary to reduce sputtering effects on the divertor plates.

The LLNL SPRED spectrometer was used to monitor the temporal behavior of impurities during the long duration H–mode experiments. Both edge and central Ni emissions decreased over the five-second H–mode operation. The decrease of both these signals suggest that this impurity concentration is decreasing, *i.e.*, there is no buildup of impurities during the H–mode with grassy ELMs.

Livermore personnel participated in the successful electron-cyclotron heating experiments with both the outside–launch O–mode and X–mode ECH systems. These experiments produced H–mode and high efficiency heating of low density plasmas. Technicians participated in installation of and conditioning of the inside launch waveguides.

The MTX experiment of LLNL will apply repetitive pulses of high power ECH from a free electron laser source to the high field, high density plasmas (in the Alcator-C tokamak relocated to LLNL). General Atomics has loaned LLNL a Michelson radiometer system for MTX temperature profile measurements. GA calibrated the MTX visible Bremstrahlung diagnostic using the technique developed for DIII–D.

UCLA

Under subcontract from GA, UCLA has installed on DIII–D a microwave reflectometer for time-dependent density profile and density fluctuation measurements. The system is being operated by UCLA, and its development will be the doctoral dissertation for a UCLA graduate student. UCLA has also mounted a FIR laser wave scattering system on DIII–D to detect plasma turbulence. Five of the seven channels of the narrow band reflectometer have been calibrated by the end of 1988. Both fluctuation and profile data from the diagnostic have been taken during DIII–D plasma shots although the profiles have not been inverted. Installation of the UCLA homodyne FIR scattering experiment is nearing completion.

ORNL

ORNL has mounted on DIII–D a low power, ICRF fast wave coupler prototypical of the kinds of couplers needed for CIT and has collaborated with GA to carry out a detailed evaluation of the coupling efficiency of this antenna. Discussions are underway on future collaboration on a fast wave current drive antenna for DIII–D.

ORNL and GA have collaborated on pellet injection research with GA mounting an ORNL pellet injector on Doublet III and ORNL personnel participating in the research program. GA proposes a pellet injector for DIII–D and supports a similar cooperative arrangement with ORNL.

Dr. Ed Lazarus has been on assignment to GA in 1988-89 and has made important advances in controlling elongated plasmas.

Johns Hopkins University

Johns Hopkins mounted a multi-chord spectrometer on DIII–D to study impurity transport. Two graduate students from Johns Hopkins University fully integrated the STRS system into the DIII–D data base, and data is taken regularly. They also reactivated the laser blowoff system. The graduate students were on site at GA and wrote their doctoral dissertations on data obtained with this instrument.

University of Maryland

A three-party arrangement was concluded between the University of Maryland, GA, and LLNL for the support of ECE measurements on DIII–D and MTX. GA has loaned its Michelson interferometer to MTX for temperature profile measurements. The University of Maryland installed its present high frequency Michelson interferometer on DIII–D in vertical viewing to detect energetic electron distributions produced during current drive. The university will seeks to develop a new, much faster time resolution grating polychrometer Michelson instrument for horizontal ECE on MTX. A new development is required because of the short-pulse nature of the FEL.

The Maryland vertical viewing ECE system (VECE) has been installed, calibrated, and brought into operation by a Maryland graduate student.

4.3. INTERNATIONAL COOPERATION

JAERI

The Doublet III/JAERI cooperation has been a long and fruitful one, starting with the five-year agreement initiated in 1979 by the governments of the United States of America and Japan for cooperative energy research. This agreement provided for 70 million dollars of JAERI support for DIII–D and sharing of Doublet III experimental time between scientific teams from GA and JAERI, with GA responsible for operation of the tokamak and its associated diagnostic systems. This agreement provides the basis for cooperation on a wide range of topics, the most notable of which is the properties of noncircular plasma configurations and especially divertors. Work at JT-60 focuses on the divertor configuration while work at JFT2-M concentrates on a wide range of noncircular cross-section configurations. The programs in rf heating and current drive compliment ICH and ECH work at DIII–D.

Under the present agreement, GA is funded by the DOE to operate DIII–D, and JAERI provides up to six scientific personnel to assist in the conduct of the experimental program. The Doublet III U.S./Japan agreement has been extended through 1993. The main areas of JAERI interest are in high power ECH and neutral beam current drive. We also propose to expand this program by sending scientists to collaborate on the JT-60 device and the JFT2-M device. Special attention will be paid to cooperating on the current drive, high power ECH and divertor physics.

During Doublet III operation JAERI had a separate team which carried out their own experiments. Now during DIII–D operation they have up to a half dozen scientists located at General Atomics who participate in DIII–D experiments. A long term leader is on site who is joined by scientists who stay for periods ranging from several months to a year or more.

JAERI has contributed to a number of research areas: L-H transition physics, differential divertor biasing, physics operations, improve shape control, ballooning mode, boundary physics, rf heating, high beta stability analysis, neutral beam current drive, ECH heating and current drive, magnetic fluctuation analysis, and Thomson data analysis.

HIDEX

From 1986 to 1988 a cooperation program, Helical Island Divertor EXperiments on the JIPP T-IIU tokamak at Nagoya, Japan were performed. GA scientists and technical staff, working together with JIPP T-IIU personnel, (1) designed, fabricated, and installed the necessary limiter modules and (2) performed experiments and analyzed results focusing on evaluating the RHD concept with $m = 3$ islands as compared to the $m = 7$ configuration TEXT.

The full power limiter was installed and experiments were performed and completed. The temperature rise of the HIDEX limiter blade edge, as measured by an infrared video camera, is much less when the O-point of an island surrounds the blade than when, for comparison, the direction of the helical coil current is zero. For operation with the limiter head between islands (*e.g.*, $q = 3.5$) little or no difference in temperature is observed. During NBI auxiliary heating, O-point operation again results in a lower limiter temperature than X-point operation, although the difference is smaller.

A high speed video camera with various interference filters is also used to view the HIDEX limiter during plasma discharges. The visible light signal is much brighter for the X-point case, confirming that the recycling and heat loading at the edge of the limiter are less when an island O-point is present.

The most obvious difference in the bulk properties of X- and O-point plasmas is a rise in the density and carbon radiation signals during the time the X-point is on the limiter. Both of these effects are thought to be due to ablation of carbon from the limiter at the high temperatures reached during operation with an island X-point on the limiter. The lack of a corresponding increase in the oxygen radiation indicates that the carbon is coming from the pump limiter rather than the impurity gases adsorbed on the other surfaces of the vacuum chamber. The limiter stays much cooler when it is in the island O-point and there is no significant change in the amount of carbon in the plasma.

Under the proper operating conditions, *i.e.*, when the density is less than 2×10^{13} cm^{-3} and the MHD activity is low enough so that the scintillating magnetic fields do not destroy the islands, the pump limiter collection efficiency is enhanced when the limiter is inside the island and the particles are discharged around into the pump chamber opening. The increase in collection efficiency is about 70%.

ASDEX

The ASDEX cooperation has concentrated on trying to maximize the useful complementary results of this machine which is similar in some ways to DIII–D. Emphasis has been on H–mode studies and participation in the ICRF experiments.

In FY85 GA sent four scientists to ASDEX to work on various joint papers and collaborations. In FY86, ASDEX sent a SPRED spectrometer and Dr. Guenther Janeschitz to DIII–D for six months for impurities studies in DIII–D. Dr. Janeschitz's studies continued until December 1986. His visit was extremely helpful to DIII–D.

DIII–D and ASDEX began the joint development of the method of principal component analysis of magnetic data originated at ASDEX. Dr. McCarthy from ASDEX worked at GA one month and Dr. St.John of GA worked at ASDEX for one month in FY86.

In addition, Dr. J. K. Lee of GA took to ASDEX and installed the nonlinear, resistive MHD code CART. Dr. K. Grassie worked with Lee at ASDEX and visited GA for one month in the fall of 1986. Dr. Gunther Haas of ASDEX installed three ASDEX pressure gauges on DIII–D and collaborated on the resulting measurements.

In FY88 Dr. Ping Lee spent 10 months at ASDEX working with the Spectroscopy group, and Dr. T. Luce spent three months working with the rf physics group. Dr. D. Thomas and Ms. M. Thomas spent 2 months at ASDEX working with Dr. K. McCormick of MPIPP to prepare a high current Li beam source to be used in a current density diagnostic to be used during LHCD experiments.

JET

An attempt has been made to coordinate the results of some of the experiments on DIII–D and JET. These two devices are the only tokamaks running similar elongated multimegampere plasmas. Moreover, in FY86 both devices found the H–mode regime.

In FY85, GA initiated a substantial cooperation with JET. GA sent Drs. Ejima (nine months), Kellman (eight months), Baker (two months), and Brooks (one month) to JET. Baker consulted on ICRF and Brooks consulted on wall conditioning. Dr. Kellman was instrumental in obtaining the first diverted plasma operation in JET.

In FY86, Dr. P. Noll of JET came to GA and worked with the plasma control group. In FY87, Dr. P. Lomas of the JET physics operations group joined the DIII–D physics operations group for a period of three months. In FY88, J. Phillips of GA continued the interaction of the two laboratory's neutral beam groups. Dr. J. Kim participated in JET neutral gas studies. In FY88 GA sent Dr. D. Schissel to JET for three months to participate in pellet experiments and size scaling studies. In FY88, Dr. A. Costley of JET visited GA to collaborate on ECE diagnostics.

TORE SUPRA

The ergodic magnetic limiter (EML) were originally performed by GA on the TEXT tokamak. It is fortunate for the development of the tokamak that the French, on TORE SUPRA, plan to carry this advanced concept forward. TORE SUPRA with strong, long pulse auxiliary heating is ideally suited to test the EML approach to plasma boundary management for particle and heat exhaust and impurity control. The EML may ultimately make possible limiter-less, H–mode tokamaks without divertor chambers.

During FY86, GA participated in exploratory discussions with the French EML group, sharing results from TEXT and making suggestions for the TORE SUPRA EML coil design. In FY87 mutual physics interaction is in progress, with GA performing magnetic mapping studies of the French design, and GA applying the French thermal transport code to TEXT experiments. A long term exchange was begun in FY88 with Dr. T. Evans moving to cadarache as part of the U.S. team.

Culham Laboratory

General Atomics is working with Culham Laboratory on an electron cyclotron heating system for the DITE experiment at Culham. GA designed and built ECH parts and participated in the installation and system tests. GA's prior experience in this area on Doublet III is a significant advantage to Culham, and this effort has provided GA with an important test bed for a new launcher concept. The new COMPASS device at Culham will use ECH heating exclusively.

SECTION 5

SUPPORT SERVICES

5. SUPPORT SERVICES

5.1. QUALITY ASSURANCE

During the period 1983 through 1988, the Fusion Quality Assurance Branch performed all relevant Quality Assurance/Quality Control tasks required to support the assigned DOE milestones. During this period, several events and associated QA activities were particularly noteworthy.

- Converting the Doublet III to the DIII–D configuration.
- Converting the short-pulse Neutral Beam Injection System (NBIS) to the long-pulse configuration.
- Installing the Electron Cyclotron Heating (ECH) System.
- Installing the Ion Cyclotron RF Heating (ICRH) System.
- Toroidal Field Coil Remaining Life Analysis.
- Machine pit and building settlement analysis.
- Fixed/Translating Roof and Peripheral Shield Wall construction and installation.
- Miscellaneous tasks.

5.1.1. CONVERTING THE DOUBLET III TO THE DIII–D CONFIGURATION

Fusion Quality Assurance assigned a Quality Engineer to Toshiba during the construction of the Big Dee vacuum vessel in Japan. In order to accommodate the frequent questions relative to design, quality and fabrication anomalies, a Telex computer link was established between the assigned engineer and the Fusion QA Manager. This system, combined with other available communications media, allowed a timely interchange of technical and managerial problems and solutions. The net result of our comprehensive planning, mature design and corporate cooperation was a vacuum vessel delivered on-time, on-budget, and superior quality.

The Fusion Quality organization reached a peak of 15 engineers and Quality Control inspectors during the DIII–D conversion. The majority of their work involved routine dimensional inspections, process surveillance and verification, and test surveillance and verification. Four of the inspectors were utilized extensively for subassembly and final assembly optical alignments of the vacuum vessel, port and flange fit-ups, neutral beam alignments, toroidal, poloidal and field-shaping coil alignments, and various auxiliary systems alignments. The inspectors designed, fabricated, and utilized special tools, fixtures, and jigs to complete their tasks. The inspectors were also utilized extensively to perform layouts for cable and conduit runs, diagnostic equipment positions, and equipment positions.

Quality Assurance tasks were thoroughly documented, collected in retrievable files, and placed in long term storage for future reference.

5.1.2. CONVERTING THE SHORT-PULSE NEUTRAL BEAM INJECTION SYSTEM (NBIS) TO THE LONG-PULSE CONFIGURATION

Fusion QA inspectors performed receiving inspections of the new long-pulse sources, performed assembly dimensional inspections and optical alignments during assembly, and devised a periodic inspection plan to assure that pit settlement did not impact the interface between the NBIS and the DIII–D vacuum vessel. Mechanical layouts were also completed to assure the proper beam firing angle existed into the vacuum vessel. Our inspectors also assisted in developing high-consequence lift procedures, witnessed proof-testing of the handling fixtures and performed nondestructive tests of those fixtures. We perform all long-pulse source lifts in accordance with written high-consequence lift procedures and witness each lift.

5.1.3. INSTALLING THE ELECTRON CYCLOTRON HEATING (ECH) SYSTEM

Our Fusion QA engineers and inspectors reviewed design drawings, developed project-specific inspection plans, performed dimensional measurements and mechanical layouts and participated in safety and technical reviews of the ECH project. The 60 GHz waveguide components were inspected utilizing state-of- the-art video optical borescope equipment, and QA monitored and inspected all microwave components and processes during fabrication. Particular emphasis was placed on the superconducting magnets which surround each 200 kW gyrotron. We inspected each gyrotron received from the supplier (Varian), examined and translated the information contained in the impact recorders, and negotiated shipping problems with Varian. Fusion QA Representatives (QAR) conducted

extensive source inspections and in-process inspections on the inside launch hardware. Our unique and complex design required very intense interaction between the GA design/engineering personnel, QA, and the supplier.

5.1.4. INSTALLING THE ION CYCLOTRON RF HEATING (ICRH) SYSTEM

Fusion QA performed a source inspection of the ICRH Power Supply at Continental Electronics, a division of Varian Corporation, and witnessed and documented the final acceptance testing. Final amplifier tube problems prevented testing to full power levels, but the general performance was such that GA made the decision to complete testing at the DIII–D site. We were extensively involved in the design and fabrication of the Ion Bernstein Wave (IBW) antenna system for the ICRH. The Fusion QA inspectors conducted both in- process and source inspections of this complex antenna to assure that the plating, brazing, welding, and flame-spray results correlated with design requirements. We also performed optical alignments and dimensional inspections of the IBW antenna-to-port fit-up.

5.1.5. TOROIDAL FIELD COIL REMAINING LIFE ANALYSIS

Fusion QA conducted a complete investigation and analysis of the remaining life of the Doublet III Toroidal Field Coils (B-Coils) during the conversion of the Doublet III to the DIII–D configuration. We reviewed original inspection data which was collected during the B-Coil fabrication cycle to determine those areas which had been identified as high stress areas and those areas where flaws were known to exist. We developed a detailed analysis plan, purchased state-of-the-art optical borescope and NDE equipment, designed and fabricated eddy current sensor probes and rotating probe fixtures. We developed precision eddy current calibration standards and radiographic techniques, and devised a semiautomatic NDE inspection system to collect data on all B-Coil finger joint bolt holes. The data was digitized and stored on magnetic tape for future analysis. Photographs of suspected and known flaws were made for further analysis and historical records.

While this inspection was in progress, each B-Coil was being machined to provide additional clearance for the new diagnostic and access ports on the DIII–D vacuum vessel. We formulated rigorous layout, NC Machine tape computer program verifications, witnessed sample cutouts in aluminum blocks, and witnessed 100% of the actual finish machining. Each lifting and handling operation was witnessed and documented. All high-strength bolts were re-torqued to original specifications and verified by QA. The entire operation was executed without incident and there was no damage to any coil.

The B-Coil inspection data was reviewed and analyzed, with the following results: After seven years of operation, the coils are in acceptable condition for continuing service. The total calculated expended life at the time the machine was shut down for the DIII–D conversion was 9.955%, after 50,573 shots were performed at various power levels. All flaws discovered as part of the B-Coil In-service Inspection were thoroughly documented and stored for future reference.

5.1.6. MACHINE PIT AND BUILDING SETTLEMENT ANALYSIS

In response to a request from the DIII–D Engineering Department, Fusion QC inspectors developed a plan to locate optical targets at strategic locations throughout the building and the machine pit to monitor any settlement of machine components or building structural components. We established baseline data utilizing the stable columns upon which the DIII–D rests. We then established a schedule of optical measurements which can be analyzed to track any settlement resulting from ground moisture, compaction over time, or seismic activity.

5.1.7. FIXED/TRANSLATING ROOF AND PERIPHERAL SHIELD WALL CONSTRUCTION AND INSTALLATION

In order to provide shielding for neutrons emanating from the DIII–D machine, a project was initiated to surround the entire machine with a boron- rich enclosure, consisting of a fixed and moveable roof, and a 12-inch thick peripheral shield wall. Fusion QA assisted the project by monitoring the subcontractor's performance with respect to weld inspections, safety inspections, operational inspections, material sample form design and construction, sample analysis and documentation, and bolt torquing. A comprehensive Quality Plan was developed, and all inspections, tests, and analyses were documented for future reference.

5.1.8. MISCELLANEOUS TASKS

Fusion QA personnel participated in a variety of miscellaneous activities since the last report. A new Measuring and Test Equipment (M&TE) Calibration program was initiated. While QA assured that only currently calibrated equipment was utilized for data collection and acceptance testing, the basic controls central to an effective calibration system were not in place. Fusion QA has assisted DIII–D management in developing and implementing an effective control system.

We have investigated means to implement an inexpensive, but effective, Preventive Maintenance program to try to increase the availability of our fusion experiment. The severe operating parameters have taken their toll over the years, and we can expect that equipment aging will eventually impact availability. Several inexpensive PC-based PM programs were reviewed, and the program is currently being developed.

Fusion QA remains committed to helping small suppliers compete for fusion- related contracts. Where possible and feasible, we assist prospective small business suppliers in refining their QA/QC programs to satisfy our stringent requirements. We have been extremely successful in achieving these goals.

The Fusion QA Branch remains committed to providing our customers with the highest quality products and services, delivered on-time, and at the lowest cost.

5.2. PLANNING AND CONTROL

The Planning and Control Group supported operation and maintenance of DIII–D facility. Planning and control provided long-term program planning, as well as day-to-day scheduling (cost control, preparation of Field Task Proposals and Cost and Fee Proposals, processing of purchase requests, expediting and reporting of status). These support activities are essential to the performance of the program within prescribed budgets and schedules. These planning activities (budget, schedule, resource) enabled us to maximize the utilization of available resources for accomplishment of program goals.

5.3. COMPUTER OPERATIONS

5.3.1. OVERVIEW

The DIII–D Computer Systems (DCS) group is dedicated to activities in direct support of the experimental physics program at General Atomics. This involves support of computers which do real time control functions for the tokamak, neutral beam and other related systems. Other computer systems are used for data acquisition and between shot analysis of tokamak data. Additional support is given to the User Service Center so that data can be accessed and restored using the formats which originate at DIII–D. Software packages have been installed and supported at the USC which are for the use of the physics community. The DIII–D computer group also supports all auxiliary systems which are used for dedicated diagnostic control. This involves system generation, backup procedures,

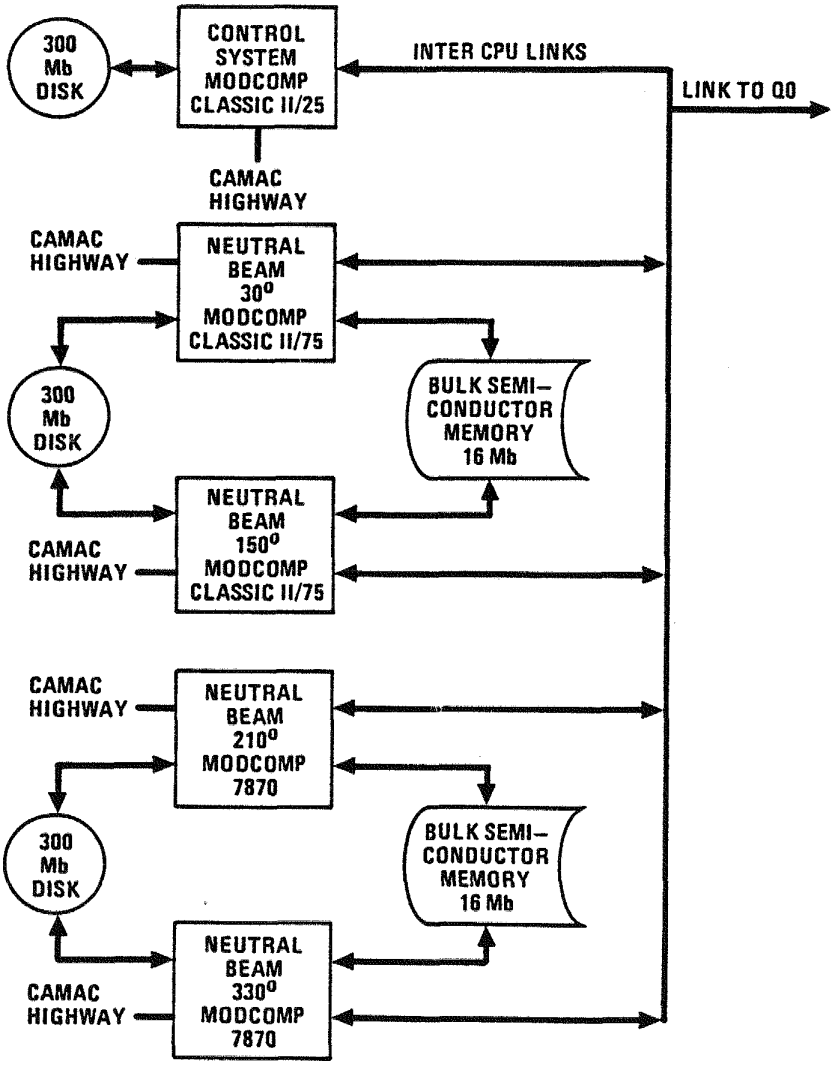

Fig. 5.3-1. Control and neutral beam system.

trouble shooting of hardware problems and maintenance of all hardware. MODCOMP computers are used to do most of the real-time control. There are eight active systems and one spare MODCOMP system. There are three bulk memory units, six disk drives, and six tape units. The DCS has a VAX cluster consisting of two VAX 11/785's, three tape drives, and eight disk drives. Attached to this on an ethernet connection are one VAX 11/750 (Thomson profile diagnostic), three Micro Vax IIs, and one VAXstation 3200. One MODCOMP is connected to the VAX cluster via a Network Systems Hyperchannel link. There are three LSI 11/23 systems, and three IBM PC systems. The DCS consists of a staff of eight, which includes a manager, one principle computer systems position, and six people in various systems programmers positions. All personnel share in responsibilities

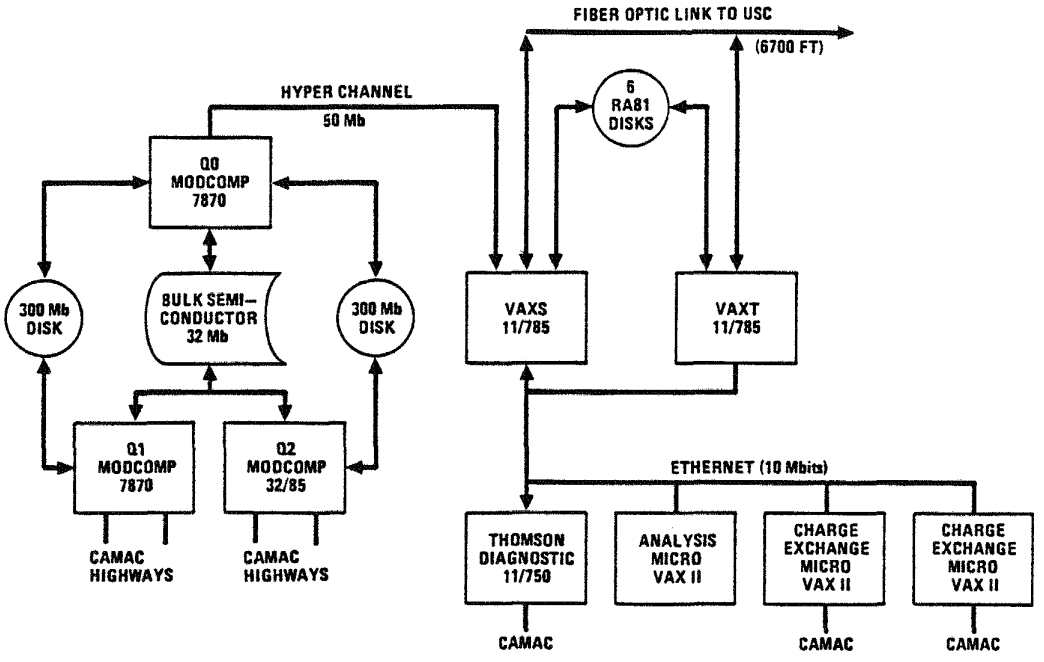

Fig. 5.3-2. Data acquisition system.

such as off-hour operation support and routine backup and maintenance. See Figs. 5.3-1 and 5.3-2 for the hardware configuration.

The User Service Center (USC) provides the computer services the GA fusion user community requires to support its investigations in theoretical and experimental plasma and reactor physics. Funding is by the Applied Plasma Physics and Toroidal Confinement divisions of the Office of Fusion Energy. Included in these services are the maintenance and continual upgrade of a large-scale, flexible computational and data collection facility. The USC currently has a VAX cluster consisting of a VAX-11/750, a VAX-11/780, a VAX 8600, and a VAX 8650. There are 9.3 gigabytes of online storage and 6 tape drives. This configuration, showing all external network links, is illustrated in Fig. 5.3-3. A 6500 foot fiber optic link connects the DCS to the USC. The two clusters share a common ethernet backbone which functions under the DECnet protocol. USC has a staff of five, which includes a manager and four systems programmers. One hundred percent of the computing performed at the USC is in support of the DOE/OFE program.

The USC computers are linked through a satellite system to the National Magnetic Fusion Energy Computer Center (NMFECC) at Livermore, California, and through this system local users have access to the CRAY supercomputers. The supercomputers of the NMFECC are used to run large codes that model Tokamak performance, make general MHD equilibrium and stability calculations, and deal with more theoretical subjects, such

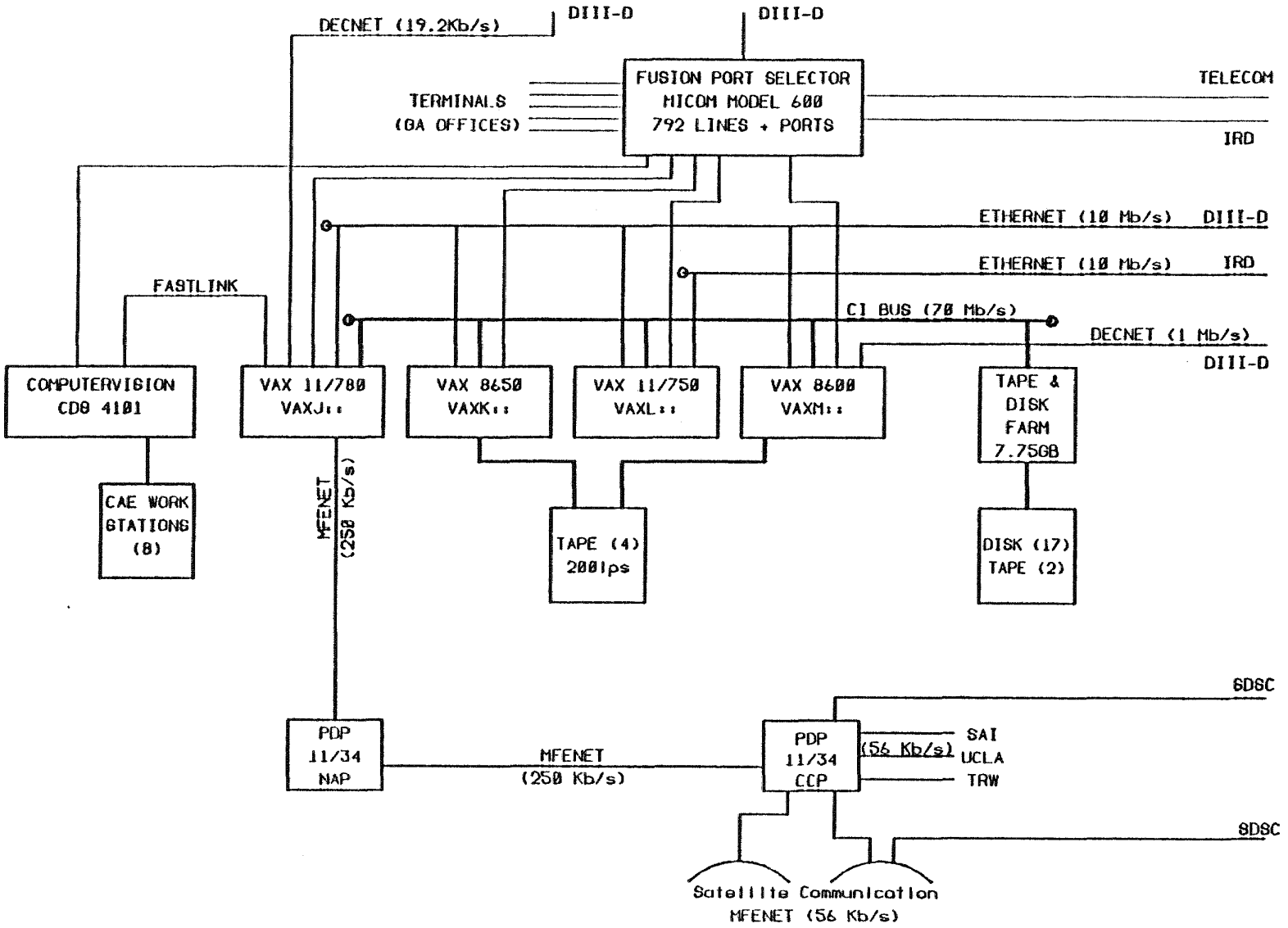

Fig. 5.3-3. DIII-D computer system facility.

as plasma/particle and plasma/wave interactions. The USC also maintains a network link to the rest of GA including the San Diego Supercomputer Center (SDSC). Through SDSC the USC has a direct connection to the Space Physics Analysis Network (SPAN) and the High Energy Physics network (HEPnet).

5.3.2. FY88 HIGHLIGHTS

During FY88, the total acquired data size grew from 17 Mb per shot to 32 Mb per shot as new diagnostics were installed on the tokamak and added to the computer systems. The bulk semiconductor memory on the MODCOMP was expanded from 24 Mb to its maximum size of 32 Mb. A large amount of data was added to help in examination of power supply fault shots. This particular data is handled differently from all others so that it is collected only for shots with faults or occasionally on demand. This lessens its impact on speedy collection of important tokamak data. The VAXstation 3200 arrived in April, and was brought on line immediately and a new version of the MFIT MHD fitting program was installed. This MFIT is modified to run on the separate processor, and has a faster bound routine. It has been used to generate up to 100 time slices between shots. Data which is computed and stored on the 3200 is networked into the shot data base. Later facilities added during the FY include plotting on the 19 inch color screen of the plasma shapes, and playback of several shots on recall in a movie-like setting. The MODCOMP Classic II/25 which had been used for several years as the main tokamak control computer reached saturation. This was mostly due to new demands including between shot glow cleaning of the tokamak. The spare MODCOMP 7870 cpu was swapped into its spot, and has performed well, but no spare computer was available during the balance of the year. Four additional disk drives, RA82's were purchased for storage of shot data and user programs. These were installed at the USC, and two of their disks were moved to the DIII-D computer room. A fiber optic link was installed between the USC and DIII–D VAXes. An 8 mm helical scan tape drive was installed to facilitate the long-term storage of shot data. The ECH control system was integrated in the total data acquisition and control system. This includes exchange of data between an IBM PC and the MODCOMP computers on availability of gyrotrons and desired power levels and gyrotrons to be used for a particular plasma shot. The local area network hardware of the MICOM was greatly improved in reliability by adding the interface hardware necessary and attaching it to the fiber optic cable between DIII-D and the USC micoms. This has greatly increased the reliability of the system, and no problems have been seen since this change was made. Several projects have improved operation of the neutral beam systems.

A new historical data collection system has been added. This includes new data base of up to 256 parameters per shot per source, sending the data through 4 computers to the USC VAXes, and eventually having all data in a S1032 data base. This information will be used for analysis of source performance, determination of problem components and other parameters relating to the long-term use of neutral beams. The central PC console was also installed and programming completed to make it a functioning unit. All four MODCOMP beam computers send information to the PC which saves it and displays a summary screen of all source information. Additional plots of timing are also available. An 8 mm tape drive was purchased after a lengthy investigation of this new type of hardware. Software for archiving of shot data to the tape was developed during the last 2 quarters of the year, and production use began in November 1988.

The USC VAX cluster performed exceptionally well, with an overall average availability of nearly 98%. The 1 Mbit per second coaxial link between the USC and DIII–D Computer Systems was replaced with a fiber optic system that provides VAX DECnet communications at 10 Mbit per second. This project was started at the end of FY87 and completed in the first quarter of FY88. The fiber optic link has proved to be more reliable and faster than the previous system, and requires fewer system resources. A terminal/printer server Xyplex was installed on the ethernet. All printer queues were converted to run off this device thus making them independent of a particular node in the cluster. This provided more flexibility and assures the users of better printer availability.

The mass storage on the VAX cluster was increased by 0.6 Gbytes with disk drives obtained in cooperation with DIII–D. The added storage was used for shot data and general user files. The CPU utilization continued to run very high with all available cycles consumed during peak periods. The USC was able to evaluate a VAX 8700. This VAX was added to the USC cluster and used primarily for between-shot analysis. Although budgetary constraints forced the rejection of the machine, the evaluation did point out the need for more cpu cycles. Funding also was not available in FY88 to achieve the planned goal of upgrading the 8600 processor to a 8650.

The USC purchased an 8 mm helical tape subsystem identical to the unit that is installed on the DIII–D computer systems. Software modifications are underway and the unit should be ready for full production by 3rd quarter FY89. The USC moved from an adjacent building into GA's commercial computer center. The move took place November 18–20, 1988. All computers were available for use on the morning of November 21 with only a few terminal lines and remote printers temporarily out of service. The move was very successful and should have no adverse impact on the Fusion user community.

5.3.3. REVIEW OF PREVIOUS CONTRACT YEARS

FY 1984

This operation year was split much of the time with JAERI running a long shift week and General Atomics then having a run period (operations was from 8 a.m. to midnight). A new model MODCOMP Classic II/25 was installed as the control computer. The control system also provided nine time slices of thermocouple data to the data base. The ability to recall power supply waveforms was added.

The neutral beam systems provided data which was incorporated into the regular shot data file. This also made the calculation of the neutral beam total injected power and shine-through power possible. These computed waveforms were added to the shot data base.

The data acquisition system serviced many diagnostics. A pellet injector experiment from Oak Ridge was added and all control was done via the MODCOMP system. Other diagnostics which involved control functions and display programs include a charge exchange diagnostic, slow Langmuir probes, and soft X–ray values. A user program was installed so that preamplifier gains could be quickly and easily changed between shots. A bulk-semiconductor memory unit was installed on the acquisition system to speed collection of data without having to rely on slow disk drive access. A new parallel CAMAC highway was installed and the optical isolaters were built. A 230 Kb line was installed between the MODCOMP computer and the USC DEC-10 computer. Limited use was made of this facility because of the load it placed on the DEC-10 system, and the slowness of data transfer. Much of the data was transferred from DIII to the USC via tape.

A VAX 11/780 and Network Systems hyperchannel were installed. Efforts were made to convert codes to the VAX, especially the data access subroutine PTDATA, and the MFIT (MHD analysis) and EFIT (energy transport) codes. The link hardware and handlers were tested, brought up, and data was transferred from the MODCOMP to the VAX. VAX software to receive the data over the hyperchannel, and format it into a usable data base was written. A code to schedule tasks on the VAX was written.

Planning for shutdown tasks continued. This included preliminary testing of data compression for VAX files, and development of the method to gather DIII–D data into the MODCOMP computers and process/analyze it on the VAX computers. A data base size of 25 megabytes was felt to be the largest which would be required. Also, plans for upgrading the neutral beam systems was started.

In FY84 processing of the experimental data required more than 65% of the total USC computing resources. To handle these requirements, several significant hardware upgrades and modifications were done during FY84. Two VAX 11/780s and a VAX 11/750 in a VAX cluster configuration were incorporated into the existing DEC-10 System environment. The VAX 11/750 was used primarily for communications processing, and the two VAX 11/780s were used for Doublet III data manipulation. A new PDP-11/44 was installed for the link to the NMFECC, and a cache memory added to the older PDP-11/34.

The DISSPLA graphics package from Computer Associates was available on the DEC-10 and was added to the VAX cluster for compatibility. The public domain typesetting program TeX was acquired for the DEC-10.

FY85

All computer systems (neutral beams, control, and acquisition) supported the final operation of the Doublet III tokamak. The acquisition system was routinely processing 5.33 Mbytes of data for each tokamak shot. After Doublet III shutdown, development began for the increased demands expected for DIII–D.

All console and computer hardware was acquired for the fourth neutral beamline. An ion source test stand was interfaced and operation of the test stand was started. All hardcopy output was reconfigured to use laser printers. Commercial software was installed to network all neutral beam, data acquisition, and control computers. Procedures for automatic power supply and source conditioning were developed.

On the Doublet III control system, the command language was upgraded to provide consistency and added capabilities for operation. The data base was restructured to improve maintenance and operator interaction.

The acquisition system has undergone major modifications to handle up to 25 Mbytes of data to be produced by DIII–D tokamak shots. The MODCOMPS were reconfigured into a master and two slave systems, with the slaves doing data acquisition via CAMAC. Hardware and software were added for a general central timing system. The analysis functions were all moved to the VAX CPUs. A second VAX 780 was added to the cluster and software to manage the data and analysis on this system was written. Additionally, programming was completed so that data for archival will be compressed (by a factor of 3) on the VAX CPUs.

This fiscal year represented a major transition period for the USC. A year long upgrade was started that would end when the DIII–D experiment came on-line. At this time Digital Equipment Corporation announced it was discontinuing the DEC-10 Systems. The DOE/OFE decided to abandon the DEC-10 Systems and adopt the VAX line of computers. The USC migration plan included hardware trade outs, software evaluation, procurement and implementation, program conversions, and user training.

A VAX 8600 was brought into the USC and one of the VAX 11/780s was moved to the DIII–D Computer Systems cluster. An 1 Mbit per second coaxial link using DECnet software was installed between the USC and the DIII–D VAX clusters. Programs running on either cluster use this link to search for requested data which may be resident on disks located in either the USC or DIII–D. The USC VAX-11/750 was changed from a communications handler to a laser printer server, thereby increasing the overall throughput of the VAX cluster. Other hardware changes included the installation of a remote line printer, several small laser printers, and more disk drives.

Several data base packages were evaluated and S1032 from CompuServe was selected. S1032 will be used for the DIII–D physics data base maintenance and analysis, and for general user needs.

FY86

Efforts on the DIII–D computers during FY86 were concentrated on finishing up development efforts so that systems would be functioning for the testing and startup of the tokamak. First plasma was in February 1986, and first long-pulse neutral beams were near the end of the fiscal year. Work was completed on the RGA vacuum monitoring system and other hardware which was needed during the pre-operation bakeout of the vessel. Data for additional pressures and temperatures was also added to the control system. The neutral beam work focused on changes needed for operation of the new source configuration.

The data acquisition system finished up work the VAX acquisition system, and completed the software reconfiguration of the MODCOMP computers into a Master/2 slave system. The second MODCOMP slave CPU was purchased and debugging started. New hardware and software was installed to do the automatic setting of waveforms to control power supplies during the shot.

The acquisition system started taking data in November during testing of some of the various power systems, and ran routinely during the rest of the year to acquire and analyze data. The new timing system was installed and improved throughout the year. It allows for much more flexibility of operation and ensures that all timing information is collected along with the shot data. A SPRED diagnostic from ASDEX was added to the data acquisition system very easily. Analysis codes which run automatically on the VAX 780 computers were added. This included a CO_2 density calculation and six MHD time slice calculations. More codes are now being run on the VAX computers which corresponds to the phase out of the DEC-10 computers at the USC in June 1986. Both VAX 11/780s were upgraded to 11/758s. All DEC-10 tapes were moved to permanent off-site storage and it was arranged to store the second copy of shot data at the SDSC Supercomputer site nearby.

The major accomplishment in FY86 for the USC was the successful migration from the DEC-10 System to the VAX cluster. Both DEC-10 processors were replaced with two VAX 8600 computers. The DIII–D physics analysis database conversion to S1032 was completed in March 1986. The fusion administrative support programs remained in Accent-r and were moved to the VAX. Every effort was made to assure that all software packages and all capabilities that existed on the DEC-10 System were available on the VAX cluster. All programs and user accounts were moved to the VAX cluster, the NMFECC link was routed exclusively through the VAX, and the DEC-10 System was decommissioned on May 30, 1986.

The memory on both VAX 8600s was expanded for efficient processing of large physics codes. A 9642S Color Graphics Output System from Tektronix was installed. It was promptly used by the physicists to compare several sets of data on one plot, to trace impurities in the plasma, and to follow plasma decay more accurately.

FY87

Procurement and installation of a fiber optic link between the DIII–D VAX cluster and the USC VAX cluster was started. This link will be approximately 6500 feet long and will provide a much more reliable connection between the two centers. During the year, the data size increased to 17 megabytes. Two Mbytes of data, collected over the ethernet, were added when the Thomson Profile experiment started operation. A Microvax II was purchased to do between shot calculations. Calculations for the multichannel VUV, Bolometer, GRECE, and neutral beam injected power are being done with resultant data added to the shot database. A VAXstation 3500 was ordered to do a similar calculation

for the MHD fitting program MFIT. The MFIT code was modified so that the time traces of parameters such as elongation, BETAT are added to the shot data file. One VAX in the cluster is used to run this code. An experiment (STRS) from Johns Hopkins was incorporated into the VAX data acquisition, adding three megabytes of data. Security on the VAX systems was improved by use of mandatory generated passwords and with some additional in-house checks. Additional memory was added to the VAX systems.

The central timing system was refined and worked well. Timing information for neutral beam firing, ECH time and laser fire times can be set from a central console. Also, capabilities using asynchronous triggers with pre- and post-sampling was added.

CAMAC equipment from Berkeley was acquired as a result of the shutdown of their neutral beam test facility. A spare MODCOMP computer was purchased at a very good rate from a private company. The control system MODCOMP was upgraded to have 1 megabyte of memory and a 300 megabyte disk drive. Problems with the interface between the MODCOMP 32/85 and CAMAC were remedied, and this computer came online. All neutral beam programming was completed to handle long pulse sequences. A PC system was designed and is running to monitor neutron generation.

At the USC, major modifications in either hardware or software were kept to a minimum so as not to interfere with the DIII–D support. Disk refresher software was purchased from Raxco, Inc. (Rabbit-7). The Performance Coverage Analyzer (PCA) software was purchased from DEC and is used to compile code and indicate possible bottlenecks.

FASTLINK was installed between the ComputerVision CAD/CAM (CV) System and the USC cluster. This link makes it possible to send CAD files, via the MFEnet, to other MFE laboratories. The Accent-r license was moved from the VAX 11/780 to one of the VAX 8600s. This upgrade, along with the memory expansion for the 11/780, increased the MFEnet throughput. The online mass storage was expanded by trading out the disk drives from the DEC-10 System (RP07s) for VAX cluster compatible RA81 drives. One megaword of dual ported external memory which had been used on the DEC-10 was transferred to the Lawrence Berkeley Laboratory (LBL) Computations Department.

The shortage of cpu cycles was the greatest problem facing the USC. Extra cpu cycles were added by upgrading the VAX 8600 to an 8650. All cpu's were totally utilized by the end of FY87. A study to solve this problem was narrowed to the minisupercomputer market, several benchmarks were run, and an initial proposal was made. Budgetary considerations postponed any purchases.

5.4. SAFETY

The DIII–D safety program is established to provide safe operation of the DIII–D facility and to provide a safe working environment for its employees. The areas that are stressed include high voltage and current, vacuum, ionizing radiation, microwave radiation, cryogenics and industrial safety. Therefore, a special two volume Safety Manual set was written entitled "Doublet III Safety Procedures for Facility and Equipment Operation;" volume #1 contains policies and volume #2 contains procedures. These two manuals point out the specific safety rules and operating procedures to be adhered to while at the DIII–D site. Both manuals refer to the company safety manual for the general safety rules and regulations. The DIII–D safety program is supported by the GA safety program which provides expertise in areas such as Health Physics, Industrial Hygiene, and Industrial Safety.

DIII–D has a Safety Committee that is made up of representatives from all facets of DIII–D, from top management to the hands-on technician. Its chairman is the DIII–D Associate Program Director and the DIII–D Safety Officer reports directly to him. The Safety Committee can also solicit specialized help from any one of the three Safety Subcommittees when additional help is required in the areas of Lasers, Electrical, or Vacuum. The Safety Committee meets twice a month to discuss safety activities and concerns such as: new hazardous work requests, radiation work authorizations, accident reports or near misses, equipment malfunctions with potential safety hazards, accident avoidance through personnel training and supervisor involvement, access control in hazardous areas and the potential hazards in high voltage areas. Minutes of each meeting are published by the Safety Officer and become the basis for discussion at the next meeting.

When new employees arrive on site to work, they go through a thorough and comprehensive safety indoctrination by the Safety Officer and the Pit Coordinator. At that time they are made aware of the specific potential hazards that are present and the safety precautions and rules that apply. Subcontractors also go through a similar indoctrination.

The DIII–D Emergency Response Team consists of individuals from various areas involved directly with maintenance and operation of the DIII–D equipment. They are all trained in CPR, first aid, SCBA and fire extinguisher usage, evacuation and crowd control. The team can respond within seconds to provide immediate first aid assistance while the company EMT's are enroute.

The neutron and gamma radiation produced at DIII–D is constantly monitored at the site boundary with the level kept below 20 mR per year. Personnel dosimeters are worn by all individuals while on the DIII–D site and if entrance into the machine pit is required between shots, an alarming dosimeter is worn in addition to the TLD badge. Prior to unrestricted machine pit access, the pit is surveyed and the necessary areas are cordoned off until a safe reading is achieved.

A series of Safety Inspections occur throughout the year in keeping with our active Hazard Prevention Program. The inspections are conducted by both DIII–D personnel and outside consultants with report provided to the Safety Committee for action. The inspection topics are: monthly site inspection, yearly electrical inspection, voluntary OSHA consultant inspection, insurance carrier inspection and the General Atomics Safety Council yearly site inspection. The Safety Officer is responsible for tracking the progress and ensuring compliance.

Training is all-important to the Safety of both personnel and equipment. Due to the complexity of the DIII–D site and its operation, numerous safety training classes are offered throughout the year or whenever necessary. These classes include but are not limited to: confined space entry, back injury prevention, radiological safety, laser safety, hazard communication, cryogenic safety, crane and forklift operation, the national electrical code, shop tool usage and basic industrial safety.

5.5. VISITOR AND PUBLIC INFORMATION PROGRAM

5.5.1. VISITOR PROGRAM

Tours of the DIII–D facilities are open to organizations and institutions interested in fusion development (colleges, schools, government agencies, manufacturers and miscellaneous organizations). These tours are conducted on a non-interference basis and are arranged through the DIII–D tour coordinator whose responsibilities include security, scheduling tour guides and tours as required. During the last 5 years over 4,200 people toured DIII–D.

SECTION 6

PUBLICATIONS

6. PUBLICATIONS

6.1. FY88 PUBLICATIONS

Allen, S.L., D.N. Hill, M. Rensink, *et al.*, "Divertor Studies on DIII–D," *Bull. 30th Annual American Physical Society Meeting*, October 31 – November 4, 1988, Hollywood, Florida, (Abstract), **33**, 1915 (1988).

Allen, S.L., M.E. Rensink, D.N. Hill, *et al.*, "Recycling and Neutral Transport in the DIII–D Tokamak," *Proc. of the 8th International Conference on Plasma Surface Interactions*, May 2-6, 1988, Jülich, Federal Republic of Germany, General Atomics Report GA-A19292, 1988.

Anderson, P.M., "Development, Installation, and Initial Operation of DIII–D Graphite Armor Tiles," General Atomics Report GA-A19202, submitted to *J. Fus. Eng. Des.* (1988).

Bhadra, D.K., J. Kim, "Injection of Neutral Beam of Different Atomic Species into Plasmas of Different Ionic Species," *Bull. 30th Annual American Physical Society Meeting*, October 31 – November 4, 1988, Hollywood, Florida, (Abstract), **33**, 2055 (1988).

Brooks, N., T. Osborne, T. Petrie, *et al.*, "Impurity Behavior During Ohmic H–Mode in DIII–D," *Bull. 30th Annual American Physical Society Meeting*, October 31 – November 4, 1988, Hollywood, Florida, (Abstract), **33**, 1963 (1988).

Brooks, N., M. Perry, S. Allen, *et al.*, "Regulative Effect on Impurities of Recurring ELMs in H–Mode Discharges on the DIII–D Tokamak," General Atomics Report GA-A19108, submitted to *Plasma Physics & Controlled Fusion*, (1988).

Burrell, K.H., R.J. Groebner, H.St. John and R.P. Seraydarian, "Confinement of Angular Momentum in Divertor and Limiter Discharges in the Doublet III Tokamak," *Nucl. Fusion*, **28**, 3, January 1988.

Burrell, K.H., "Error Analysis for Parameters Determined in Nonlinear Least Squares Fits," General Atomics Report GA-A19251, submitted to *Am. Journ. of Physics* (1988).

Burrell, K.H., S.L. Allen, G. Bramson, *et al.*, "Energy Confinement in Auxiliary–Heated Divertor and Limiter Discharges in DIII–D Tokamak," *Proc. 12th International Conference on Plasma Physics and Controlled Nuclear Fusion Research*, October 12 – 19, 1988, Nice, France, General Atomics Report GA-A19443, 1988.

Callis, R.W., *et al.*, "An Overview of the DIII–D Long Pulse Neutral Beam System," *Proc. of the 15th Symposium on Fusion Technology*, September 19-23, 1988, Utrecht, Netherlands.

Carlstrom, T.N., N. Ohyabu, K.H. Burrell, *et al.*, "H–Mode Transition Studies in DIII–D," *Bull. 30th Annual American Physical Society Meeting*, October 31 – November 4, 1988, Hollywood, Florida, (Abstract), **33**, 1964 (1988).

Carlstrom, T., N. Ohyabu, P. Gohil, *et al.*, "Edge Electron Density & Temperature Behavior Following the H–Transition in DIII–D," General Atomics Report GA-A19169.

Colleraine, A., "Neutral Beam Long Pulse Project Final Report," General Atomics Report GA-A19139, January 1988.

Colleraine, A.P., *et al.*, "Stray Magnetic Field Interference with Ion Source Operation on the DIII–D Beamline," *Proc. 12th Symposium on Fusion Engineering*, IEEE, Monterey, 1987, **2**, 1157.

Content, D., H.W. Moos, M.E. Perry, *et al.*, "Impurity Profile Analysis in DIII–D H–Mode Discharges," *Bull. 30th Annual American Physical Society Meeting*, October 31 – November 4, 1988, Hollywood, Florida, (Abstract), **33**, 1915 (1988).

Content, D., H.W. Moos, M.E. Perry, *et al.*, "Impurity Profiles in DIII–D H–Mode Discharges," General Atomics Report GA-A19288, submitted to *Nucl. Fusion* (1988).

Davis, L.G., "DIII–D Vessel Modification Project Final Report," General Atomics Report GA-A19327, (1988).

DeBoo, J.C., K.H. Burrell, T. Carlstrom, *et al.*, "Energy Confinement Studies in the DIII–D Tokamak," *Bull. 30th Annual American Physical Society Meeting*, October 31 – November 4, 1988, Hollywood, Florida, (Abstract), **33**, 1915 (1988).

Ferron, J.R., E.J. Strait, T. Taylor, *et al.*, "High β Discharges in DIII–D Doublet Null Divertor Equilibria," *Bull. 30th Annual American Physical Society Meeting*, October 31 – November 4, 1988, Hollywood, Florida, (Abstract), **33**, 1960 (1988).

Gohil, P., K.H. Burrell, L. Lao, *et al.*, "Giant ELMs in DIII–D and Ballooning Instabilities," *Bull. 30th Annual American Physical Society Meeting*, October 31 – November 4, 1988, Hollywood, Florida, (Abstract), **33**, 1960 (1988).

Gohil, P., M. Ali Mahdavi, *et al.*, "Study of Giant ELMs and Comparison with Ballooning Theory in DIII–D," General Atomics Report GA-A19035, *Phys. Rev. Lett.* **61**, 1603 (1988).

Greenfield, C.M., J. Kim, R.L. Lee, "Analysis of Profile Measurements in the DIII–D Long Pulse Neutral Beam System," *Bull. 30th Annual American Physical Society Meeting*, October 31 – November 4, 1988, Hollywood, Florida, (Abstract), **33**, 2055 (1988).

Groebner, R.J., D.P. Schissel, H. St. John, *et al.*, "Thermal Diffusivity Variation with Current in H–Mode Discharges in the DIII–D Tokamak, *Bull. 30th Annual American Physical Society Meeting*, October 31 – November 4, 1988, Hollywood, Florida, (Abstract), **33**, 1964 (1988).

Heidbrink, W.W., "Charge Exchange Measurements from DIII–D," *Bull. 30th Annual American Physical Society Meeting*, October 31 – November 4, 1988, Hollywood, Florida, (Abstract), **33**, 1961 (1988).

Heidbrink, W.W., "The DIII–D $E_{\|}B$ Charge Exchange Diagnostics," General Atomics Report GA-A19185, *Rev. Sci. Instru.* **59(8)**, 1679 (1988).

Heidbrink, W.W., J. Kim, R.J. Groebner, "Comparison of Experimental and Experimental Fast Ion Slowing-Down Times in DIII–D," *Nucl. Fusion*, **28**, 1897 (1988).

Heidbrink, W.W., "Beam Density Fluctuation Diagnostic," General Atomics Report GA-A19071, *Rev. Sci. Instru.* **59(9)**, 2008 (1988).

Hill, D.N., C. Baxi, R. Ferguson, *et al.*, "Infrared Thermography of the DIII–D Divertor Targets," General Atomics Report GA-A19183, *Rev. Sci. Instru.*, **59(8)**, 1878 (1988).

Hill, D.N., "Particle Transport in DIII–D H–Mode Plasmas," *Bull. 30th Annual American Physical Society Meeting*, October 31 – November 4, 1988, Hollywood, Florida, (Abstract), **33**, 1978 (1988).

Hong, R., *et al.*, "Operational Experience with the DIII–D Neutral Beam 12 cm × 48 cm Common Long Pulse Source," *Proc. 12th Symposium on Fusion Engineering*, IEEE, Monterey, 1987, **2**, 1133.

Hong, R., A.P. Colleraine, J. Kim, *et al.*, "DIII–D Neutral Beam Long Pulse Source Operational Characteristics of Various Source Gas Flow Rates," *Bull. 30th Annual American Physical Society Meeting*, October 31 – November 4, 1988, Hollywood, Florida, (Abstract), **33**, 2054 (1988).

Hsieh, C.L., R. Chase, J.C. Deboo, *et al.*, "Multipoint Thomson Scattering Diagnostic for DIII–D," General Atomics Report GA-A19192, *Rev. Sci. Instru.*, **59(8)**, 1467 (1988).

Jackson, G.L., K.H. Burrell, J.R. Ferron, *et al.*, "Enhanced Confinement in DIII–D Beam–Heated Limited Discharges," *Bull. 30th Annual American Physical Society Meeting*, October 31 – November 4, 1988, Hollywood, Florida, (Abstract), **33**, 1963 (1988).

Jackson, G.L., T.S. Taylor, S.L. Allen, *et al.*, "Reduction of Recycling in DIII–D by Degassing and Conditioning of the Graphite Tiles," *Proc. of the 15th European Conference on Controlled Fusion and Plasma Heating*, May 16–20, 1988, Dubrovnik, Yugoslavia, General Atomics Report GA-A19295, 1988.

Jackson, G.L., "Experiments to Reduce Recycling in DIII–D by Degassing of the Graphite Divertor Tiles," *Proc. of the 8thy International Conference on Plasma Surface Interactions*, May 2-6, 1988, Jülich, Federal Republic of Germany.

James, R.A., S. Janz, R. Snider, *et al.*, "Experimental Plans for Electron Cyclotron Current Drive Experiments in DIII–D," *Bull. 30th Annual American Physical Society Meeting*, October 31 – November 4, 1988, Hollywood, Florida, (Abstract), **33**, 1963 (1988).

James, R.A., S. Janz, R. Ellis, *et al.*, "Vertical Viewing ECE Diagnostic for the DIII–D Tokamak," General Atomics Report GA-A19174, *Rev. Sci. Instru.*, **59(8)**, 1611 (1988).

Janz, S., D.A. Boyd, R.F. Ellis, *et al.*, "Vertical Viewing ECE Diagnostic on DIII–D," *Bull. 30th Annual American Physical Society Meeting*, October 31 – November 4, 1988, Hollywood, Florida, (Abstract), **33**, 1962 (1988).

Kellman, A., D. Schissel, R. Snider, *et al.*, "Confinement Studies in Low q, H–Mode Discharges," *Bull. 30th Annual American Physical Society Meeting*, October 31 – November 4, 1988, Hollywood, Florida, (Abstract), **33**, 1964 (1988).

Kellman, D.H., R. Hong, J. Kim, *et al.*, "Modification of the DIII–D Neutral Beam Power Systems for Operation of the Common Long Pulse Source," *Proc. 12th Symposium on Fusion Engineering*, IEEE, Monterey, 1987, **1**, 420.

Kim, J., M. Matsuoka, T.C. Simonen, *et al.*, "Neutral Beam Current Drive Experiments on DIII–D," *Bull. 30th Annual American Physical Society Meeting*, October 31 – November 4, 1988, Hollywood, Florida, (Abstract), **33**, 1963 (1988).

Matsuda, "Current Drive from a Langmuir Wave Excited by a Decay Instability of an Electromagnetic Wave in the Range of Electron Cyclotron Harmonics," *Bull. 30th Annual American Physical Society Meeting*, October 31 – November 4, 1988, Hollywood, Florida, (Abstract), **33**, 2014 (1988).

Kim, J., "Foil Activation Measurements of Energy and Flux of Neutrons from D–T Mixed Beams Driven into a Target," General Atomics Report GA-A19289, submitted to *Nuc. Instrum. & Method* (1988).

Kim, J., *et al.*, "Performance of the DIII–D Neutral Beam Injection System," *Proc. 12th Symposium on Fusion Engineering,* IEEE, Monterey, 1987, **1**, 290.

Kim, J., A.P. Colleraine, J. Haskovec, "Permeability Measurement of Ferromagnetic Components in the DIII–D Beamlines," *Proc. 12th Symposium on Fusion Engineering,* IEEE, Monterey, 1987, **2**, 1149.

Kim, J., A.P. Colleraine, R. Hong, *et al.*, "Discharge Characteristics of Magnetic-Bucket Long Pulse Plasma Generator Used in DIII–D Neutral Beam Injector," *Bull. Am. Phys. Soc.*, **32**, 1894 (1987).

Kinoshita, S., H. Fukumoto, G.L. Jackson, *et al.*, "Independent Control of the Gaps in Single–Null Divertor Discharges in the DIII–D Tokamak," *Bulletin of the Japanese Physical Society Meeting*, October 3–6, 1988, Hiratsuka, Japan (Abstract) (1988).

Lao, L.L., M. Chu, J. Ferron, *et al.*, "MHD Stability in DIII–D Divertor Discharges," *Bull. 30th Annual American Physical Society Meeting*, October 31 – November 4, 1988, Hollywood, Florida, (Abstract), **33**, 1914 (1988).

Lao, L.L., E.J. Strait, T.S. Taylor, *et al.*, "MHD Stability in High Beta$_T$ DIII–D Divertor Discharges," *Proc. of the 15th European Conference on Controlled Fusion and Plasma Heating*, May 16–20, 1988, Dubrovnik, Yugoslavia, General Atomics Report GA-A19218, 1988.

Lao, L., M.S. Chu, T. Ozeki, *et al.*, "Ideal Ballooning Stability in High Beta$_T$ DIII–D Divertor Discharges," General Atomics Report GA-A19247, accepted for publication in *Nucl. Fusion*, (1988).

Lazarus, E.L., J.B. Lister, "Axisymmetric Stability in DIII–D," *Bull. 30th Annual American Physical Society Meeting*, October 31 – November 4, 1988, Hollywood, Florida, (Abstract), **33**, 1961 (1988).

Lee, R.L., A. Colleraine, R. Hong, *et al.*, "Measurement of Neutral Beam Profiles on DIII–D Inner Wall Armor Tiles Using Scanning Infrared Optics," *Bull. 30th Annual American Physical Society Meeting*, October 31 – November 4, 1988, Hollywood, Florida, (Abstract), **33**, 2055 (1988).

LeHecka, T., E.J. Doyle, R. Philipona, *et al.*, "Multichannel, Narrowband Reflectrometry on DIII–D," *Bull. 30th Annual American Physical Society Meeting*, October 31 – November 4, 1988, Hollywood, Florida, (Abstract), **33**, 1962 (1988).

Lohr, J., "Electron Density Measurements from Cutoff of Electron Cyclotron Emission in the DIII–D Tokamak," General Atomics Report GA-A19107, *Rev. Sci. Instru.*, **59(8)**, 1608.

Lohr, J., T.C. Luce, R. James, *et al.*, "H–Mode Confinement with High Field Launched ECH on DIII–D," *Bull. 30th Annual American Physical Society Meeting*, October 31 – November 4, 1988, Hollywood, Florida, (Abstract), **33**, 1962 (1988).

Luce, T.C., R. James, J. Matsuda, *et al.*, "Inside Launch ECH on DIII–D," *Bull. 30th Annual American Physical Society Meeting*, October 31 – November 4, 1988, Hollywood, Florida, (Abstract), **33**, 1915 (1988).

Luxon, J.L., *et al.*, "DIII–D Annual Report for the Period FY87," Annual Report, GA-A19222, 1988.

Luxon, J., K. Burrell, R. Callis, *et al.*, "DIII–D: Summary of Recent Results and Program Plans," *Bull. 30th Annual American Physical Society Meeting*, October 31 – November 4, 1988, Hollywood, Florida, (Abstract), **33**, 1914 (1988).

Mahdavi, M.A., D. Hill, S. Allen, *et al.*, "Modification of the Scrape–Off Layer By Edge Plasma Modes," *Proc. of the 8th International Conference on Plasma Surface Interactions*, May 2-6, 1988, Jülich, Federal Republic of Germany, General Atomics Report GA-A19291, 1988.

Matsuoka, M., T.C. Simonen, D.K. Bhadra, *et al.*, "Neutral Beam Current Drive Experiments on DIII–D," *Bulletin of the Japanese Physical Society Meeting*, October 3–6, 1988, Hiratsuka, Japan (Abstract), 1988.

Mayberry, M.J., R.I. Pinsker, R.D. Phelps, *et al.*, "Ion Bernstein Wave Experiments on DIII–D – I. Heating," *Bull. 30th Annual American Physical Society Meeting*, October 31 – November 4, 1988, Hollywood, Florida, (Abstract), **33**, 1961 (1988).

Moeller, C.P., J.M. Lohr, T. Luce, *et al.*, "Operation of the DIII–D ECH High Field Launch System," *Bull. 30th Annual American Physical Society Meeting*, October 31 – November 4, 1988, Hollywood, Florida, (Abstract), **33**, 1962 (1988).

Moeller, C.P., "A Survey of ECH Microwave Technology," *Proc. of the 8th Topical Meeting on Technology of Fusion Energy*, October 9–13, 1988, Salt Lake City, Utah, General Atomics Report GA-A19424, (1988).

Ohyabu, N., "Optimization of H–Mode Discharges by Fine Ergodic Structure," *Bull. 30th Annual American Physical Society Meeting*, October 31 – November 4, 1988, Hollywood, Florida, (Abstract), **33**, 1965 (1988).

Ohyabu, N., S. Allen, N.H. Brooks, *et al.*, "H–Mode Study in DIII–D," *Proc. of the 15th European Conference on Controlled Fusion and Plasma Heating*, May 16–20, 1988, Dubrovnik, Yugoslavia, General Atomics Report GA-A19204, 1988.

Ohyabu, N., T.S. Osborne, G.L. Jahns, *et al.*, "Features of Edge Magnetic Turbulence in DIII–D Expanded Boundary Divertor Discharges," General Atomics Report GA-A19176, submitted to *Nucl. Fusion* (1988).

Okazaki, T., K. Yoshioka, M. Sugihara, *et al.*, "Analysis of Temperature Effects on RF Current Drive by Relativistic and Bounce–Averaged Fokker–Planck Equation," *Bull. 30th Annual American Physical Society Meeting*, October 31 – November 4, 1988, Hollywood, Florida, (Abstract), **33**, 2014 (1988).

Osborne, T., N. Brooks, T. Carlstrom, *et al.*, "H–Mode with Ohmic Heating Alone in DIII–D," *Bull. 30th Annual American Physical Society Meeting*, October 31 – November 4, 1988, Hollywood, Florida, (Abstract), **33**, 1915 (1988).

Osborne, T., N. Brooks, K.H. Burrell, *et al.*, "Observation of H–Mode in Ohmically Heated Divertor Discharges on DIII–D," General Atomics Report GA-A19362, submitted to *Phys. Rev. Lett.* (1988).

Ozeki, T., L.L. Lao, T.S. Taylor, "Effects of Shape on Ballooning Stability Near the Separatrix in DIII–D," *Bulletin of the Japanese Physical Society Meeting*, October 3–6, 1988, Hiratsuka, Japan (Abstract) (1988).

Perry, M.E., D. Content, H.W. Moos, *et al.*, "Impurity Transport Correlations with Electron Density Profiles," *Bull. 30th Annual American Physical Society Meeting*, October 31 – November 4, 1988, Hollywood, Florida, (Abstract), **33**, 1964 (1988).

Perry, M.E., N. Brooks, D. Content, *et al.*, "Impurity Transport During Density Profile Variations in DIII–D H–Mode with Giant ELMs," General Atomics Report GA-A19286, submitted to *Nucl. Fusion* (1988).

Petrie, T., N. Brooks, A. Kellman, *et al.*, "High–Density Limits in Ohmic- and Beam–Heated Plasmas in DIII–D," *Bull. 30th Annual American Physical Society Meeting*, October 31 – November 4, 1988, Hollywood, Florida, (Abstract), **33**, 1965 (1988).

Philipona, R., E.J. Doyle, T. Lehecka, *et al.*, "η_i Mode/Microturbulence Studies on DIII–D via Far–Infrared Heterodyne Scattering," *Bull. 30th Annual American Physical Society Meeting*, October 31 – November 4, 1988, Hollywood, Florida, (Abstract), **33**, 1962 (1988).

Phillips, J.C., *et al.*, "Fault Analysis of the DIII–D Neutral Beam Safety Interlock System," *Proc. 12th Symposium on Fusion Engineering*, IEEE, Monterey, 1987, **2**, 1101.

Pinsker, R.I., M.J. Mayberry, S.C. Chiu, *et al.*"Ion Bernstein Wave Experiments on DIII–D – II. Coupling," *Bull. 30th Annual American Physical Society Meeting*, October 31 – November 4, 1988, Hollywood, Florida, (Abstract), **33**, 1961 (1988).

Prater, R., N.H. Brooks, K.H. Burrell, *et al.*, "Electron Cyclotron Heating Experiments in the DIII–D Tokamak," *Proc. 12th International Conference on Plasma Physics and Controlled Nuclear Fusion Research*, October 12 – 19, 1988, Nice, France, General Atomics Report GA-A19448, 1988.

Rensink, M.E., "Particle Confinement Time for Divertor Discharges in DIII–D," *Bull. 30th Annual American Physical Society Meeting*, October 31 – November 4, 1988, Hollywood, Florida, (Abstract), **33**, 1965 (1988).

Sager, G.T., K.H. Burrell, A.G. Kellman, *et al.*, "Disappearance of Sawteeth During DIII–D Neutral Beam Counter–Injection," *Bull. 30th Annual American Physical Society Meeting*, October 31 – November 4, 1988, Hollywood, Florida, (Abstract), **33**, 1961 (1988).

Schaffer, "Oscillating Fluxes Current Drive on DIII–D," *Bull. 30th Annual American Physical Society Meeting*, October 31 – November 4, 1988, Hollywood, Florida, (Abstract), **33**, 1963 (1988).

Schissel, D.P., K.H. Burrell, J.C. DeBoo, *et al.*, "Results of Counter Neutral Beam Injection on DIII–D," *Bull. 30th Annual American Physical Society Meeting*, October 31 – November 4, 1988, Hollywood, Florida, (Abstract), **33**, 1915 (1988).

Schissel, D.P., R.E. Stockdale, H. St. John, *et al.*, "Measurements and Implications of Z_{eff} Profiles on the DIII–D Tokamak," General Atomics Report GA-A19049, *Physics of Fluids*, **31(12)**, 3738 (1988).

Schissel, D.P., K.H. Burrell, J.C. DeBoo, *et al.*, "Energy Confinement Properties of H–Mode Discharges in the DIII–D Tokamak, General Atomics Report GA-A19243, (1988), to be published in *Nucl. Fusion*, Feb. 1989.

Scoville, T., A. Kellman, T. Osborne, *et al.*, "The Effect of an Externally–Applied n=1 Field on Locked Modes in DIII–D Plasmas," *Bull. 30th Annual American Physical Society Meeting*, October 31 – November 4, 1988, Hollywood, Florida, (Abstract), **33**, 1961 (1988).

Seraydarian, R., K.H. Burrell, R.J. Groebner, "Multichordal Visible/Near UV Spectroscopy in the DIII–D Tokamak," General Atomics Report GA-A19178, *Rev. Sci. Instru.* **59(8)**, 1530 (1988).

Shimada, M., R. Stambaugh, A. Mahdavi, *et al.*, "Limiter Bias and Divertor Bias Experiments," *Bull. 30th Annual American Physical Society Meeting*, October 31 – November 4, 1988, Hollywood, Florida, (Abstract), **33**, 1965 (1988).

Simonen, T.C., D.K. Bhadra, K.H. Burrell, *et al.*, "Neutral Beam Current Drive Operation of the DIII–D Tokamak," *Proc. of the 15th European Conference on Controlled Fusion and Plasma Heating*, May 16–20, 1988, Dubrovnik, Yugoslavia, General Atomics Report GA-A19186, 1988.

Simonen, T.C., M. Matsuoka, D.K. Bhadra, *et al.*, "DIII–D Neutral Beam Current Drive Experiments at High Beta Poloidal," *Proc. 12th International Conference on Plasma Physics and Controlled Nuclear Fusion Research*, October 12 – 19, 1988, Nice, France, General Atomics Report GA-A19447, 1988.

Simonen, T.C., *et al.*, "Neutral Beam Current Driven High Poloidal Beta Operation of the DIII–D Tokamak," *Phys. Rev. Lett.*, **61**, 1720 (1988).

Sleaford, B.W., G.A. Cottrell, J. Kim, "Use of Balmer Radiation from Injected Neutral Beams for Measurement of Beam Deposition and Plasma Density Profiles," *Nucl. Fusion*, **28**, 523 (1988).

Snider, R., R. James, A. Kellman, *et al.*, "Experiments on Suppression of Sawteeth in DIII–D," *Bull. 30th Annual American Physical Society Meeting*, October 31 – November 4, 1988, Hollywood, Florida, (Abstract), **33**, 1915 (1988).

Snider, R.T., R. Evanko, J. Haskovec, "Toroidal and Poloidal Soft X–Ray Imaging System on the DIII–D Tokamak," General Atomics Report GA-A19159, *Rev. Sci. Instru.*, **59(8)**, 1807 (1988).

Snider, R.T., D. Content, R. James, *et al.*, "Modification of Sawteeth by Second Harmonic Electron Cyclotron Heating in a Tokamak," General Atomics Report GA-A19057, *Physics of Fluids-B*, **1#2**, 404 (1988).

St. John, H., K. Burrell, R. Groebner, *et al.*, "Analysis of Toroidal Rotation Data for the General Atomics DIII–D Tokamak," *Bull. 30th Annual American Physical Society Meeting*, October 31 – November 4, 1988, Hollywood, Florida, (Abstract), **33**, 1964 (1988).

Stallard, B., R. James, J. Lohr, *et al.*, "Heating and Confinement in DIII–D Using Inside Launch ECH," *Bull. 30th Annual American Physical Society Meeting*, October 31 – November 4, 1988, Hollywood, Florida, (Abstract), **33**, 1962 (1988).

Stambaugh, R.D., S. Allen, G. Bramson, *et al.*, "High Beta and ECRH Studies in DIII–D," *Proc. of the 15th European Conference on Controlled Fusion and Plasma Heating*, May 16–20, 1988, Dubrovnik, Yugoslavia, General Atomics Report GA-A19306, 1988.

Stambaugh, R.D., "Doublet III Annual Report, GA-A19133, 1988.

Stockdale, R.E., K.H. Burrell, W.M. Tang, "Perturbative Transport Experiments on DIII–D," *Bull. 30th Annual American Physical Society Meeting*, October 31 – November 4, 1988, Hollywood, Florida, (Abstract), **33**, 1977 (1988).

Strait, E., J. Ferron, G. Jackson, *et al.*, "Recent High Beta Results on DIII–D," *Bull. 30th Annual American Physical Society Meeting*, October 31 – November 4, 1988, Hollywood, Florida, (Abstract), **33**, 1914 (1988).

Strait, E.J., L. Lao, A.G. Kellman, *et al.*, "MHD Instabilities Near the Beta Limit in the DIII–D Tokamak," General Atomics Report GA-A19214, 1988, to be published by *Phys. Rev. Lett.*, March 1989.

Strait, E.J., L.L. Lao, T.S. Taylor, *et al.*, "Stability of High Beta Discharges in the DIII–D Tokamak," *Proc. 12th International Conference on Plasma Physics and Controlled Nuclear Fusion Research*, October 12 – 19, 1988, Nice, France, General Atomics Report GA-A19444, 1988.

Taylor, P.L, G.L. Jackson, P.I. Petersen, *et al.*, "Graphite Conditioning Techniques and Vent Recovery in the DIII–D Tokamak," *Bull. 30th Annual American Physical Society Meeting*, October 31 – November 4, 1988, Hollywood, Florida, (Abstract), **33**, 1963 (1988).

Taylor, T.S., E.J. Strait, L. Lao, *et al.*, "Achievement of Reactor–Relevant Beta in Low q Divertor Discharges in the DIII–D Tokamak," General Atomics Report GA-A19134, 1988, to be published by *Phys. Rev. Lett.*, March 1989.

Taylor, T.S., "Stability at High Beta in DIII–D," *Bull. 30th Annual American Physical Society Meeting*, October 31 – November 4, 1988, Hollywood, Florida, (Abstract), **33**, 1862 (1988).

Wight, J., A. Colleraine, R. Hong, *et al.*, "Maximization and Measurement of Ion–to–Neutral Conversion Efficiency in the DIII–D Beamlines," *Bull. 30th Annual American Physical Society Meeting*, October 31 – November 4, 1988, Hollywood, Florida, (Abstract), **33**, 2055 (1988).

Wight, J., *et al.*, "Beam Transmission Properties in the DIII–D Neutral Beamlines," *Proc. 12th Symposium on Fusion Engineering,* IEEE, Monterey, 1987, **2**, 1125.

Wood, R.D., S.L. Allen, N. Brooks, *et al.*, "Impurity Trends During DIII–D Plasma Operations," *Bull. 30th Annual American Physical Society Meeting*, October 31 – November 4, 1988, Hollywood, Florida, (Abstract), **33**, 1964 (1988).

6.2. FY87 PUBLICATIONS

C.B. Baxi, *et al.*, "Thermal-Stress Analysis and Testing of DIII–D," General Atomics Report GA-A18974, *Proc. 12th Symposium on Fusion Engineering,* IEEE, Monterey, 1987, **1**, 231 (1987).

N.H. Brooks, P. Petersen, and the DIII–D Group, "Initial Conditioning of the Vessel Wall and the Graphite Limiters in DIII–D," presented at the Seventh International Conference on Plasma-Surface Interactions in Controlled Fusion Devices, and published in *J. Nucl. Matl.*, **145, 146** (1987).

K.H. Burrell, S. Ejima, D.P. Schissel, N.H. Brooks, R.W. Callis, T.N. Carlstrom, A.P. Colleraine, J.C. DeBoo, H. Kukumoto, R.J. Groebner, D.N. Hill, *et al.*, "Observation of an Improved Energy Confinement Regime in Neutral Beam Heated Divertor discharges in the DIII–D Tokamak," *Phys. Rev. Lett.* **59**, 1432 (1987).

R.W. Callis et al., "Start-Up Performance of the DIII–D Tokamak," published in the *Proc. of the 14th Symposium on Fusion Technology*, Avignon, France, September 1986; GA Technologies Report GA-A18589 (1986); Vol. 2 (1987) page 347.

G.L. Campbell, *et al.*, "Automatic Laser Alignment for DIII–D Thomson Scattering," General Atomics Report GA-A18988, *Proc. 12th Symposium on Fusion Engineering,* IEEE, Monterey, 1987, **1**, 577 (1987).

V.S. Chan and S.K. Wong, "Poloidal Electric Field Generated by Electron Cyclotron Heating in a Collisional Tokamak Plasma," *Physics of Fluids,* **30**, 830 (1987).

M.S. Chu, "Equilibria in an Ellipsoidal Coordinate System," GA Technologies Report GA-A18481, *Nucl. Fusion*, **27**, 611 (1987).

M.S. Chu, L. Lao, R.W. Moore, H. St.John, R.D. Stambaugh, E.J. Strait and T.S. Taylor, "Beta Limit and Localized Ballooning Mode Stability in Doublet III," GA Technologies Report GA-A18546, *Nucl. Fusion*, **27**, 735 (1987).

A. Colleraine, "Doublet III Neutral Beam Heating Project Final Report," General Atomics Report GA–A18892, May 1987.

A.P. Colleraine, *et al.*, "Stray Magnetic Field Interference with Ion Source Operation on the DIII–D Beamline," General Atomics Report GA-A18995, *Proc. 12th Symposium on Fusion Engineering,* IEEE, Monterey, 1987, **2**, 1157 (1987).

L.G. Davis, *et al.*, "Status and Near-Term Plans for DIII–D," General Atomics Report GA–A18997, *Proc. 12th Symposium on Fusion Engineering,* IEEE, Monterey, 1987, **2**, 991 (1987).

S. Ejima, and R. Prater, "Interpretation of Electron Cyclotron Heating Results in Overdense Plasma in Doublet III," *Nucl. Fusion* **27**, 1135 (1987).

R. Evanko, "A Compact, Multiple Fiber-Optic Bundle Viewing System," to General Atomics Report GA–A18973, *Proc. 12th Symposium on Fusion Engineering,* IEEE, Monterey, 1987, **2**, 1504 (1987).

T.E. Evans, J.S. deGrassie, G.L. Jackson, N. Ohyabu, A. Wootton, K. Gentle, W. Hodge, S. McCool, P. Phillips, T. Rhodes, B. Richards, C. Ritz, W. Rowan, F. Karger and G. Haas, "Experiments to Test an Intra-Island Scoop Limiter on TEXT," *J. Nucl. Mater.*, **145-147**, 812 (1987).

A.S. Glad, "Microprocessor-Based Neutron Counter for DIII–D," General Atomics Report GA–A18990, *Proc. 12th Symposium on Fusion Engineering,* IEEE, Monterey, 1987, **1**, 561 (1987).

J.S. Haskovec, *et al.*, "Analog Computation System for DIII–D Plasma Control," General Atomics Report GA–A18972, *Proc. 12th Symposium on Fusion Engineering,* IEEE, Monterey, 1987, bf 1, 603 (1987).

D.N. Hill, T. Petrie, M.A. Mahdavi, L. Lao, and W. Howl, "Power Flow to the DIII–D Divertor Tiles," *Nucl. Fusion*, **28**, 902 (1988).

R. Hong, *et al.*, "Operational Experience of the DIII–D Neutral Beam 12 cm × 48 cm Long Pulse Source," General Atomics Report GA–A18993, *Proc. 12th Symposium on Fusion Engineering,* IEEE, Monterey, 1987, **2**, 1133 (1987).

J.Y. Hsu and M.S. Chu, "On the Tokamak Equilibrium Profile," GA Technologies Report GA-A18275, *Phys. Fluids*, **30**, 1221 (1987).

R.A. James, E. Silver, D. Boyd, R.F. Ellis, S. Janz, C.J. Lasnier, M.R. O'Brien, R.W. Harvey, J.M. Lohr, and R. Prater, "Measurements of High Harmonic, Optically Think ECE from Hot, Relativistic Electrons," to be published in *Proc. of the EC–6 International Workshop on Electron Cyclotron Emission and Electron Cyclotron Heating*, Oxford, England, September 10–14, 1987, General Atomics Report GA–A18980 (1987).

R.A. James, S. Janz, R.F. Ellis, D. Boyd, and J. Lohr, "Vertical viewing ECE Diagnostic for the DIII–D Tokamak," General Atomics Report GA–A19174, *Rev. Sci. Instru.*, **59(8)**, 1611 (1987).

J. Kim, A.P. Colleraine, and J.S. Haskovec, "Permeability Measurement of Feromagnetic Components in the DIII–D Beamlines," General Atomics Report GA–A18991, *Proc. 12th Symposium on Fusion Engineering,* IEEE, Monterey, 1987, **2**, 1149 (1987).

J. Kim, *et al.*, "Performance of the DIII–D Neutral Beam Injection System," General Atomics Report GA–A18992, *Proc. 12th Symposium on Fusion Engineering,* IEEE, Monterey, 1987, **1**, 290 (1987).

M.J. Mayberry, F.W. Baity, D.J. Hoffman, J.L. Luxon, T.L. Owens, and R. Prater, "Coupling of an ICRF Compact Loop Antenna to H–Mode Plasmas in DIII–D," *Proc. Applications of Radio–Frequency Power to Plasmas Seventh Topical Conference*, Kissimmee, Florida, 1987 (American Institute of Physics, New York, 1987), p. 278.

B.B. McHarg, Jr., "The Use of Networking in the DIII–D Data Acquisition," General Atomics Report GA–A18971, *Proc. 12th Symposium on Fusion Engineering,* IEEE, Monterey, 1987, **1**, 636 (1987).

C.P. Moeller, and J. Lohr, "Operation and Calibration of the DIII–D Grating Radiometer," to be published in *Proc. of the EC–6 International Workshop on Electron Cyclotron Emission and Electron Cyclotron Heating*, Oxford, England, September 16–17, 1987, General Atomics Report GA–A18987 (1987).

N. Ohyabu, G.L. Jahns, R.D. Stambaugh, and E.J. Strait, "Correlation of Magnetic Fluctuation and Edge Transport in the Doublet III Tokamak," *Phys. Rev. Lett.*, **58** (1987) 120.

N. Ohyabu, and J.S. deGrassie, "Possible Application of a Resonant Helical Magnetic Field in the Tokamak Boundary," *Nucl. Fusion* **27**, 2171 (1987), General Atomics Report GA–A18424.

N. Ohyabu, G.L. Jahns, R.D. Stambaugh, and E.J. Strait, "Correlation of Magnetic Fluctuations and Edge Transport in the Doublet III Tokamak," *Phys. Rev. Lett.* **58** 120 (1987).

R. Prater, R.J. Groebner, J.M. Lohr, K. Matsuda, C.P. Moeller, T.W. Petrie, R.T. Snider, B.W. Stallard, "Confinement in H–Mode Discharges in the DIII–D Tokamak with Electron Cyclotron Heating," to be published in *Proc. of the EC–6 International Workshop on Electron Cyclotron Emission and Electron Cyclotron Heating*, Oxford, England, September 10–14, 1987, General Atomics Report GA–A19116 (1987).

R. Prater, S. Ejima, R.W. Harvey, R.A. James, K. Matsuda, C.P. Moeller, B.W. Stallard, and T.C. Simonen, "Electron Cyclotron Heating at the Fundamental and Second Harmonic on DIII–D," 14th European Conference on controller Fusion and Plasma Physics, Madrid, 1987 (European Physical Society, 1987) **3**, p. 885.

R. Prater, S. Ejima, R.W. Harvey, J.Y. Hsu, R.A. James, K. Matsuda, J.M. Lohr, M.J. Mayberry, C.P. Moeller, B.W. Stallard, and T.C. Simonen, "Electron Cyclotron Heating Using the Fundamental Extraordinary Mode Launched from the Low Field side on DIII–D," *Proc. Applications of Radio–Frequency Power to Plasmas Seventh Topical Conference*, Kissimmee, Florida, 1987 (American Institute of Physics, New York, 1987), p. 9.

R. Prater, V.S. Chan, and T.C. Simonen, "The Status of Electron Cyclotron Heating and Current Drive and the Role of DIII–D," General Atomics Report GA–A18795 (1987).

E.E. Reis, *et al.*, "Assessment of Vertical Motions of DIII–D Vacuum Vessel," General Atomics Report GA–A18976, *Proc. 12th Symposium on Fusion Engineering,* IEEE, Monterey, 1987, **1**, 212 (1987).

J.T. Scoville, and P.I. Petersen, "The Ground-Fault Detection System for DIII–D," General Atomics Report GA–A18975, *Proc. 12th Symposium on Fusion Engineering,* IEEE, Monterey, 1987, **2**, 1532 (1987).

M. Shimada, *et al.*, "H–Mode Investigations in DIII–D," 14th European Conference on controller Fusion and Plasma Physics, Madrid, 1987 (European Physical Society, 1987) **1**, p. 9, General Atomics Report GA–A18864 (1987).

T.C. Simonen, G.R. Smith, R. Prater, and K. Matsuda, "Third Harmonic Electron Cyclotron Heating for Tokamak High Beta Profile Control Studies," Applications of Radio–Frequency Power to Plasmas Seventh Topical Conference, Kissimmee, Florida, 1987 (American Institute of Physics, New York, 1987), p. 45.

J.P. Smith, *et al.*, "Design of DIII–D Armor Tiles," General Atomics Report GA–A18977, *Proc. 12th Symposium on Fusion Engineering,* IEEE, Monterey, 1987, **1**, 144 (1987).

J.J. Wight, *et al.*, "Beam Transmission Properties in the DIII–D Neutral Beamlines," General Atomics Report GA–A18996, *Proc. 12th Symposium on Fusion Engineering,* IEEE, Monterey, 1987, **2**, 1126 (1987).

Yamaguchi, S. and M. Schaffer, "Current Drive Experiments in DIII–D by an Oscillating Flux Method," *Bull. 30th Annual American Physical Society Meeting*, October 31 – November 4, 1988, Hollywood, Florida, (Abstract), **33**, 1900 (1987).

6.3. FY86 PUBLICATIONS

V.S. Chan, C.S. Liu and Y.C. Lee, "Runaway Effects on Lower Hybrid Current Ramp-Up," Thirteenth European Conference on Controlled Fusion and Plasma Heating, Schliersee 14-18 April 1986 (*European Physical Society*, G. Brifford and M. Kaufmann, Eds.), **10C, II**, 382.

M.S. Chu, E.J. Strait, J.K. Lee, L. Lao, R.D. Stambaugh, K.H. Burrell, R.J. Groebner, J.M. Greene, F.J. Helton, J.Y. Hsu, J.S. Kim, H. St.John, R.T. Snider and T.S. Taylor, "Beta Limit Disruption," GA Technologies Report GA-A18594, presented at the 11th International Conference on Plasma Physics and Controlled Nuclear Fusion Research, Kyoto, Japan, November 13-20, 1986.

J.C. DeBoo, K.H. Burrell, S. Ejima, A.G. Kellman, N. Ohyabu, T.W. Petrie, D.P. Schissel, R.D. Stambaugh, "Doublet III Operating Regimes with Improved Energy Confinement," *Nucl. Fusion,* **26,** (1986) 211–221.

H.R. Garner, *et al.*, "Azimuthal Nonuniformities Induced by ECH and ICH in the RFC-XX-M Mirror Plasma," *Nucl. Fusion*, **26**, 611 (1986).

A.S. Glad, "Personal Computer Applications in DIII–D Neutral Beam Operation," presented at the Sixth Topical Conference on High Temperature Plasma Diagnostics, March 1986, Hilton Head Island, So. Carolina, *Rev. Sci. Instrum.*, **57,8**, 1921 (1986).

R.J. Groebner, W. Pfeiffer, F.P. Blau, K.H. Burrell, E.S. Fairbanks, R.P. Seraydarian, H. St. John, R.E. Stockdale, "Experimentally Inferred Ion Thermal Diffusivity Profiles in the Doublet III Tokamak: Comparison with Neoclassical Theory," *Nucl. Fusion,* **26,** 543–554 (1986).

R.J. Groebner for the Doublet III Group, "Comparison of Experimentally-Inferred Ion Thermal Diffusivities with Neoclassical Theory for Neutral Beam-Heated Discharges in the Doublet III Tokamak," presented at the Thirteenth European Conference on Controlled Fusion and Plasma Heating, Schliersee, 14–18 April 1986, and published in the Europhysics Conference Abstracts, **10C** (1986) 25–28.

P.A. Henline, "Experiences with Delta Compression of Data Produced by Doublet III," presented at the Sixth Topical Conference on High Temperature Plasma Diagnostics, March 1986, Hilton Head Island, So. Carolina, *Rev. Sci. Instrum.*, **57,8**, 1924 (1986).

J.Y. Hsu and M.S. Chu, "Minimum Energy State of MHD Equilibria," GA Technologies Report GA-A18474, Presented at International Workshop on Small Scale Turbulence and Anomalous Transport in Magnetized Plasmas, Cargèse, France, July 6-12, 1986.

J.Y. Hsu and M.S. Chu, "Kink Stability of a Low q High β Circular Tokamak," GA Technologies Report GA-A18211, submitted to *Nucl. Fusion* (1986).

G.L. Jahns, S.K. Wong, R. Prater, S.H. Lin, and S. Ejima, "Measurement of Thermal Transport by Synchronous Detection of Modulated Electron Cyclotron Heating in the Doublet III Tokamak," *Nucl. Fusion,* **26**, 226–231 (1986).

C. Kahn, K.H. Burrell, S. Ejima, E. Fairbanks, T. Petrie, M. Shimada, M. Washizu, "Divertor and Edge Plasma Properties in Doublet III Expanded Boundary Discharges," *Nucl. Fusion*, **26**, 73 (1986).

J.K. Lee, C.L. Bernard, F.J. Helton, R.D. Stambaugh and E.J. Strait, "Stability Analyses of High-Beta Doublet III Discharges," *Plasma Phys. and Contr. Fusion*, **28**, 259 (1986).

P. Lee, "Tokamak as an X-Ray/XUV Light Source," presented at the Soc. of Photo-Optical Instrumentation Engineering (SPIE), San Diego, CA, and published in the *Proc. of X-Ray Calibration Techniques, Sources, and Detectors*, **689**, 238 (1986).

P. Lee, A.J. Lieber, A.K. Pradan, and Y. Xu, "Time-Resolved Measurements of Non-thermal X-Ray Emission of TiXXI Lines in Electron-Cyclotron-Heated Tokamak Plasmas," *Phys. Rev. A*, **34**, 3210 (1986).

J. Lohr, and T. Ohkawa, "Parametric Decay During Lower Hybrid Heating on Doublet IIA," *Phys. Fluids,* **29**, 892 (1986).

J. Lohr, G. Jahns, C. Moeller, and R. Prater, "Grating Spectrometer Installation for Electron Cyclotron Emission Measurements on the DIII–D Tokamak using Circular Waveguide and Synchronous Detection," presented at the Sixth Topical Conference on High Temperature Plasma Diagnostics, Hilton Head Island, SC, 9–13 March 1986, and published in *Rev. Sci. Instrum.*, **57**, 1956 (1986).

J.L. Luxon et al., "Initial Results from the DIII–D Tokamak," *Proc. of the Eleventh International Conference on Plasma Physics and Controlled Nuclear Fusion Research*, (Kyoto, Japan), IAEA, Vienna, 1987, **3**, 159 (1986),

M. Ali Mahdavi, "Status of Poloidal Divertor Experiments," *Trans. Am. Nucl. Soc.*, **52**, 159 (1986).

N. Ohyabu, J.S. deGrassie and T.E. Evans, "Model for Divertor Function in H-Mode Onset and Proposed for H-Mode Operation with the Island Divertor," *J. Nucl. Mater.*, **145-147**, 844, 1987.

N. Ohyabu, J.K. Lee, and J.S. deGrassie, "A Simple Model of Energy Confinement in Tokamaks," *Nucl. Fusion*, **26**, 593 (1986).

N. Ohyabu, J.S. deGrassie, and T.E. Evans, "Model for Divertor Function in H-Mode Onset and Proposal for H-Mode Operation with the Island Divertor," GA Technologies Report GA-A18454, *J. Nucl. Materials.*, **145-147**, 844 (1986).

N. Ohyabu and J.S. deGrassie, "Consideration of Ergodic and Resonant Magnetic Divertor for Tokamak Reactors," GA Technologies Report GA-A18259, and presented at the IAEA Specialists Meeting on Tokamak Concept Innovation, January 1986.

R. Prater, S. Ejima, R.W. Harvey, A.J. Lieber, K. Matsuda, C.P. Moeller, "Confinement in Electron Cyclotron Heating Experiments on Doublet III," to be published in the *Proc. of the Eleventh International Conference on Plasma Physics and Controlled Nuclear Fusion Research*, (Kyoto, Japan), (IAEA, Vienna, 1987), paper F-III-3; GA Technologies Report GA-A18630 (1986).

R. Prater, J. Lohr, editors, *Proc. of the EC-5 Fifth International Workshop on Electron Cyclotron Emission and Electron Cyclotron Heating*, GA Technologies Report GA-A18294 (1985).

R. Prater and A.J. Lieber, "Heating Effectiveness in Electron Cyclotron Heating Experiments in the Doublet III Tokamak," GA Technologies Report GA-A18358 (1986); published in the *Proc. of the EC-5 Fifth International Workshop on Electron Cyclotron Emission and Electron Cyclotron Heating* GA-A18294 (1985).

D.P. Schissel, G. Bramson, and J.C. DeBoo, "Physics Analysis Database for the DIII–D Tokamak," presented at the Sixth Topical Conference on High Temperature Plasma Diagnostics, March 1986, Hilton Head Island, S. Carolina, and published in *Rev. Sci. Instrum.*, **57**, 1932 (1986).

D.P. Schissel, "Pellet Injection Experiments on Doublet III and DIII–D," presented at the CIT Pellet Fueling Workshop, Massachusetts Institute of Technology, August 1986.

R.P. Seraydarian and K.H. Burrell, "Multichordal Charge Exchange Recombination Spectroscopy on the DIII–D Tokamak," presented at the Sixth Topical Conference on High Temperature Plasma Diagnostics, Hilton Head Island, S. Carolina, March 9–13, 1986, and published in *Rev. Sci. Instrum.*, **57**, 2012–2014 (1986).

R.P. Seraydarian, K.H. Burrell, N.H. Brooks, R.J. Groebner, and C. Kahn, "Multichordal Charge Exchange Recombination Spectroscopy on the Doublet III Tokamak," presented at the Fifth Topical Conference on High Temperature Plasma Diagnostics, and published in *Rev. Sci. Instrum.*, **57**, 155-163 (1986).

M. Shimada, A.T. Ramsey, D.K. Owens, H.F. Dylla, R. Bundy, P.H. LaMarche, J. Schivell, R.H. Groebner, D. Heifetz, and M. Murakami, "Global Particle Recycling with Ohmic and Neutral Beam Heating in TFTR," presented at the Seventh International Conference on Plasma Surface Interactions in Controlled Fusion Devices, and published in *J. Nucl. Materials.*

M. Shimada, M.G. Bell, P. Couture, R.J. Fonck, G. Gammel, W. Heidbrink, K. Ida, R. Kaita, S. Kaye, H. Kungel, B. LaBlanc, D. Manos, W. Morris, N. Ohyabu, S. Paul, S. Sesnic, H. Takahashi, and M. Okabayashi, "Limiter Bias Experiments in PBX," presented at the Seventh International Conference on Plasma Surface Interactions in Controlled Fusion Devices, and published in *J. Nucl. Materials.*

E.J. Strait, M.S. Chu, G.L. Jahns, J.S. Kim, A.G. Kellman, L.L. Lao, J.K. Lee, R.W. Moore, H. St. John, D.O. Overskei, R.T. Snider, R.D. Stambaugh, and T.S. Taylor, "Beta and Current Limits in the Doublet III Tokamak," presented at the Thirteenth European Conference on Controlled Fusion and Plasma Heating (European Physical Society), Schliersee, Federal Republic of Germany, 14-18 April 1986, and published in the *EUROPHYSICS Conf. Abstracts*, **10-C, Part I**, 204.

6.4. FY85 PUBLICATIONS

C.J. Armentrout, "Improved Performance for Large Area Triple Layer Microchannel Plate Detector for a Neutral Particle Spectrometer in Doublet III," *Rev. Sci. Instrum.*, **56** (1985).

C.J. Armentrout, "Large Area Triple-Layer Microchannel Plate Arrays," *Rev. Sci. Instrum.*, **56**, 1179 (1985).

C.J. Armentrout and E.J. Strait, "Evidence for Prompt Fast Ion Loss from Plasmas During Neutral Beam Injection in Doublet III," GA Technologies Report GA-A17891, submitted to *Nucl. Fusion.*

C.J. Armentrout, G. Bramson and R.G. Evanko, "E Parallel B Canted Detector Neutral-Particle Spectrometer," *Rev. Sci. Instrum.*, **56**, 2103 (1985).

V.S. Chan, C.S. Liu and Y.C. Lee, "Modification of Lower Hybrid Current Ramp-up by Runaways," GA Technologies Report GA-A18001.

V.S. Chan, S.C. Chiu and S.K. Wong, "Impurity Transport in ICRH Tokamak Plasmas," *Nucl Fusion*, **25**, 697 (1985).

V.S. Chan and C.S. Liu, "Nonlinear Ion Heating in Lower Hybrid Current Drive," *Fusion Technol.*, **7**, 288 (1985).

G.A. Cottrell, E.S. Fairbanks and R.E. Stockdale, "Determination of Experimental Tokamak Plasma Profiles Using Maximum Entropy Analysis," *Rev. Sci. Instrum.*, **56** (1985).

J.C. DeBoo and the Doublet III Physics, Operations, and Neutral Beam Groups: "Energy Confinement Experiments on Doublet III with High Power Neutral Beam Heating," presented at the Twelfth European Conference on Controlled Fusion and Plasma Physics, Sept. 2-6, 1985, Budapest, Hungary, and published in the *Proceedings*, **9F, I**, 2.

S. Ejima, G. Jahns, S.-H, Lin, C. Moeller, R. Prater and R. Snider, "Heating and Confinement in the Doublet III Tokamak with Electron Cyclotron Heating," presented at the Twelfth European Conference on Controlled Fusion and Plasma Physics, Sept. 2-6, 1985, Budapest, Hungary, and published in the *Proceedings.*

E.S. Fairbanks, "CO_2 Laser Interferometer Array for Big Dee," *Rev. Sci. Instrum.*, **56** (1985).

K. Hoshino, T. Yamamoto, A. Funahashi, N. Suzuki, T. Matoba, T. Yamaguchi, H. Matsumoto, T. Kawakami, H. Kimura, S. Konoshima, M. Maeno, T. Matsuda, Y. Matsuzaki, K. Odashima, K. Ohasa, S. Sengoku, T. Shoji, T. Sudie, S. Yamamoto, Y. Tanaka, C.P. Moeller, R.J. LaHaye, and R. Prater, "Electron Cyclotron Heating and Pre-Ionization in the JFT-2 Tokamak," *J. Phys. Soc. Japan,* **54**, 2503–2515 (1985).

L. Lao, H. St.John, R. Stambaugh and W. Pfeiffer, "Separation of $\bar{\beta}_p$ and ℓ_i in Tokamaks of Non-Circular Cross-Sections," *Nucl. Fusion,* **25**, 1421 (1985).

L. Lao, H. St.John, R. Stambaugh, A. Kellman and W. Pfeiffer, "Reconstruction of Current Profile Parameters and Plasma Shapes in Tokamaks," GA Technologies Report GA-A17910.

L. Lao, J. Greene, T. Wang, F.J. Helton and E. Zawadzki, "Equilibrium and Stability by a Variational Spectral Method," *Phys. Fluids,* **28**, 869 (1985).

J.K. Lee, M.S. Chu, C.S. Liu and J.F. Drake, "Half-Coalescence Ideal MHD Instability of the q=1 Magnetic Island in Tokamaks," *Phys. Fluids*, **25**, 1585 (1985).

P. Lee, A.J. Lieber and R.P. Chase, "Helium-Like Titanium Spectra Produced by Electron-Cyclotron-Heated Tokamak Plasmas, *Phys. Rev. Lett.*, **55**, 386 (1985).

P. Lee, A. Lieber and S. Wojtowicz, "Observation of the Helium-Like Ti XXI Emission Lines from Doublet III Tokamak Plasmas," *Phys. Rev. Lett.*, **31**, 3996 (1985).

P. Lee, "Soft X-Ray Optics Using Multilayer Mirrors," *Opt. Eng.*, **24(1)**, 197-201 (1985).

A.J. Lieber, "Sequentially-Framing Soft X-Ray Pinhole Camera for Tokamak Plasma Studies," *Rev. Sci. Instrum.*, **56** (1985).

A. Lieber, R. Snider and P. Lee, "Electron Cyclotron Heating Correlation with Plasma Rotation in the Doublet III Tokamak," GA Technologies Report GA-A18039.

A. Lieber, P. Lee, R. Snider and S. Wojtowicz, "ECH Induced Toroidal Plasma Rotation in the Doublet III Tokamak," GA Technologies Report GA-A17880.

C.S. Liu, V.S. Chan and Y.C. Lee, "Runaway Electrons and Plasma Turbulence in Current Ramping by Lower Hybrid Waves in Tokamak Plasmas," *Phys. Rev. Lett.*, **55**, 2583 (1985).

J. Lohr and C.J. Armentrout, "Charge Exchange Measurements on the Doublet III Tokamak," in *Proc. of the Conference on Basic Physical Processes in Toroidal Fusion Plasmas,* August 26-Sept. 3, Varenna, Italy (1985).

J. Lohr and C.J. Armentrout, "Neutral Flux Measurements During Neutral Beam Injection on Doublet III," *Rev. Sci. Instrum.*, **56**, 1127 (1985).

J.L. Luxon and L.G. Davis, "Big Dee – A Flexible Facility Operating Near Breakeven Conditions," Sixth Topical Meeting on the Technology of Fusion Energy, *Fusion Technology*, **8**, 441-449 (1985).

C.P. Moeller, "A Survey of ECH Microwave Technology," in *Proc. of the Course and Workshop on Application of RF Waves to Tokamak Plasmas,* Sept. 5-14, Varenna, Italy (1985).

C. Moeller, J. Lohr and R. Prater, "The Transmission System for the DIII–D ECE Radiometer," presented at the Fifth International Workshop on Electron Cyclotron Emission and Electron Cyclotron Heating, Nov. 9-12, 1985, San Diego, CA and to be published in the *Proceedings.*

T. Ohkawa, R. Stambaugh and the Doublet III Physics Group, "Energy Confinement in Doublet III," presented at the Twelfth European Conference on Controlled Fusion and Plasma Physics, Sept. 2-6, 1985, Budapest, Hungary and to be published in *Plasma Physics and Controlled Fusion.*

N. Ohyabu, J.S. deGrassie, N. Brooks, T. Taylor, H. Ikezi, K. Gentle, R. Bengtson, R. Bravenec, W. Hodge, K. Nelin, P. Phillips, B. Richards, C. Ritz, W. Rowan, Y. Wan, C. Kleeper, J. Porter and J. Snipes, "Ergodic Magnetic Layer Experiment," *Nucl. Fusion,* **25**, 1684 (1985).

N. Ohyabu, K.H. Burrell, J.C. DeBoo, S. Ejima, R. Groebner, D. Overskei, W. Pfeiffer, R. Stambaugh, C. Armentrout, J. Baur, F. Blau, G. Bramson, N. Brooks, R. Chase, E. Fairbanks, C. Hsieh, G. Jahns, C. Kahn, A. Kellman, D. Knowles, A. Lieber, J. Lohr, T. Petrie, L. Rottler, D. Schissel, R. Seraydarian, J. Smith, R. Snider, H. St.John, E. Strait, T. Taylor, D. Vaslow, S. Wojtowicz, S. Wong, G. Zawadzki and the Doublet III Operations, Neutral Beam and Theory Groups, "A Regime of Improved Energy Confinement in Beam Heated Expanded-Boundary Discharges in Doublet III," *Nucl. Fusion,* **25**, 49 (1985).

T.W. Petrie and J.T. Scoville, "Infrared Camera and Data Acquisition System in Doublet III," *Rev. Sci. Instrum.*, **56**, (1985)

R. Prater, "A Review of ECH Experiments in Toroidal Devices," in *Course and Workshop on Applications of RF Waves to Tokamak Plasmas*, ed. S. Bernabei, U. Gasparino, and E. Sindoni, pp. 354-376 (International School for Plasma Physics, Italy, 1985); GA Technologies Report GA-A18149 (1985).

R. Prater, "Review of Electron Cyclotron Heating Experiments in Tokamaks and Stellerators," GA Technologies Report GA-A18149), to be published in *Proc. of the Course and Workshop on Application of RF Waves to Tokamak Plasmas,* Sept. 5-14, 1985, Varenna, Italy.

R. Prater, K.H. Burrell, S. Ejima, G.L. Jahns, S.-H. Lin and C.P. Moeller, "Doublet III Electron Cyclotron Heating Physics Summary," GA Technologies Report GA-C17810.

R. Prater, K.H. Burrell, S. Ejima, S.-H. Lin, C.P. Moeller and the DIII Physics Group, "Summary of Electron-Cyclotron Heating Physics Results from the Doublet III Tokamak," GA Technologies Report GA-A17939.

D.P. Schissel, "Comment on Energy Transduction in Pellet-Injected Plasmas," GA Technologies Report GA-A18239.

D.P. Schissel, J. Baur, G. Bramson, A. Kellman, R.T. Snider, R. Stockdale, S.S. Wojtowicz and C.A. Foster, "The Results of Pellet Fueled Discharges on the Doublet III Tokamak," GA Technologies Report GA-A17958.

R.P. Seraydarian, K.H. Burrell and C. Kahn, "Multichordal Charge Exchange Recombination Spectroscopy on Doublet III," *Rev. Sci. Instrum.*, **56** (1985).

R.D. Stambaugh, "Investigations of MHD Activity in ASDEX Discharges," *Max-Planck-Institut Report* IPP III/103 (June 1985).

E.J. Strait, L.C. Bernard, A.G. Kellman, R.W. Moore, R.D. Stambaugh, D.O. Overskei, C.J. Armentrout, J.F. Baur, K.H. Burrell, J.C. DeBoo, R. Groebner, F.J. Helton, G.L. Jahns, L. Lao, J.K. Lee, J. Lohr, R.T. Snider and H. St.John, "Doublet III Beta Limits and the Role of Discharge Shape," GA Technologies Report GA-A17837.

R.W. Moore, R.R. Dominguez and M.S. Chu, "Resistive Ballooning Modes in the Doublet III Tokamak," GA Technologies Report GA-A17416.

W. West, A.J. Lieber, "Transfer of Analog Temporal Data Via Standard Duel-Channel Digital Fiberoptic Links," GA Technologies Report GA-A17260.

S.K. Wong, "Hypotheses on L-H Transition," *Max-Planck-Institut Report* IPP III/106 (June 1985).

6.5. FY84 PUBLICATIONS

P.L. Andrews, V.S. Chan and C.S. Liu, "A Simple Model for Lower Hybrid Current Drive in Tokamaks," GA Technologies Report GA-A17567, 1984.

S.C. Bates, K.H. Burrell, "Fast Gas Injection System for Plasma Physics Experiments," *Rev. Sci. Instrum.*, **55**, 934 (1984).

K.H. Burrell, R. Prater, S. Ejima, *et al.*, "Comparison of Energy Confinement in Doublet III Limiter and Divertor Discharges with Ohmic, Neutral Beam, and Electron Cyclotron Heating," Tenth International Conference on Plasma Physics and Controlled Nuclear Fusion Research, London, 1984, IAEA-CN-44/A-I-5.

K.H. Burrell, N. Ohyabu, R. Chase, *et al.*, "On Means of Varying Conditions in the Expanded Boundary Divertor Without Affecting Energy Confinement," *J. Nucl. Mater.*, **128 & 129**, 275 (1984).

K.H. Burrell, R.J. Groebner, N.H. Brooks, *et al.*, "Magnetic Dipole Transitions in the n=3 Level of Highly Ionized Zinc, Germanium, and Selenium," *Phys. Rev. A*, **29**, 1343 (1984).

J.C. DeBoo, C.J. Armentrout, J.F. Baur, *et al.*, "Beta Confinement Experiments on Doublet III with High Power Neutral Beam Heating," GA Technologies Report GA-A17613.

J.S. deGrassie, N. Ohyabu, N.H. Brooks, K. Gentle, R. Bengtson, R. Bravenec, W. Hodge, T. Kochanski, K. Nelin, P. Phillips, T. Price, B. Richards, C. Ritz, W. Rowan, S. Kim, S. Levinson, K. Leung, J. Porter and J. Snipes, "EML Experiments on TEXT with 7/3 Resonance," *J. Nucl. Mater.*, **128, 129**, 266 (1984).

T.E. Evans, J.F. Benesch, R.D. Bengtson, Y.-M. Li, S.M. Mahajan, M.E. Oakes, D.W. Ross, P.M. Valanju, X.-Z. Wang, J.G. Watkins, and C.M. Surko, "Structure of the Global Alfvén Eigenmode," *Phys. Rev. Lett.*, **53**,1743 (1984).

F.L. Hinton, M.-S. Chu, R.R. Dominguez, R.W. Harvey, L.L. Lao, J.K. Lee, C.S. Liu, R.W. Moore, T. Ohkawa, S.K. Wong and Y.C. Lee, "Physics of the H-Mode," GA Technologies Report GA-A17645, 1984, presented at the Tenth IAEA International Conference on Plasma Physics and Controlled Nuclear Fusion, London, September 1984.

J.-Y. Hsu, V.S. Chan, R.W. Harvey, R. prater and S.K. Wong, "Resonance Localization and Poloidal Electric Field Due to Cyclotron Wave Heating in Tokamak Plasmas," *Phys. Rev. Lett.*, **53**, 564 (1984).

C. Kahn, K.H. Burrell, E. Fairbanks, *et al.*, "The Scaling of Edge Properties with Main Plasma Parameters in Doublet III Discharges," *J. Nucl. Mater.*, **129**, (1984).

J.K. Lee and M.-S. Chu, "MHD Stability of High-Beta Tokamak Equilibria with pedestal and Line-Tying," *Nucl. Fusion*, **24**, 1360 (1984).

J.K. Lee, M.-S. Chu, F.J. Helton and W. Park, "Magnetic Fluctuations in High-β_p Tokamak Plasmas," *Phys. Fluids*, **27**, 607 (1984).

R. Little and J.M. Rawls, "Large Tokamak Experiments," *Nucl. Fusion,* **24**, 657 (1984).

C.P. Moeller, R. Prater, S.-H. Lin, "Components and Transmission Systems for ECH," *Proc. of the Fourth International Symposium on Heating in Toroidal Plasmas*, Rome, **II**, March 1984.

N. Ohyabu, J.S. deGrassie, N.H. Brooks, T.S. Taylor, H. Ikezi and the TEXT group, "Preliminary Results from the EML Experiment on TEXT," *J. Nucl. Mater.,* **121**, 263 (1984).

N. Ohyabu, J.S. deGrassie, N. Brooks, *et al.*, "Ergodic Magnetic Layer Experiment," GA Technologies Report GA-A17786, November 1984.

N. Ohyabu, N.H. Brooks, K.H. Burrell, *et al.*, "Role of Particle Recycling in Beam Heated Expanded Boundary Divertor Discharges in D-III," *J. of Nucl. Mater.,* **121** (1984).

D.O. Overskei, C.J. Armentrout, J.F. Baur, *et al.*, "High Power Neutral Beam Heating on Doublet III," *Proc. of the Fourth Varenna/Grenoble International Symposium on Heating in Toroidal Plasmas,* Rome, 1984.

R. Prater, S. Ejima, S.-H. Lin, *et al.*, "Electron Cyclotron Heating Experiments on Doublet III," *Proc. of the Fourth International Symposium on Heating in Toroidal Plasmas,* Rome, **II**, 736 (1984).

J.M. Rawls, D.R. Baker, A.P. Colleraine, *et al.*, "Design of Long Pulse Heating Systems for Doublet III-D," *Fusion Technology 1984,* **1**, 645, Pergamon Press.

J. Smith, R. Chase, J. Garcia, *et al.*, "An Intensified CCD Camera System for Plasma Diagnostics," *Rev. Sci. Instrum.,* **29**, 1364 (1984).

R.D. Stambaugh, W.R. Moore, L.C. Bernard, *et al.*, "Tests of Beta Limits as a Function of Plasma Shape in the Doublet III Device," presented at the Tenth International Conference on Plasma Physics and Controlled Nuclear Fusion Research, London, 1984, IAEA-CN-44/A-IV-2-1.

R.E. Waltz, M.-S. Chu, D.K. Bhadra and F.L. Hinton, "Plasma Diffusion in an Ergodic Magnetic Limiter," *J. Nucl. Mater.*, **128,129**, 118 (1984).

S.K. Wong and F.L. Hinton, "Rotational Suppression of Pfirsch-Schluter Ion Thermal Conductivity for a Plasma," *Phys. Rev. Lett.,* **52**, 827 (1984).